Department of Electrical Engineering and Automation

Reliability aspects of network planning for meshed subtransmission networks

Bruno Jorge de Oliveira e Sousa

Aalto University

DOCTORAL DISSERTATIONS

Aalto University publication series
DOCTORAL DISSERTATIONS 167/2015

Reliability aspects of network planning for meshed subtransmission networks

Bruno Jorge de Oliveira e Sousa

A doctoral dissertation completed for the degree of Doctor of Science (Technology) to be defended, with the permission of the Aalto University School of Electrical Engineering, at a public examination held at the lecture hall S5 of the school on 17 November 2015 at noon.

Aalto University
School of Electrical Engineering
Department of Electrical Engineering and Automation
Power Systems and High Voltage Engineering

Supervising professor
Prof. Matti Lehtonen, Aalto University, Finland

Preliminary examiners
Assoc. Prof. Herwig Renner, Graz University of Technology, Austria
Prof. Saulius Gudžius, Kaunas University of Technology, Lithuania

Opponents
Assoc. Prof. Herwig Renner, Graz University of Technology, Austria
Assoc. Prof. Jako Kilter, Tallinn University of Technology, Estonia

Aalto University publication series
DOCTORAL DISSERTATIONS 167/2015

ISBN 978-952-60-6495-6 (printed)
ISBN 978-952-60-6496-3 (pdf)
ISSN-L 1799-4934
ISSN 1799-4934 (printed)
ISSN 1799-4942 (pdf)
http://urn.fi/URN:ISBN:978-952-60-6496-3

Unigrafia Oy
Helsinki 2015

Finland

NORDIC ECOLABEL
441 697
Printed matter

Aalto University

Abstract

Aalto University, P.O. Box 11000, FI-00076 Aalto www.aalto.fi

Author
Bruno Jorge de Oliveira e Sousa

Name of the doctoral dissertation
Reliability aspects of network planning for meshed subtransmission networks

Publisher School of Electrical Engineering

Unit Department of Electrical Engineering and Automation

Series Aalto University publication series DOCTORAL DISSERTATIONS 167/2015

Field of research Power Systems and High Voltage Engineering

Manuscript submitted 11 August 2015 **Date of the defence** 17 November 2015

Permission to publish granted (date) 14 October 2015 **Language** English

☐ **Monograph** ☒ **Article dissertation (summary + original articles)**

Abstract

As the intermediate part of the power system connecting transmission and distribution systems, the subtransmission networks incorporate a great number of intrinsic features. Despite their ambiguous role, sometimes being treated as distribution or as transmission, the subtransmission networks have a clear and direct effect on power quality issues for end-customers. Therefore, they must be handled and appropriately modeled, because of their particularities and operational practices.

This thesis proposes modifications to the generic network cost function which is adjusted to the subtransmission networks. These modifications are located in the outage cost component, in the inclusion of the voltage sag cost component, and in the network assessment of two-dimensional time-related scenarios. More particularly, this work is focused on urban meshed topology with underground cable and overhead line connections. This type of network is well represented by the typical 110-kV Nordic subtransmission network which constitutes a realistic example in cold countries.

Furthermore, this thesis develops four modules that complement the subtransmission network assessment algorithm. The Reliability Module assesses networks in a block-layer structure from the perspective of the delivery point. The Voltage Sag Module determines the voltage sag distribution function and its severity coefficients. The Network Cost Module compiles statistical data and results from the previous modules to estimate the total network cost over a project period. As an ancillary tool, the Sensitivity Module identifies zones of low reliability within the tested network and suggests remedial actions.

The results show that this sort of subtransmission network with short and medium-length lines contains large voltage sag and outage costs. For instance, overhead networks are susceptible to meteorological phenomena, thus producing high rates of failures, interruptions and voltage sags. Conversely, underground networks are virtually immune to these, consequently resulting in an extremely low number of interruptions and voltage sags. Despite the aggregated investments, the gradual replacement of overhead networks with underground networks would most likely yield several operational benefits, including reinforcement of grid resilience and reliability, as well as supporting power quality to end-customers.

Keywords outage cost, reliability analysis, sensitivity analysis, subtransmission network, voltage sag distribution function

ISBN (printed) 978-952-60-6495-6 **ISBN (pdf)** 978-952-60-6496-3

ISSN-L 1799-4934 **ISSN (printed)** 1799-4934 **ISSN (pdf)** 1799-4942

Location of publisher Helsinki **Location of printing** Helsinki **Year** 2015

Pages 198 **urn** http://urn.fi/URN:ISBN:978-952-60-6496-3

A! Aalto-yliopisto

Tiivistelmä

Aalto-yliopisto, PL 11000, 00076 Aalto www.aalto.fi

Tekijä
Bruno Jorge de Oliveira e Sousa

Väitöskirjan nimi
Luotettavuus silmukoitujen suurjännitteisten jakeluverkkojen suunnittelussa

Julkaisija Sähkötekniikan korkeakoulu

Yksikkö Sähkötekniikan ja automaation laitos

Sarja Aalto University publication series DOCTORAL DISSERTATIONS 167/2015

Tutkimusala Sähköverkot ja suurjänniteteknikka

Käsikirjoituksen pvm 11.08.2015 **Väitöspäivä** 17.11.2015

Julkaisuluvan myöntämispäivä 14.10.2015 **Kieli** Englanti

☐ **Monografia** ☒ **Yhdistelmäväitöskirja (yhteenveto-osa + erillisartikkelit)**

Tiivistelmä

Suurjännitteinen jakeluverkko yhdistää kanta- ja jakeluverkot. Suurjännitteisellä jakeluverkolla on monia sähkön jakeluun vaikuttavia ominaispiirteitä. Monissa tutkimuksissa suurjännitteistä jakeluverkkoa käsitellään joko vain kantaverkkona tai jakeluverkkona. Sen vuoksi suurjännitteistä jakeluverkkoa on käsiteltävä ja mallinnettava sen erityispiirteitä tarkastellen.

Tässä tutkimuksessa esitetään muutoksia verkon geneeriseen funktioon, joka muodostetaan suurjännitteisiin verkkoihin. Muutoksia tehtiin keskeytyskustannuksen lohkoon, lisättiin jännitekuoppakustannuksen lohko ja verkon analyysi simuloitiin kahdella aikasuureella, jotka olivat jaettu skenaarioiden mukaan. Tässä väitöskirjassa keskitytään silmukoituihin kaupunkiverkkoihin, joissa on sekä maakaapeleita että avolinjoja. Hyvä esimerkki tällaisesta verkosta on silmukoitu 110-kV pohjoismaalainen suurjännitteinen jakeluverkko.

Tämän lisäksi tässä väitöskirjassa kehitetään neljä moduulia, jotka yhdessä sisältyvät suurjännitteisten jakeluverkkojen analyysin algoritmiin. Luotettavuus-moduuli arvioi verkkoja lohkokerrosrakenteessa suurjännitteisen jakeluverkon kuormapisteen kohdalta. Jännitekuoppa-moduuli määrittelee jännitekuopparakennefunktion ja sen vakavuuskertoimen. Verkkokustannus-moduuli kerää tietoja ja tuloksia edellisiltä moduuleilta ja laskee verkon kokonaiskustannukset projektien pitoaikana. Apuvälineenä herkkyys-moduuli tunnistaa matalan luotettavuuden alueita testatussa verkossa ja ehdottaa mahdollisia korjauksia.

Tulokset osoittivat, että tällaiset lyhyitä johtoja sisältävät suurjännitteiset jakeluverkot aiheuttavat suuria jännitekuoppa- ja keskeytyskustannuksia. Avolinjat ovat alttiina säätilojen vaikutuksille, jotka saavat aikaan korkeita keskeytys-, katko- ja jännitekuoppamääriä. Sitä vastoin maakaapeleihin sääolosuhteet eivät vaikuta ja sen takia keskeytyksiä ja jännitekuoppia on erittäin vähän. Huolimatta investointikustannuksista asteittainen siirtyminen avoverkosta maanalaisiin kaapeleihin sisältää useita etuja. Tämä mm. lisää verkon kestävyyttä ja luotettavuutta sekä parantaa sähkön laatua loppuasiakkaille.

Avainsanat herkkyysanalyysi, jännitekuopparakennefunktio, keskeytyskustannus, luotettavuusanalyysi, suurjännitteinen jakeluverkko

ISBN (painettu) 978-952-60-6495-6 **ISBN (pdf)** 978-952-60-6496-3

ISSN-L 1799-4934 **ISSN (painettu)** 1799-4934 **ISSN (pdf)** 1799-4942

Julkaisupaikka Helsinki **Painopaikka** Helsinki **Vuosi** 2015

Sivumäärä 198 **urn** http://urn.fi/URN:ISBN:978-952-60-6496-3

Acknowledgments

This work was performed in the Department of Electrical Engineering & Automation of Aalto University under the supervision of Professor Matti Lehtonen and sponsored by the Smart Grid & Energy Markets (SGEM) and the Smart Control Architecture for Smart Grids (SAGA) projects. I would like to express my sincere gratitude to my supervisor, Prof. Matti Lehtonen, who believed me by offering this incredible journey throughout the academic world and for his wise advices. I would like to extend my gratitude to my dear colleagues and personnel of the Department of Electrical Engineering & Automation in Otakaari 5 for these great five years of acquaintanceship and collaboration.

My gratefulness to Atte Pihkala, main co-author of several of my publications, who has provided me with indispensable real world perspective on my research and has always critiqued my work with eloquence and professionalism. And to my dear colleagues John Millar and Muhammad Humayun, also co-authors of mutual research, with whom I spent several moments of fruitful discussions and ideation on the development of my research and academic skills. Also to John Millar who generated the figure on urban distribution network topologies.

À minha família, meu pai Jorge que sempre me é fonte de inspiração, minha mãe Nilma, minha irmã Laura Uacila e meu irmão Luís Felipe, que sendo de perto ou de longe incondicionalmente sempre me apoiaram nesta longa caminhada com muito amor, suporte e entendimento. Dedico esta tese também ao meu primo Maurício Araquam de Sousa, que me é exemplo genuíno de competência, e aos membros das famílias Oliveira e Souza.

Special thanks to my great friends Adalgisa Santos, Adriana Chis, Alexey Zhukovskiy, Cintia Kawai, Evisa Collaku, Filipe Oliveira, Flavia Restitutti, Juho Rukkila, Márcio Bispo, Markus Laitala, Mehrnaz Farzam Far, Mehrnoosh Farzam Far, Reetta Peltola, Simon Le Roux and Veera Yliniemi who were indispensable part in this journey here in Finland motivating me with positive vibes. My special thanks to my dear friend Anita Bisi who not only checked the translation of the abstract of this thesis, but also motivated me in the course of learning Finnish language, and to Patrik Wikman for his motivation and support. And finally, to Anya Siddiqi, John Millar, Patrik Wikman, Pirjo Heine and William Martin for helping with the language check of this thesis.

Kiitos teille ystävyydestänne ja tuestanne!

Espoo, October, the 22nd, of 2015
Bruno Jorge de Oliveira e Sousa

Index

Abstract iii
Tiivistelmä v
Acknowledgments vii
List of Publications xi
Author's Contribution xiii
List of Symbols xv
List of Abbreviations & Terminology xix
I. Introduction 1
I.1 Literature 2
I.2 Research Problem Formulation 4
I.3 Objectives 6
I.4 Contributions 7
II. The Network Cost Assessment & Subtransmission Networks 11
II.1 The Subtransmission Networks 11
II.1.1 The typical 110-kV Nordic subtransmission network 12
II.1.2 The Nordic urban distribution networks 14
II.2 General Considerations 17
II.2.1 Generation and combined heat & power (CHP) 17
II.2.2 Seasons & meteorological phenomena 19
II.3 The Proposed Cost Function for Subtransmission Networks 20
II.3.1 Assessment into scenarios 21
II.3.2 The Network Cost Module 23
III. The Reliability Assessment 31
III.1 The Three-Layer Reliability Assessment of Subtransmission Networks 31
III.1.1 Component Clustering 33
III.1.2 Blocks 34
III.1.3 Layers 39
III.1.4 Delivery points 42

III.1.5 Other concepts 43
III.1.6 Expansion to distribution network assessment..................45
III.2 The Reliability Module..49
III.3 The Sensitivity Analysis 54
IV. The Voltage Sag Assessment 59
IV.1 The Voltage Sag Distribution Model 59
IV.1.1 Considerations for the subtransmission networks 59
IV.1.2 Voltage sag propagation...62
IV.1.3 Derivation of the voltage sag distribution function 63
IV.2 The Voltage Sag Module 65
V. Discussion 69
V.1 Results & Discussion 69
V.2 Prospective Future Research on the Topic.............................78
V.3 Conclusions 78
References 81
Appendices 91
A. The Urban Nordic 110-kV Meshed Subtransmission Network Parameters...91
A.1. Inter-network & inter-substation connections...........................91
A.2. Generation Output & Load Demand..93
B. Equipment & Device Data 94
B.1. Fault statistics & related coefficients..94
B.2. General parameters..95
C. Customer Categories & Penalties 96
D. Discount Factors (k_c, k_l & k_q) 97
E. Residual Voltages from Symmetrical & Asymmetrical Faults ... 98
E.1. Residual voltages 98
E.2. Currents from symmetrical short circuits................................100
Publications I – VII

List of Publications

This doctoral dissertation consists of a summary and of the following publications which are referred to in the text by their numerals:

I. Sousa, B. J. O., Humayun, M., and Lehtonen, M. (2014). “Inclusion of voltage sag cost to underground and overhead subtransmission network planning”. *International Review of Electrical Engineering*, volume 9, issue 3, pages 548–558. ISSN: 1827-6660.

II. Sousa, B. J. O., Pihkala, A., and Lehtonen, M. (2014). “Comparison of voltage sag and outage costs in urban meshed 110-kV subtransmission network planning”. In *the 5th IEEE PES Innovative Smart Grid Technologies Europe* (ISGT 2014). Istanbul, Turkey. October 12–15. ISBN: 978-1-4799-7720-8. DOI: 10.1109/ISGTEurope.2014.7028744.

III. Sousa, B. J. O., Humayun, M., Pihkala, A., and Lehtonen, M. (2014). “Three-layer seasonal reliability analysis in meshed overhead and underground subtransmission networks in the presence of co-generation”. *International Journal of Electrical Power and Energy Systems*, volume 63, pages 555–564. ISSN: 0142-0615. DOI: 10.1016/j.ijepes.2014.06.026.

IV. Millar, R. J., Sousa, B. J. O., Lehtonen, M., Pihkala, A., and Saarijärvi, E. (2015). “Impact of investment in primary substation double 110-kV busbars versus inter-primary substation backup on urban MV network topology and costs”. In *the 5th Conference on Power Engineering, Energy and Power Drives* (POWERENG 2015). Riga, Latvia. May 11–15. ISBN: 978-1-4799-9978-1.

V. Sousa, B. J. O., Millar, R. J., Pihkala, A., and Lehtonen, M. (2015). “Layered reliability assessment of a typical Finnish medium voltage network under multiple weather and load scenarios”. In *the 23rd International Conference and Exhibition on Electricity Distribution* (CIRED 2015). Lyon, France. June 15–18. ISBN: 2032-9644.

VI. Sousa, B. J. O., Pihkala, A., and Lehtonen, M. (2015). “Sensitivity and viability analyses of overhead and underground meshed subtransmission networks”. *International Review of Electrical Engineering*, volume 10, issue 2. pages 221–232. ISSN: 1827-6660.

VII. Sousa, B. J. O., Humayun, M., Pihkala, A., and Lehtonen, M. (2015). “Block-layer reliability assessment of distribution systems under various operating scenarios”. Submitted to the journal *IEEE Transactions on Power Systems*.

Author’s Contribution

I hereby declare that I am the sole author of this thesis. I have also the main responsibility for the contents of this thesis, including all the developed methods, analyses and simulations, as well as the writer and corresponding person of all published papers in which I am the first author.

Publication I: “Inclusion of voltage sag cost to underground and overhead subtransmission network planning”

The author proposed the method, performed the simulations and wrote the paper. The other authors commented on the pre-submission manuscript and checked the calculations.

Publication II: “Comparison of voltage sag and outage costs in urban meshed 110-kV subtransmission network planning”

The author proposed the topic, performed the calculations and wrote the paper. The other authors commented on the pre-submission manuscript and checked the calculations.

Publication III: “Three-layer seasonal reliability analysis in meshed overhead and underground subtransmission networks in the presence of co-generation”

The author proposed the method, performed the simulations and wrote the paper. The other authors commented on the pre-submission manuscript and checked the calculations.

Publication IV: “Impact of investment in primary substation double 110-kV busbars versus inter-primary substation backup on urban MV network topology and costs”

The author performed part of the simulations and participated in the writing of the paper. The main author wrote the paper and the other authors commented on the pre-submission manuscript.

Publication V: “Layered reliability assessment of a typical Finnish medium voltage network under multiple weather and load scenarios”

The author proposed the topic, performed the calculations and wrote the paper. The other authors commented on the pre-submission manuscript and checked the calculations.

Publication VI: “Sensitivity and viability analyses of overhead and underground meshed subtransmission networks”

The author proposed the method, performed the simulations and wrote the paper. The other authors commented on the pre-submission manuscript and checked the calculations.

Publication VII: “Block-layer reliability assessment of distribution systems under various operating scenarios”

The author proposed the method, performed the simulations and wrote the paper. The other authors commented on the pre-submission manuscript and checked the calculations.

List of Symbols

a	Fortescue operator
a	unavailability of block a [p.u.]
A	unavailability of block A [p.u.]
b	unavailability of block b [p.u.]
B	unavailability of block B [p.u.]
b_{Tsw}	unavailability of block b between zero and the switching time [p.u.]
c	unavailability of block c [p.u.]
C	unavailability of block C [p.u.]
$\mathrm{c_c}$	voltage sag penalty per event according customer category [€/sag]
C_{cap}	capital cost [€]
C_{loss}	losses cost [€]
C_{netg}	general objective network cost function [€]
C_{netp}	proposed objective network cost function [€]
C_{out}	outage cost [€]
$C_{o\&m}$	operational and maintenance cost [€]
c_{repair}	cost of repair [€/fault.unit]
C_{sag}	voltage sag cost [€]
c_{teamh}	cost of technical team, including salaries and related costs [€/h]
$\mathrm{cic_e}$	customer interruption cost for non-delivered energy [€/kWh]
$\mathrm{cic_p}$	customer interruption cost for non-delivered power [€/kW]
d	unavailability of block d [p.u.]
D	unavailability of block D [p.u.]
h_{pL}	price for equipment load losses in the considered scenario [€/kW.scenario]

h_{p0}	price for equipment no-load losses in the considered scenario [€/kW.scenario]
m_x	slope of the independent variable x (block x) [p.u.]
N	number of substations in the test network
N_{annual}	number of annual scenarios
n_c	number of end-customers per unit of power according customer category [cust/MW]
N_{daily}	number of daily scenarios
$N_{inter.substi}$	number of inter-substation connections in substation i
n_{trip}	number of trips given fault duration
N_s	total number of scenarios
P_a	generated/transferred power in block a [kW]
P_A	generated/transferred power in block A [MW]
$P_{a\|b}$	share of fault type a given fault duration b
P_b	transferred power through block b [kW]
P_B	transferred power through block B [MW]
P_c	transferred power through block c [kW]
P_C	transferred power through block C [MW]
P_{cc}	sagged load according customer category per substation [MW/subst]
P_{cap}	power transfer capacity [MW]
P_{curtq}	curtailed load at risk state q [MW]
P_d	generated/transferred power in block d [MW]
P_D	generated/transferred power in block D [MW]
P_{dem}	demanded load [MW]
P_{demi}	demanded power for the considered substations [MW]
$P_{demisec}$	demanded power for the test secondary substation [kW]
P_{demF}	demanded power for the test feeder [kW]
P_{dg}	generated power by the local DG [kW]
P_{demN}	demanded power for the considered network [MW]
P_{demx}	demanded power at given block [MW]
p_{els}	price of energy for load losses [€/kWh.scenario]

p_{e0s}	price of energy for no-load losses [€/kWh.scenario]
$P_{inter.feed}$	generated/transferred power by each inter-feeder connection with power injection capacity [kW]
$P_{inter.net}$	generated/transferred power by each inter-network connection with power injection capacity [MW]
P_L	equipment nominal load losses [kW]
$P_{loc.gen}$	generated power by the local generation [MW]
P_{nsb}	equivalent power not supplied directly connected to the transformer bay [kW]
P_{nseq}	equivalent power not supplied [kW]
p_{pl}	price of power for load losses [€/kW.a]
P_{pns}	probable power not supplied [MW]
P_{ps}	probable power supplied [MW]
P_0	equipment nominal no-load losses [kW]
pf_s	power factor in the considered scenario
q_s	number of hours in the considered scenario [h/scenario]
r_{eq}	equivalent repair time [h/fault]
R_q	probability of the risk state q
S_{avg}	average power in the considered scenario [MVA]
S_N	nominal rated power [MVA]
S_p	peak power in the considered scenario [MVA]
T_i	average outage time [h]
T_p	peak utilization time [h/a]
T_s	given scenario duration [h]
T_{sw}	switching time, distribution [h]
T_{SW}	switching time, subtransmission [h]
U	normalized unavailability over the scenario [p.u.]
U_{eq}	equivalent unavailability [h/scenario]
$\mathbf{u_{pri}}$	residual voltage vector at the transformer primary terminals [p.u.]
U_s	unavailability at given scenario [h]
$\mathbf{u_{sec}}$	residual voltage vector at the transformer secondary terminals [p.u.]

U_i	unavailability of layer i [p.u.]
U_I	unavailability of layer I [p.u.]
U_{ii}	unavailability of layer ii [p.u.]
U_{II}	unavailability of layer II [p.u.]
U_{iii}	unavailability of layer iii [p.u.]
U_{III}	unavailability of layer III [p.u.]
v_i	post-fault residual voltage distribution in substation *i* [occ./season]
v_{ir}	total inter-substation post-fault residual voltage rate [occ/season]
$v_{net}\|_{tolerance}$	post-fault residual voltage sag below the tolerance [occ/season]
α	failure rate coefficient at given day scenario
β	failure rate coefficient at given year scenario
ε_p	power transfer utilization rate
η	ratio between peak utilization time and year
θ_x	angle of incline of the slope m_x [$^\circ$]
λ_b	transformer bay failure rate [fault/scenario]
λ_e	average annual failure rate [failure/unit.a]
λ_{eq}	equivalent failure rate [fault/scenario]
Λ_i	equivalent interruption rate at the delivery point [interr/scenario]
$\lambda_{inter.substir}$	failure rate in the inter-substation connection *ir* [occ/season]
λ_{ir}	total inter-substation failure rate [occ/season]
μ_i	voltage sag rate per substation [sag/season]
μ_{net}	network voltage sag rate [sag/season]
ρ_{a}	severity coefficient for fault type a
φ	phase-shift angle of transformer class [rad]
$[A]$	transform matrix of the transformer in focus
$[T]$	sequence-to-phase component transform matrix
$[T]^{-1}$	phase-to-sequence component transform matrix

List of Abbreviations & Terminology

AC	alternating current
CHP	combined heat and power
cm	common mode
DAR	delayed auto-reclosure
DG	distributed generation
DSO	distribution system operator
EHV	extra-high voltage, 400-kV† equipment, transmission network
HV	high voltage, 110-kV† equipment, subtransmission network
LC	load curtailment
LV	low voltage, 0.4-kV† equipment, [secondary] distribution network
MV	medium voltage, 20-kV† equipment, [primary] distribution network
n.c.	normally closed (logical state)
n.o.	normally open (logical state)
NTOA	network topology optimizing algorithm
OHL	overhead line
PCC	point of common coupling
RAR	rapid auto-reclosure
RESs	renewable energy sources
RMS	root mean square
TSO	transmission system operator
UGC	underground cable

†*Typical operational voltage levels in Finland* [Hei03].

Bay	the interconnection of related equipment forming three types of bays: feeder, line or transformer bay
Component	the smallest piece of equipment considered in the reliability assessment
Delivery point (distr.)	the low-voltage side of the secondary substation
Delivery point (subtr.)	the medium-voltage side of the primary substation
Distributed generation	generation units connected to either the low-voltage or medium-voltage distribution networks
End-customer	the single customer consuming electricity at the end point of any part of the power system hierarchy being directly connected to the low, medium, high or extra-high voltage network.
Faulted equipment	piece of equipment or device that is out of service due to faults or non-scheduled purposes
Fault duration	classification according to the duration of the fault (momentary, temporary and permanent)
Fault type	classification according to the type of fault (single phase-to-ground, phase-to-phase, two phase-to-ground and three phase)
Fixed cost	cost independent of annual load growth
Healthy equipment	piece of equipment or device that operates according to its functions
Interruption	"*the loss of electric power supply to one or more loads*" [Iee98], "*this does not include sags, swells, impulses, or harmonics*" [Iee12]
Inter-feeder	connections between the feeder in focus and adjacent primary substations directly or indirectly connected to this feeder and DG within this feeder
Inter-network	connections between the network in focus and adjacent subsystems via step-up transformers (generation), line connections (same voltage level) and step-down transformers (from the grid upstream)
Intra-network	all devices and equipment within the network in focus
Inter-substation	connections between the considered substation and adjacent substations within the network in focus at the same voltage level (for both primary and secondary substations)
Intra-substation	line and equipment connections within the considered substations (for both primary and secondary substations)

Line	all line types (including underground cables and overhead lines) with their respective protection components
Local generation	generation units directly connected to the tested substation
Outage	"*the loss of ability of a component to delivery power*" [Iee12]
Peak short circuit current	the peak short-circuit current (I_p) is "*the maximum possible instantaneous value of the possible (available) short-circuit current*" [Iec01]
Primary substation	HV/MV (110/20-kV) substation
Remote generation	generation units out of the considered substation, but still within the tested network
Risk state	state at the risk assessment that incorporates total or partial load curtailment, at calculated probability and curtailed load
Secondary substation	MV/LV (20/0.4-kV) substation
Short-circuit current	the initial symmetrical short-circuit current (I_k'') is "*the RMS value of the AC symmetrical component of a possible (available) short-circuit current applicable at the instant short circuit if the impedance remains at zero-time value*" [Iec01]
Substation	electrical substation with transformers in the same network, *i.e.*, at the same primary voltage level
System	collective of associated components, in this context, the main physical subdivisions of the power system (distribution, generation, subtransmission and transmission)
Switching time	parcel of time when "*a switching operation is required due to a component failure until that switching operation is completed*" [Iee98]
Unavailability	parcel of time in which a system or a component is out of service, over a given period
Variable cost	cost depending on annual load growth (with linear or quadratic relation)

I. Introduction

Fueled by the technological possibilities, environmental and socio-political concerns in the current world order, recent achievements have shifted the power system towards a more complex, multivalent, coordinated and interconnected infrastructure [Ene15b],[Eur11],[Fin15a],[Gud11],[Mac10],[Mil12]. Indeed, these new aspects also extend to subtransmission networks which are in the intermediate position connecting the two major systems of the grid and are often located within the urban environment.

Since reliability evaluation with probabilistic techniques first started in Power Systems, several studies have investigated important parts of the power system utilizing a number of methods and approaches [Bil01]. Since then, relevant studies [Mil12],[Jal14b],[Roc15] have incorporated distributed generation (DG) into risk analysis and have implemented economic assessment. More recently, the concept of the smart grid [Gel09],[Ham15],[Jär11],[Men14],[Uni14] has also reshaped and enriched reliability analysis particularly due to the advent and popularization of new technologies, such as storage systems, electric vehicles, generation from renewable resources, as well as revolution in automation, communication, control and protection. In addition, the power system is currently experiencing a major shift from the traditional monopolized structure to non-hierarchical values in which the individual end-customers play an active role in a deregulated and more competitive power market [Eur13],[Nor15]. These new global achievements have brought a multidisciplinary aspect to power system assessment, thus resulting in an urge to include the effect of non-technical features on the system and local performance.

Moreover, the present welfare state is implementing tighten improvements in measuring and regulation, with particular concern to power quality issues [Bol06], prioritizing the end-customer. Grid operators and utility companies have been gradually improving their networks and apparatus in order to supply electricity with quality determined by local policy [Dug96]. In order to do that, it is important to consider the influence of power quality constraints which have been originated by technical and operational as well as external factors intrinsically related to each part of the power system. These factors must be transcribed into monetary figures in order to assess the operation performance and planning of networks.

I.1 Literature

Reliability evaluation techniques combined with economic assessment incorporates several benefits to network planning [Haa13],[Hyv08],[Kaz11],[Lak03],[Li11],[Mil12],[Roc15],[Saa13],[Sal12],[Wil10]. Appropriate parameterization allied to specific equipment and device modelling reinforces the accuracy and validity of this type of study. Moreover, attributing monetary burden from voltage sags introduces a new comprehensive aspect to subtransmission network assessment. Together, these and related features describe and decode an objective subtransmission network cost function.

Subtransmission network reliability analysis with weather-related constraints & sensitivity analysis

Under the classical hierarchical level in adequacy assessment [Bil94], several studies have focused on composite systems [Gau10],[Saf14],[Und06],[Vél10], having described techniques to estimate customer-oriented reliability indices employing a number of different approaches. One classic approach for calculating system reliability is to use Monte Carlo simulation [Bil04],[Bil94],[Bil96]. In addition, the association of this simulation with other techniques and approaches, for instance, the Markov Model and demand response, have proven to be successful when assessing networks and their components [Ama10],[Abd14],[Gre13],[Hum13],[Pin11],[Sil07].

The smart grids, however, integrate the three functional zones (generation transmission and consumption) within each of the hierarchical levels, particularly when transitioning to islanded-mode is allowed [Kah12]. Similarly, the same occurs to the modern urban subtransmission networks. In these, inspection is required in a differentiated fashion. This is due to their network topology, the intermediate position in the power systems, the increasing dependency on local generation, the type and the arrangement of substation. In addition, in many situations, these networks present both overhead lines (OHLs) and underground cables (UGCs). Moreover, in urban areas, as in the Nordic countries, subtransmission networks include several categories of customers in costly real estate with high penalties and customer interruption costs [Hei02],[Kjø08],[Küf13],[Küf15a],[Küf15b].

In acknowledgement of these factors, this thesis classifies failures according to their possible category of causes, weather conditions and instant of the day and of the year, thus distributing the collected data to the specific case of this type of network. This thesis regards, firstly, generation within the network, such as combined heat and power (CHP); secondly, connections to adjacent subsystems (HV/HV connections) and to the transmission grid (EHV/HV connections); thirdly, substation arrangement; and, fourthly, power flow scenarios in different seasons to provide a multivalent reliability analysis.

Similar works have been proposed for subtransmission systems focusing on reliability assessment [Goe05],[Goe07],[Mar13],[Per13],[Sha13]. These studies describe reliability techniques at substation level using a branch-node model [Mar13], algorithms on emergency response to faults [Per13] and on penetration of distributed generation [Jal14a],[Sha11]. However, they do not include seasonal and weather variations nor model components in function of time and scenario, thus ignoring differences between underground and overhead networks.

The reliability technique developed in this thesis is structured on four blocks: (i) adjacent connections; (ii) infeed (distinguished by UGCs and OHLs); (iii) substation; and (iv) local generation. Featuring each of these blocks, arranged into layers, by a number of indices at the considered delivery points, the developed technique assesses both the local and the system reliabilities and identifies areas of vulnerability (denominated as layer) within the network under analysis. This technique returns equivalent partial parameters in these areas for further comparison and provides input for the economic assessment to plan and operate subtransmission networks.

The reliability assessment incorporates two modules as part of the developed technique: the Reliability Module and the Sensitivity Module. The first serves as a pillar for a reliability-centered network planning. The latter determines variations at chosen network operation points and detects zones of low availability. From that, the Sensitivity Module maps the zones of low reliability and proposes remedial actions in the prospective zones of the test network. Altogether, these two modules assess the effect of both low and high-order failures in all parts of the network by investigating the calculated reliability indices at the structures of this model. This occurs because of the several stratifications of the test network and the multi-leveled analyses. The two modules jointly converge the network on focus into the optimal region from a reliability-cost perspective. Moreover, this proposed technique is supported by detailed data collected from regional utility companies and operators.

Voltage sag distribution function in meshed subtransmission networks

Short interruptions and voltage sags constitute significant impact on modern network planning [Bro09],[Cha07]. These power quality issues are of much concern particularly for a meshed and interconnected network where the propagation of voltage sags reaches wider areas. These events have, in principle, originated from faults of different types and fault-clearing maneuvers in other parts of the system [Hei05],[Nai12]. In urban meshed subtransmission networks, voltage sags propagate through multidirectional paths and, due to their network circuital nature including relatively short lines, severe voltage sags are perceived in a broader area by high-penalty customer categories [Bol00],[Olg05]. Moreover, in these, the connections with downstream networks, *i.e.*, the transformers, form the key element in voltage sag propagation to the end-customer [Aun06],[Kan08].

The economic impact of short interruptions on voltage-sensitive equipment can be extremely negative, as, for instance, equipment involved in industrial and commercial processes, such as adjustable speed drives and electronic devices [Kar05],[Yas12]. Bollen *et al.* [Bol11] have proposed a categorization of equipment in terms of immunity to voltage sags. Notwithstanding the broad and demanding task of equating voltage sags with monetary values, penalties from these events must be accounted into the total network cost, according to customer category, in order to evaluate the benefit of the different lines and network types. A survey on losses from voltage sags and short interruptions in networks can be found in [Hei02]. [Nai12].

Previous research on the topic [Djo05],[Djo08],[Gos08],[Mok10],[Nai12] have developed a number of analytical techniques to characterize voltages under fault conditions. These techniques determine residual voltages as a function of impedance (sequence domain) and pre-fault voltages. However, neither distinguishes line types, whether overhead lines or underground cables for instance, nor the number of reclosing maneuvers which were identified in order to quantify the voltage sag rates at the delivery points. Similarly, stochastic methods [Alv01],[Juá06],[Wan10] determined the residual voltage effects in large systems. Conversely, the inclusion of voltage sag cost to the total cost function is required to provide realistic parameters when designing or upgrading network, particularly with different line types. Additionally, in the case of subtransmission networks, because of their intermediate position, it is an indispensable approach to estimate total network cost, considering parametrical differences between both UGCs and OHLs and assessing pertinent assumptions, for instance, related to weather-related failures and power flow patterns under different scenarios and seasons.

This thesis describes the Voltage Sag Module that consists of an algorithm to estimate the voltage sag rates in urban meshed subtransmission networks and includes a voltage sag cost addend to the network cost function. First, this module determines the voltage sag distribution function that quantifies voltage sag cost, considering fault types, the number of short interruptions (depending on the fault origin), neutral connections, voltage sag severity and customer category. The algorithm assumes that a large portion of the effect on the residual voltages, given the residual voltages on the primary side due to fault type, relies on the transformer. This is assumed, for the HV/MV transformer is in series with the delivery points (at both subtransmission and distribution level) and consists of a significantly larger equivalent impedance than the transfer-element from the network impedance matrix. And second, this thesis proposes the inclusion of the voltage sag cost addend to the objective network cost function. This is essential in order to accurately assess the viability of underground and overhead networks. This developed module is framed, within the algorithm proposed in this thesis, under the two-time dimension domain analysis.

I.2 Research Problem Formulation

This thesis observes the lack of a comprehensive objective cost function for urban meshed subtransmission networks that would parameterize constraints intrinsically pertaining to these networks. The goal is to combine reliability assessment, sensitivity analysis, voltage sag calculation (together with short-circuit and fault calculations) and economic assessment in urban subtransmission networks. The four-module method proposed in this thesis involves important features intrinsic to this class of networks in order to assist network planning and operation. In order to tackle this, the present method improves instruments to specifically assess underground and overhead networks and their viability in the urban environment. This method includes both deterministic and probabilistic processes with a distinct approach in quasi-sequential analysis and can be coupled to network planning algorithms and probabilistic techniques, such as the Monte Carlo methods.

Table I summarizes the main aspects developed in previous research within the fields of reliability-based network planning and reliability assessment of subtransmission networks. The method described in the following chapters involves a number of features not observed in the listed references in addition to a sensitivity module that assists in the identification of low-reliability zones. This method is expressed in the last row of Table I.

TABLE I. OVERVIEW OF APPROACHES TO RELATED NETWORK RELIABILITY ASSESSMENT

Reference	Network in focus	Main techniques involved	Cost assessment?	Weather considered?	Volt. sag distribution & penalty?	Local generation?	Resolution of the analysis
[And09]	*distribution & subtransmission*	*Monte Carlo*	*yes* [a]	*no*	*no*	*yes*	*year*
[Ama10]	*composite*	*Monte Carlo*	*no*	*no*	*no*	*HL2* [b]	*year*
[Goe05]	*subtransmission*	*reliability-worth indices*	*yes* [a]	*no*	*no*	–	–
[Gon13]	*composite*	*Cross-entropy & Monte Carlo*	*no*	*no*	*no*	*HL2* [b]	*year*
[Haj14]	*composite distribution*	*reliability block diagram*	*no*	*no*	*no*	*no*	*year*
[Jal14a]	*subtransmission*	*MINLP* [c]	*yes* [d]	*no*	*no*	*yes*	*1500 h*
[Kil14]	*composite*	*EMPS* [e]	*no*	*no*	*no*	*yes*	*10400 scenarios in 50 years*
[Mar13]	*subtransmission*	*branch-node*	*no*	*no*	*no*	*no*	–
[Roc15]	*distributed generation*	*Monte Carlo*	*yes* [g]	*yes*	*no*	*yes*	–
[Sha13]	*subtransmission*	*DCGA & LP* [f]	*yes* [d]	*no*	*no*	*yes*	*year*
[Sil07]	*composite*	*Monte Carlo*	*no*	*no*	*no*	*yes*	*year*
Proposed method	*subtransmission & distribution*	*three-layer technique*	*yes*	*yes*	*yes*	*yes*	*1 hour*

*Fields in blank correspond to not observed feature
[a] Only expected cost of interruption
[b] Hierarchy level 2 (transmission and generation)
[c] Mixed integer non-linear programming
[d] Neither outage cost nor voltage sag cost are considered
[e] Multi area power-market simulator
[f] Decimal codification generic algorithm & linear programming
[g] Implicitly

The thesis utilizes and parameterizes the collected databases and statistics for distribution and subtransmission equipment from [Ant03], [Ene15a], [Eur14b], [Hei03], [Hyv08], [Kaz11], [Kjø06] and [Ren08], in addition to unpublished data from the local utility company.

I.3 Objectives

Motivated by the enhancing cost-benefit ratio posed by UGC in high-voltage systems and the inexistence of such comprehensive evaluation for this section of the power system, this study assesses the cost drivers and estimates the monetary and non-monetary aspects of engaging HV underground cables and gas-insulated substation equipment (GIS) in opposition to HV overhead lines and air-insulated substation equipment (AIS). The basis of this study is on the adaptation of the generic network cost function to urban meshed subtransmission networks supported by specific reliability and risk assessments and the determination of a voltage sag distribution function. Additionally, as an important feature of this research, sensitivity analysis with diagnosis based on decision making aspects assesses subtransmission networks point-by-point and proposes multi-level remedial actions.

The thesis proposes a comprehensive network analysis method described as a multi-module algorithm for underground and overhead urban subtransmission networks. The method is framed in the objective network cost function regarding technical, operational and external conditions intrinsically related or affecting to this part of the power system. The proposed economic evaluation method assesses networks in a two-dimensional time-domain (divided into daily and year scenarios) analysis that delineates with adjustable resolution the dynamic changes in the tested network grounded in specific statistical data collected by local grid operators. These changes originated from meteorological, operational and technical constraints, and their economic impact is counted to estimate the total network cost given project requirements.

The inclusion of weather-related phenomena and the subdivision into several scenarios are both crucial for this investigation; the collection of statistical data and their interpretation must be performed acknowledging the dynamics of this type of network. This encompasses the multidirectionality of the power flows as well as the daily and yearly variations in both load demand and local generation output, included in the modeling of network equipment.

The method developed herein is suitable for the planning and operation of subtransmission networks as well as for resolving optimization issues. In the operation conditions, this method diagnoses and assists in the refurbishment of the existing network, while in the planning and optimization of networks, it develops a new network based on the stipulated project requirements. The formulation and requirement enunciation of each module and process of this method is detailed in the following chapters.

The thesis is organized into five chapters. *Chapter I* integrates the literature review on the topics developed through this thesis; the formulation of the research problems and the framework of this study; and the contributions of this research. *Chapter II* describes the network cost function with its components and includes the parameterization and considerations for the developed algorithm for subtransmission networks and their connected distribution networks. *Chapter III* develops the reliability assessment and how it is connected to the other parts of the algorithm. *Chapter IV* delineates the voltage sag distribution function and from that the voltage sag cost component. *Chapter V* concludes by highlighting the main findings and the prospective alternatives in the planning of networks. The Appendices compile statistical data and necessary formulation in the course of this research and, at the end of this work, is found the collection of seven publications upon which this thesis was based.

I.4 Contributions

The developed method is divided into four modules. The Reliability Module processes data collected by the local utility for the network in focus. This module embodies a novel reliability assessment technique structured in blocks and layers that identifies and groups equipment and devices with similar function from the perspective of the delivery point. This eliminates the number of states in the risk analysis, thus being able to assess the effect of significantly higher-order failures (not only N-1 failures). In addition, this module identifies the critical zones, denominated layer, where partial reliability indices and values are calculated, and provides input for the sensitivity analysis. Employing the same block-layer structure of the latter module, the Sensitivity Module determines the influence of each block on the availability at each delivery point for the system operation point. This module assesses substations according to their type and addresses possible remedial actions to performance from the perspective of each of them. This module can be utilized as an ancillary tool or in the iterations of a network planning algorithm in order to optimize reliability and minimize total network costs.

The Voltage Sag Module determines a voltage sag distribution function for urban meshed subtransmission networks, given the employed protection philosophy and network parameters. The method herein developed incorporates the calculation of symmetrical faults for the test network to obtain the voltage sag distribution function. This minimizes computational time and eliminates the need for more specific details about the network, such as, for instance, the zero-sequence network, and a larger number of calculations to obtain the unsymmetrical faults for each scenario. Additionally, the module requires, nevertheless, information about the transformer connections.

From this distribution function, the voltage sag costs are estimated at the considered delivery points. However, it should be added that due to the great number of fault possibilities (type, duration, position, network parameters) and their effect on adjacent feeders [Sou15], it is virtually impossible to obtain an accurate voltage sag distribution function. Nevertheless, this is possible when considering the features of urban meshed subtransmission networks resulting in negligible differences, as shown in **Publication I**.

From these three modules, the Network Cost Module calculates the total network cost. The thesis proposes the introduction of the voltage sag cost to the total subtransmission network cost. It shows, thoroughout the manuscript, the propagation of voltage sags in HV networks to the end-customers, and the adaptation of the outage cost to the subtransmission networks. Moreover, the thesis introduces the scenario-based bidimensional time analysis, determined by the collected statistical data, weather-related failures, generation and load profiles as well as other relevant parameters.

This study is further expanded to distribution networks with appropriate adaptation for topologies and features intrinsic to this part of the network and considers the impact of local and distributed generation. This was possible due to the comprehensive reach of results observed in this analysis at subtransmission level. Altogether, the analyses in this study are centered around the end-customers (at LV, MV and HV levels), represented by the respective delivery points, and offer partial, substation and system reliability and power quality indices, thus thoroughly describing performance in all parts of the network.

Contributions in the publications of this thesis

The main contributions and findings from each of the seven publications of this article-based thesis are, as follows:

Publication I determines a voltage sag distribution function for urban meshed subtransmission networks, utilizing only information related to the network in focus and considering type of line connections, number of trippings per fault and weather-related failures, and estimates the voltage sag cost. Results suggested that due to the length, position and topology of this type of network, the developed voltage sag distribution function is valid and can be extended to networks fulfilling this description.

Publication II compares voltage sag cost and outage cost in the example of the 110-kV subtransmission network of Helsinki, regarding power flow patterns during the base year influenced by combined heat and power (CHP) plants. This study confirmed the high magnitude of the voltage sag costs versus the outage costs in an existing network.

Publication III structures a block-layer reliability analysis employed in urban meshed subtransmission networks to identify regions of low reliability and considers a comprehensive set of data particularly collected for these types of networks. The three-layer reliability method showed that the substation equipment, in many situations, constitutes the most prospective areas for improving reliability and that underground cables (as well as GIS equipment) support grid resiliency throughout the base year regardless of the weather conditions.

Publication IV assesses the influences of primary substation reliability on MV network planning mainly focusing on the differences originating from single and double-busbar HV substations versus the inclusion of backup from adjacent HV substations. This customer-oriented analysis favored the installation of underground cables and remote disconnectors in opposition to the less reliable and slow-operating devices.

Publication V applies the layered reliability assessment tool to feeders from MV networks generated by the network topology optimizing algorithm (NTOA) sampled in an urban area of Helsinki. This study indicated that distributed generation directly connected to the MV networks might impose technical constraints particularly during faults in the MV feeder and adds marginal reliability support.

Publication VI aims at improving the line connections in subtransmission networks, backed by economic assessment. Using the sensitivity analysis of the three-layer reliability tool, it addressed the considerable influence of number and type of inter-substation connections on substations without local generation. The publication also shows the relatively low influence of the same on substations with generation. The viability analysis confirmed that laying underground cables constitutes a costlier alternative, yet it is more robust and resilient. The use of overhead lines inserted higher power losses and a higher number of voltage sags both locally, in the sampled substation, and systematically, in the entire network.

Publication VII delineates a block-layer reliability algorithm applied to distribution systems adding principles from the three-layer reliability method. The reliability assessment in distribution systems is quite particular and negligible features to other parts of the power system must be acknowledged in this, such as the protection philosophy. This study indicates that the MV feeders compose the most sensitive area to improve reliability independently of the network topology. The reliability assessment of several network topologies with the same feeder lengths indicated an enormous variation in terms of the unavailability at the delivery points, ranging from 20 min/subst.a up to 180 min/subst.a.

II. The Network Cost Assessment & Subtransmission Networks

II.1 The Subtransmission Networks

By definition, the subtransmission network is the part of the power system connecting transmission to the distribution networks [Bro09],[Fin00],[Wil04]. It is mainly characterized by its function rather than current type (AC or DC system), magnitude of power transferred or voltage levels (although subtransmission voltage level ranges from a dozen kilovolts up to hundreds of kilovolts in AC systems being able to transferring large amounts of power) [Fin00],[Gön08],[Nor11]. In the Nordic countries [Fin15b],[Nor11], this spans from 110 kV to 220 kV for longer-distance connections, and 30 kV or over for local interconnections and urban networks. Moreover, depending on the position, subtransmission lines can be included in the distribution or in the transmission networks, as well as being operated by either the local DSO or the TSO [Nor11].

The urban subtransmission networks differ in a number of ways. First, they are located in urban areas, in many situations as partially or fully underground networks, thus characterized by looped (radially-operated) and meshed topology with short/medium-length lines. Second, this type of subtransmission can cluster as a system due to its complexity, the existence, in many cases, of local generation and the number of inter-network interfaces and connections, thus constituting a relatively autonomous niche (in same situations, as in Helsinki in the past, it can operate in islanded mode). These factors imply a clear independency from adjacent systems and require individualized operational practices and specific tailor-made assessments (described throughout the thesis). Finally, these types of networks are connected to a substantial number of customers (at LV, MV and HV levels), many of them with a high level of priority, such as hospitals, public services and industry.

As examples of urban subtransmission networks in cold regions, Calgary, Canada [Alb14], for instance, is fed by 240/138-kV transformers and contains 69-kV and 138-kV connections as subtransmission network; Berlin and Hamburg, Germany [Pih06], are supplied by 380/110-kV transformers and embody significant participation of local generation (50 % and 20 % respectively of the total load demand). The Canadian network consists of meshed topology, while the

German ones consist of radially-operated topology. The city of Stockholm, Sweden, currently experiences alterations in its electric system [Sto15]. The 220-kV and 70-kV networks link the 400-kV connections to the distribution network within the city area. The subtransmission network of the city of Helsinki, Finland, incorporates 110-kV UGCs and OHLs in meshed topology serving over 360,000 customers [Hel15],[Pih06]. Additionally, the five examples embody local generation (directly connected to the subtransmission) and CHP plants.

II.1.1 The typical 110-kV Nordic subtransmission network

The typical 110-kV Nordic subtransmission network is the test network used in this thesis and in most of the produced publications. It is based on urban meshed subtransmission networks in the Nordic countries and, further, based on the IEEE 14-bus and 30-bus test networks [Als73],[Bak13],[Sou13],[Sou14].

This network was created to model a subtransmission network that has meshed topology accounting for a considerably large rate of installed UGCs and UGCs and OHLs assembled in parallel. In addition, it includes large CHP plants with varying power outputs typical of cold regions throughout the base year. These features support high grid resiliency to meteorological phenomena. Furthermore, this test network includes several inter-network connections to different adjacent subsystems and contains substations interconnected by two to ten lines.

Figure 1 depicts the diagram of the typical 110-kV Nordic subtransmission network with its twenty five primary substations. It is comprised of four EHV/HV inter-network connections constituted by 400/110-kV transformers; three HV/HV connections to adjacent subtransmission networks (being the two in substations 1 and 3 negligible, for they are not able to inject power into this test network); and three MV/HV connections formed by CHP plants. **Appendix A.1** covers the relevant information for these connections, including line length, rated powers and type of connections. **Appendix A.2** incorporates the load profile and generation output.

This test network is designed to show large variation in reliability at both network and substation levels. One other interesting feature is the large variance and direction of the power shifted through this network in the course of a year. The average seasonal load is 486 MW in summer and 663 MW in winter. The hourly peak load reaches up to 900 MW in the base year. In addition, the local generation output varies from zero, in summer, to 890 MW, in winter. This reflects the direct influence of weather and seasonal conditions on the load profile. During summers, part of industry and services are closed, while during the winter part of the total load is directed to heat production. For simplification purposes, load curtailment actions are proportionally distributed to the delivery point load demand in this study.

Moreover, the typical 110-kV Nordic subtransmission network is comprised of UGCs and OHLs in different combinations of number of connections and the positioning of these connections. UGCs are noted for the small failure rates in comparison with other line types. Conversely, UGCs are characterized by a high repair time, for they are installed underground and access to trenches within urban areas during busy hours might be difficult. UGCs also include low equivalent series resistance and high susceptance, due to their insulation. OHLs are characterized by high failure rates and relatively low repair times. This is caused by their exposed structure. OHLs include higher equivalent series resistance and small susceptance. Line data for this test network can be found in **Appendix A.1**.

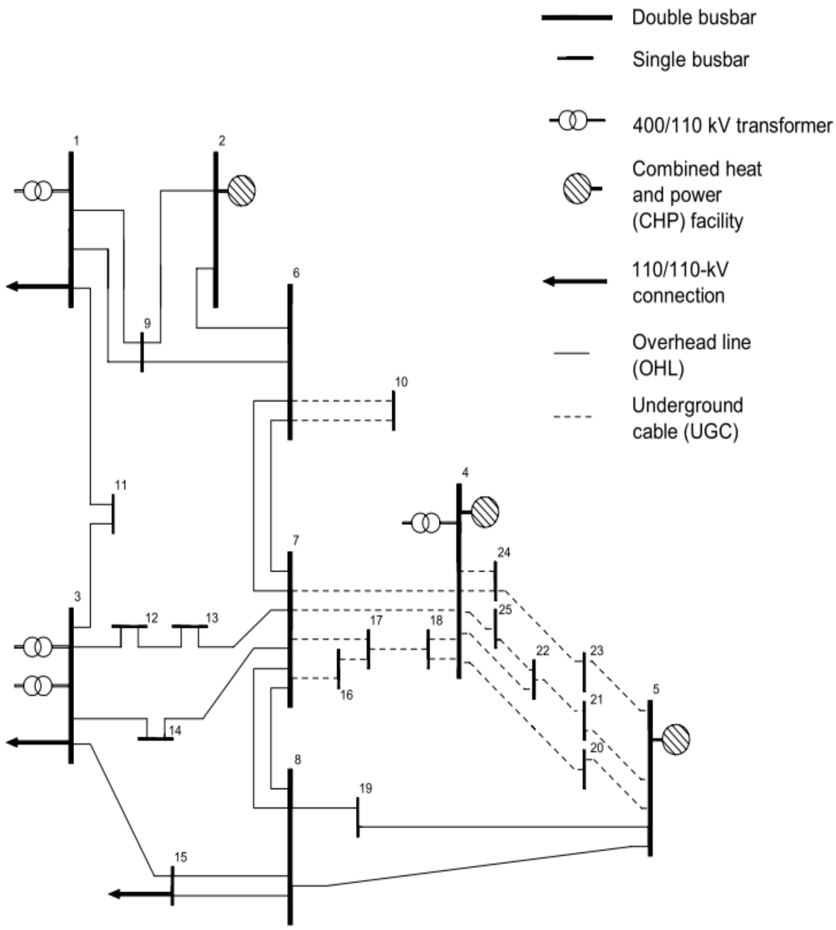

Figure 1. The test 110-kV Nordic subtransmission network based on similar networks in the Nordic region.

The HV/MV substations (primary substation)

One other essential part of this study is to schematize and model the main equipment and arrangement of the primary substations. This test network embodies two types of primary substations: single-busbar and double-busbar arrangements on the HV side.

In terms of insulation technologies, all primary substations are indoors with GIS, which is a realistic practice within urban subtransmission networks in the

Nordic countries. Figure 2 schematizes in detail the intra-substation connections in the two substation types, both of which are comprised of two-transformer bays connected to the busbar set.

Arrangements in primary and secondary substations are diverse in different parts of the power system, including the mechanisms of tripping during maintenance or fault [Cos14],[Iee98],[Moa13],[Sie14],[Won91]. In Figure 2, the MV-side is comprised of a two-section double-busbar arrangement.

The HV busbars can be divided by a normally-closed (n.c.) 110-kV disconnector operated during failures in the line or transformer bays. This study, nonetheless, considers the busbar arrangements depicted in Figures 2 and 4 to investigate substation busbar, transformer and circuit breaker influence on the delivery point in details.

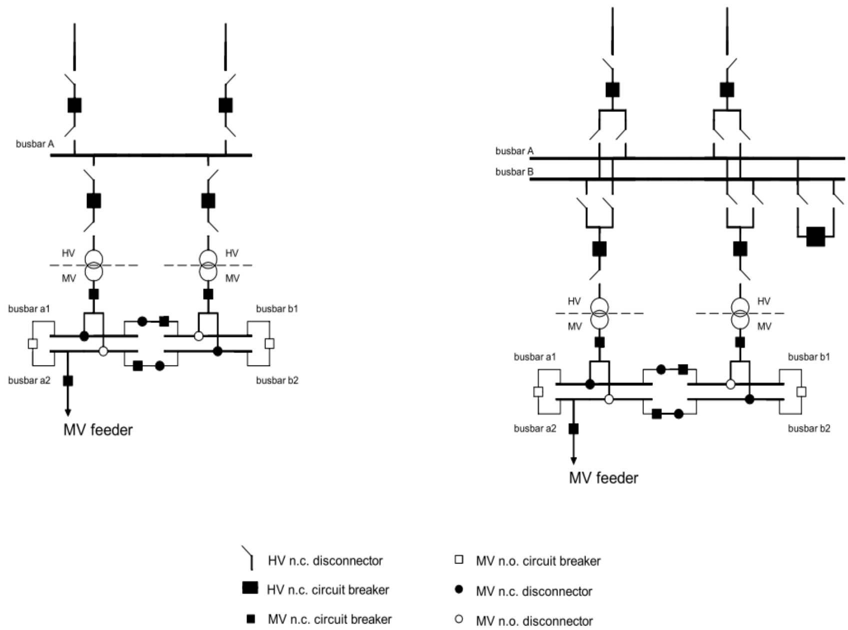

Figure 2. Schematic of two-transformer bay HV/MV primary substations present in typical 110-kV Nordic subtransmission network: (left) single-busbar arrangement; and (right) double-busbar arrangement.

II.1.2 The Nordic urban distribution networks

The urban distribution networks in the Nordic countries consist almost entirely of underground cables and most secondary substations are located indoors. These UGCs are usually laid into trenches along streets, due to lower installation and maintenance costs [Saa13]. These urban MV networks embody radially-operated backed-up relatively short feeders (rarely exceeding 5 km of length, depending on the voltage level), and, in many cases, they are supplied by at least two different primary substations to support high availability. Each feeder is headed by an n.c. circuit breaker close to the point of common coupling (PCC) and at the other extremity, connected via a normally-open (n.o.) disconnector, *i.e.*, linked to the reserve connection. Figure 3 maps a realistic MV-network simulated in the metropolitan area of Helsinki.

The distribution network in Figure 3 embodies radially-operated backed-up UGC feeders. The secondary substations are mainly supplied by one primary substation and backed-up via reserve connections by at least one different primary substation. In urban areas of Helsinki, radial sections of feeders are not allowed in this network.

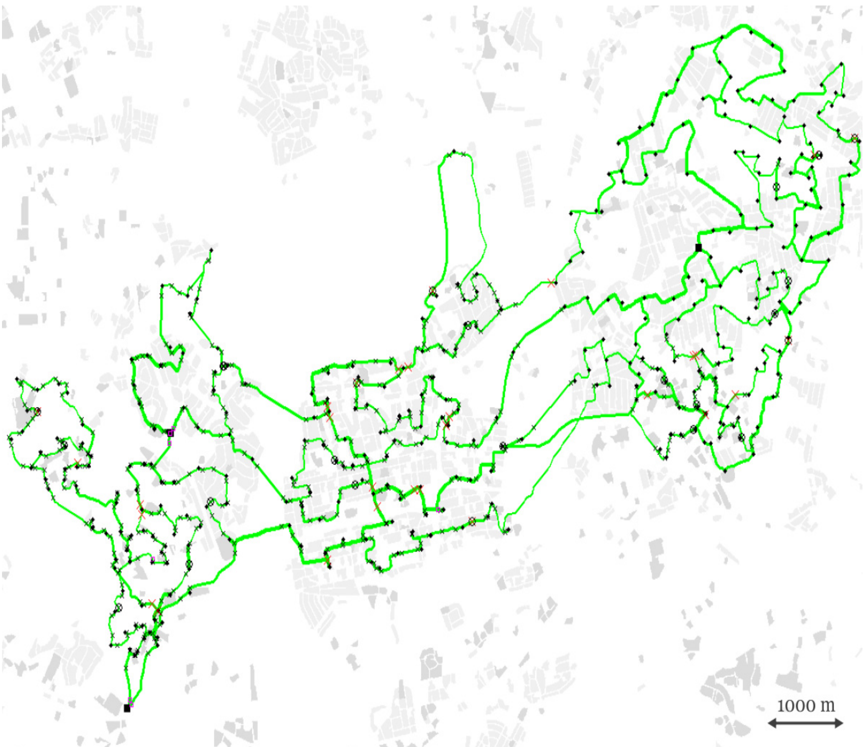

Figure 3. Realistic 10-kV distribution network in suburban area in the municipality of Helsinki. Primary substations (larger squares), secondary substations (smaller squares), n.o. points (circles), remote switches (red crosses) and manual switches (black crosses). *Courtesy of John Millar*

The features intrinsic to these types of distribution networks imply low voltage sag rates, low interruption rates and a certain level of immunity to weather phenomena (indoor substation equipment). Moreover, in Finland, the MV networks operate at 10 kV or 20 kV, while the LV networks, at 0.4 kV [Hei05].

The MV/LV substation (secondary substation)

Secondary substations are more compact and encompass less complex intra-substation connections than their primary counterparts. Figure 4 schematizes the two MV/LV substations used. The MV side does not contain circuit breakers in series with the feeder nor with the MV/LV transformer, instead, fuses are installed at this point (not represented in this schematic). This implies dependency on the technology of disconnector used (*e.g.*, manual, remote, automatic), thus the switching time has a direct influence on the unavailability at this feeder.

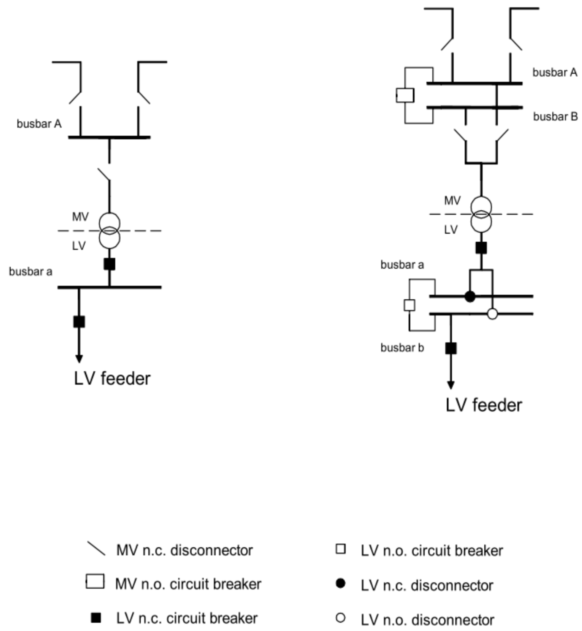

Figure 4. Schematic of transformer bay MV/LV secondary substations present in the test subtransmission network: (left) single-busbar arrangement; and (right) double-busbar arrangement.

Customer categories

This thesis classifies substations and customers regarding two main aspects: land use and main activity. The first is employed to describe primary substations (delivery points) in the reliability analysis and outage cost calculation and it is divided into share of load. It is split into rural, suburban, suburban mixed, urban and urban core substations. The latter is used to define individual customers. These are divided, furthermore, into agricultural, commercial & public services, industrial and residential categories, according to their main activity. This division is used in the voltage sag distribution function and cost calculations as well as in the load distribution by substation categories. End-customers, at HV, ML and LV levels, are divided into agricultural, commercial & public services, industrial and residential categories.

Distribution of load share within each substation category is shown in **Appendix C**. A detailed customer category description is available in [Hyv08] with the technical terminology indexed by the Association of Finnish Electric Utilities.

II.2 General Considerations

This thesis proposes the inclusion of a number of factors intrinsic to urban sub-transmission networks and to the Nordic region as to model equipment and devices in this functional part of the power system more accurately. It is imperative to understand common local practices and the influence of weather reflected through load demand and generation output patterns.

Unavailability is intrinsically small in high voltage networks in comparison to systems operating at lower voltage levels [Iee07],[Iee98]. However, a failure in HV networks can extend to a significantly larger area; while in MV networks outages have more local effect [Bil96]. Particularly, the existence of common-mode (cm) failures in double-circuited OHLs considerably compromises the ruggedness of HV networks and must be computed to this developed reliability assessment [Li05a]. Additionally, common-mode failures can be considered in multiple-transformer substations, for instance, when considering equipment thermal modeling.

Common-mode failures can be quite frequent, as observed in this test sub-transmission network, where approximately 85 % of its OHLs share towers in two-circuit connections (*vide* **Appendix A.1**). They are second-order failures that act as single failures, involving both OHLs [Bil04],[Bil96]. From the perspective of network planning, Common-mode failures assist in orienting certain project requirements, including inter-substation routing and connections to different busbars or possible substations.

Furthermore, this study considers failures up to the fourth order in each considered subdivision of the system. Higher-order failures cause negligible effect, as they are usually characterized by minimal probability (below 10^{-10}). Nevertheless, the herein proposed reliability technique proposed herein assesses systems in a gradual multi-level structure, thus indirectly considering much higher-order failures at a system level.

II.2.1 Generation and combined heat & power (CHP)

Electricity production from CHP plants forms a substantial parcel of the electricity in temperate regions and it is used, particularly in Denmark and Finland, for district heating [Fin13a],[Int08],[Nor08]. In Finland, the generation of district heat can reach up to 70 % originating from co-generation, *i.e.*, from CHPs, and the electricity from CHP accounts for approximately 17 % of the total share of the market [Fin13a]. In addition, including the CHP generated in industry increments, this share rises to about 28 % of the total generation [Fin13a],[Fin13b].

CHP consists of the simultaneous utilization of both heat and power originated from a given or many energy sources, for instance, gas, geothermal energy or biomass, in its surrounding area [Int08]. The efficiency of the processes involved in the CHP cycle in recent technologies can achieve 90 % [Int08]. CHP is a secure, reliable and relatively inexpensive process for energy generation with low emission of greenhouse gases, including carbon-based pollutants, and has immense potential to expand its usage [Con14],[Int14],[Tor15]. From the grid perspective, it promotes network stability by decreasing network congestion through its peak-shaving characteristic.† In addition to district heating, CHP can have industrial and institutional purposes, being employed also in agriculture, hospitals or large commercial facilities, with generation capacity varying from 500 kW to several hundreds of megawatt (electrical) [Int14].

Small CHP units can be directly connected to distribution networks, as exemplified in [Cos11],[Kar11]. This has emerged as a recent measure for the development of DG in network planning. However, the test cases simulated in **Publication V** indicated that at certain positions in MV networks, *e.g.*, directly connected to a secondary substation, the commission of CHP facilities does not directly contribute to the network reliability. In HV networks, nonetheless, large CHP facilities can be directly connected to primary substations, as, for instance, in the municipalities of Berlin, Hamburg [Pih06] and Helsinki [Sou14].

As most thermal processes, CHP units incorporate a relatively slow response to changes in output. Due to that, this type of generation is only modeled on the year-related time scenarios in which each unit within a CHP plant generates its output according to the season of the year. This thesis models CHP units in the commonly accepted two-state model: online and offline. However, more complex models could be utilized, only increasing computational time and adding little of relevance to the assessment.

Renewable energy sources (RESs) have been consolidated in power systems and within the urban environment [Aco10]. In addition, consumers in urban areas have acquired photovoltaic panels and there has been steady growth in the number of electric vehicles that can be smartly coordinated as storage systems [Had15],[Ond14]. Moreover, the shift from fossil-fueled public transportation to electricity-driven transportation has been consistently changing the pattern of electricity and energy consumption within the urban environment. These factors are clearly perceived, although indirectly, in the urban subtransmission networks and must be represented in this method.

The effect of this additional generation and storage via the MV and LV networks is represented in the delivery point load profiles. The total load demand is the difference between the total load demand subtracted by the output of the distributed generation (including injection of power from storage). In other words, the generation decreases the load demand at the delivery point.

In places with high penetration of RESs, particularly solar systems, their load profiles experience a reduction particularly during the summer and during hours of daylight. Moreover, consideration of these RESs in the urban environment should also bring higher-resolution analysis into the assessment of daily scenarios. As currently observed in the electricity market [Eur14a], the day-ahead markets net data are in an hourly time frame.

†*Term used to describe the elimination of peaks in load demand profiles.*

II.2.2 Seasons & meteorological phenomena

The Nordic countries experience well-defined seasons. The disparities among the seasons are characterized by multiple climate variations; therefore, causing changes in the patterns of load profiles throughout the year. The inclusion of certain loads, such as heating and the growing installment of air conditioning systems [All13],[Mah13], is seasonal in these countries. Several studies, *e.g.*, [Mal10],[Ras15],[Sin10],[Sin12],[Zha12], involve demand response, including seasonal loads, electric vehicles and electrification of public transport systems. Therefore, these loads embody a considerable part of the total power demand.

This thesis segments weather into two scenarios: normal and adverse. The duration of each is determined by the daily average wind speed in the year (values above 20 m/s were included as adverse scenario based on [Lec07]) and the season in which they were located was defined by the cause of equipment failure from the local utility reports. This classification is based on research on reliability, insurance and compensation from natural disasters [Bil05],[Bil06],[Eti12],[Lec07]. Figure 5 shows the average wind speed in Finland in the winter (left) and in the summer (right) from the interface developed by the Finnish Meteorological Institute [Fin15c].

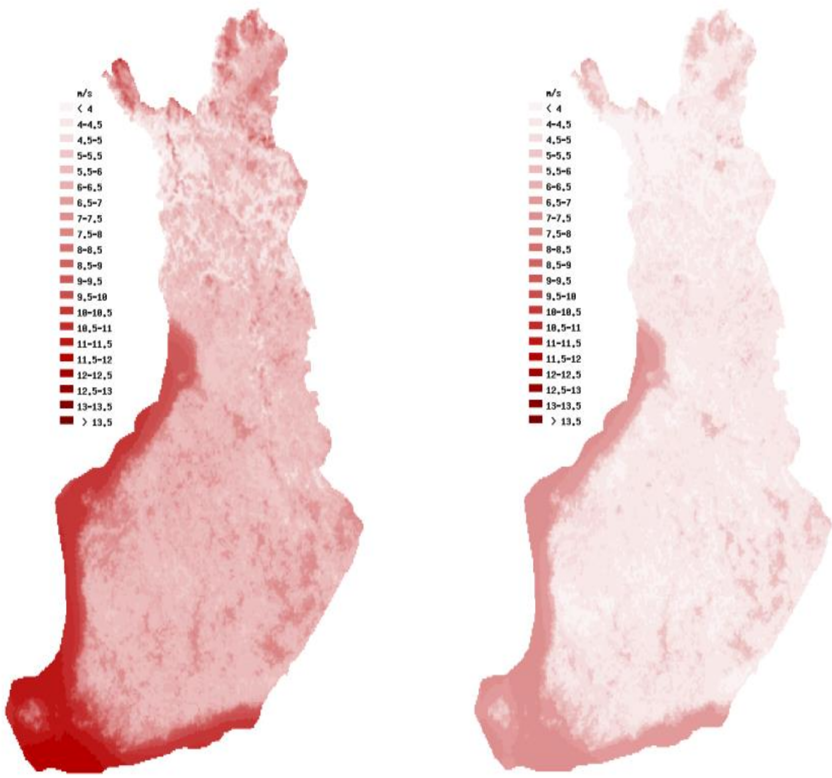

Figure 5. Wind speed maps in Finland in m/s measured fifty meters above the ground: (left) average wind speed in January; (right) average wind speed in July in m/s [Fin15c].

The segmentation of weather-related phenomena is essential for evaluation of grid resiliency to weather [Ent12] and the differentiation between underground and overhead networks. A distinguished approach for estimation of failure rates, based on weather conditions, is introduced, handling collected statistical data and characterizing natural phenomena intrinsic to warm and freezing seasons in temperate and subarctic regions. Based on ENTSO-E statistics [Eur14b] and backed by the reported data in [Hyv08], [Ene15a], [Kjø06] and from the local utility company, weather significantly impacts overhead lines and other outdoor equipment.

It is usual that reports and statistical data divide the equipment failure causes, for instance, into: *lightning*, *wind*, *icing*, *storms*, *other environmental*, *external*, *operational*, *technical* and *unknown* [Eur14b]. All weather-caused phenomena resulting in equipment failure, including external causes, are computed as adverse weather and weighted by the period duration (intrinsically to winter and to summer). The other failure causes, related to operational-technical constraints, are evenly distributed throughout the year and averaged by the number of days in each scenario. As a result, normal scenarios exhibit the same failure rates. The weather-related phenomena are not considered to affect the parameters of either underground lines or indoor equipment.

One other approach, investigated in [Sou15], divides the collected data according to the four seasons of the year. This has been shown to be relevant, particularly at urban distribution levels in Nordic countries, for in these countries most of the distribution networks are underground (*i.e.*, not directly affected by adverse weather). In addition, the correlation between network utilization (load demand) and failure rate is observed and affects both the day and year scenarios. This is further described in Subsection II.3.1.

II.3 The Proposed Cost Function for Subtransmission Networks

A typical approach to estimate the total network cost of a project (C_{net}) is schematized in Figure 6 and is divided into four main components: (i) capital cost (C_{cap}); (ii) operational and maintenance cost ($C_{o\&m}$), (iii) outage cost (C_{out}); and (iv) losses cost (C_{loss}). This equation is a time-variant object function that depends on load growth and interest rate over a specified project lifetime.

In this present thesis special attention is concentrated on the outage cost and voltage sag cost. These two components showed potential for improvement when assessing power quality issues in subtransmission networks and when evaluating the viability of high voltage underground networks in urban areas (contributions from **Publications I** to **VII**).

The outage cost is reinterpreted in this research by the block-layer reliability technique, described in *Chapter III*. This technique investigates in great detail both substation and system indices for reliability. Furthermore, the thesis proposes the inclusion of the voltage sag cost component into the total network cost function for subtransmission networks. This cost component is formulated in *Chapter IV*.

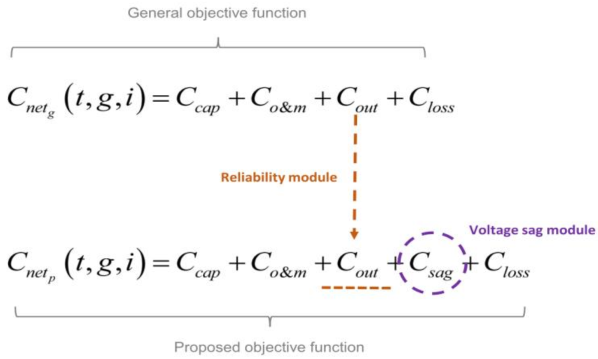

Figure 6. The general objective function for total network cost (above) and proposed objective function for subtransmission and distribution networks (below). The dashed orange line represents the different approach to reliability analysis, developed in *Chapter III*, and the violet dashed circle indicates inclusion of the voltage sag cost component, detailed in *Chapter IV*.

C_{cap}	capital cost [€]
C_{loss}	losses cost [€]
C_{netg}	general objective network cost function [€]
C_{netp}	proposed objective network cost function [€]
C_{sag}	voltage sag cost [€]
C_{out}	outage cost [€]
$C_{o\&m}$	operational and maintenance cost [€]

The entire network economic evaluation in this research is restructured by breaking the base year into several relevant scenarios (in several analyses the year corresponds to the highest time resolution, from Table I in *Chapter I*) for accurate assessment of reliability and comprehensive investigation of the different cost components. The proposed network cost function accredits the large seasonal variance directionality of the power flows, the multivalent position at which urban subtransmission networks stand and the great impact that meteorological phenomena and seasonal variation represent on the network in the course of a year.

The summation of the capital cost and the loss cost addends versus the summation of the voltage sag cost and outage cost addends indicate the differences between the financial benefit of installing underground or overhead networks. Particularly with regard to network improvements, these two summations consistently vary, depending on the number, length and power transfer capacities of the intra-network connections.

II.3.1 Assessment into scenarios

As one of the driving forces of this research, network assessment in several scenarios delineates a novel approach to reliability assessment and economic evaluation of network planning and operation. In addition, scenario assessment of networks embodies benefits that annual analyses neglect, including statistically and probabilistically expected changes, such as voltage sags and interruption rates under a number of weather-related phenomena.

The base year is analyzed on a two-dimensional level: one as *year scenario* and another as *daily scenario*. In the first, the year scenario includes both the seasonal generation outputs and load demands that are provided by the local utility and must be manipulated with engineering judgement and diligence [Li05b] to obtain the average values, for instance, when selecting the adverse and normal weather conditions. In Finland, for instance, within urban areas, the large seasonal differences in load demand and generation output suggest the subdivision of seasons of the year into several scenarios. This considers the number of days within the seasons in which each CHP generation unit is online at different outputs. **Appendix B.2** details the context in which CHP plants were modeled. The suggested division of the year for the typical 110-kV Nordic urban subtransmission network is given in Figure 7. These definitions are the fundamental information upon which the four modules developed in this thesis are founded.

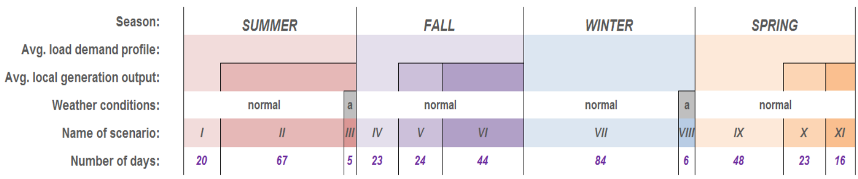

Figure 7. Criteria for division of the base year to determine the number of year scenarios (a, in grey, stands for adverse weather scenarios).

In the other time analysis, the daily scenario is fixed on an hourly-basis resolution for subtransmission systems, since at this level, the average load demands do not abruptly vary if compared to higher resolutions [Wil04]. This analysis can be changed to include higher daytime resolution. However, this increases the computational time and will probably not include any additional benefit, particularly at delivery points far from the LV end-customer.

This model is based on a quasi-chronological frame. The temporal structure of this algorithm is transformed into discrete values fixed in time. Also, within each period (*i.e.*, scenario) time-dependency is irrelevant. For each annual scenario there will be a uniformly-divided daily scenario with the appropriate resolution. The total number of scenarios in this proposed network assessment is:

$$N_s = N_{annual} \cdot N_{daily} \tag{1}$$

N_{annual} number of annual scenarios
N_{daily} number of daily scenarios
N_s total number of scenarios

Moreover, this thesis includes only CHP plants directly connected to the subtransmission network that depicts a typical scenario encountered in cold regions. However, in case of different sources of power at the same positions (*i.e.*, as local generation), for instance solar and wind power plants, the number of scenarios due to generation can be much larger and, therefore, will likely compromise the computational time-accuracy tradeoff. For these cases, the total intra-network and intra-substation generation outputs should also be distributed according to the daily scenario with an hourly-basis (or higher) resolution.

A study [Rid14] commissioned by the British and Italian governments indicated patterns in equipment failure rates and repair times during the timespan of a day. The curves drawn for these two variables were obtained through probabilistic techniques employing hundreds of random variables. In many cases, due to the insufficient number of samples from the statistical data provided for a network, it is not possible to delineate curve for failure rates and repair times for the main equipment.

During inspection of the available data for the test subtransmission network, a high correlation between the load demand and equipment failure rates was observed: during daytime (between 7 AM and 7 PM), there was a high demand and a higher probability of equipment failure (more congestion and bottlenecks in the system). Conversely, during the night, lower demand suggested a lower probability of equipment failure (smaller congestion). This variance is computed as the failure rate coefficients shown in **Appendix B.1**.

Additionally, the variance over the day for repair time can be disregarded. This is valid for urban areas because of the promptness of the technical teams to operate and the easier accessibility to faulty equipment in comparison with rural areas that might be a distance of several dozens of kilometers from the operation centers. Therefore, the equipment repair time, as it is described in literature, is the average repair time [Bil96],[Wil04].

II.3.2 The Network Cost Module

The method proposed in this thesis embodies the comprehensive cost function for subtransmission network planning, upgrading and evaluation and can be expanded to distribution networks with the appropriate parameterization and component modeling. It incorporates four main modules: (i) the Reliability Module; (ii) the Voltage Sag module; (iii) the Sensitivity Module; and from these, (iv) the Network Cost Module.

The subtransmission network cost function, represented in Figure 8, includes the voltage sag cost evaluation and the adjustment of the reliability assessment of the subtransmission networks to calculate the outage cost parcel. This algorithm is proposed as an approach to estimate the total network cost when planning, upgrading or evaluating a project over its lifetime. The values **T**, **R** and **V**, (being **R** and **T** from the Reliability Module, and **V** from the Voltage Sag Module) are determined and described in *Chapters III* and *IV*.

Inputs

The inputs involved in the Network Cost Module are, from Figure 8, in addition to inputs **R** and **T**, described in *Chapter III*, and input **V**, described in *Chapter IV*.

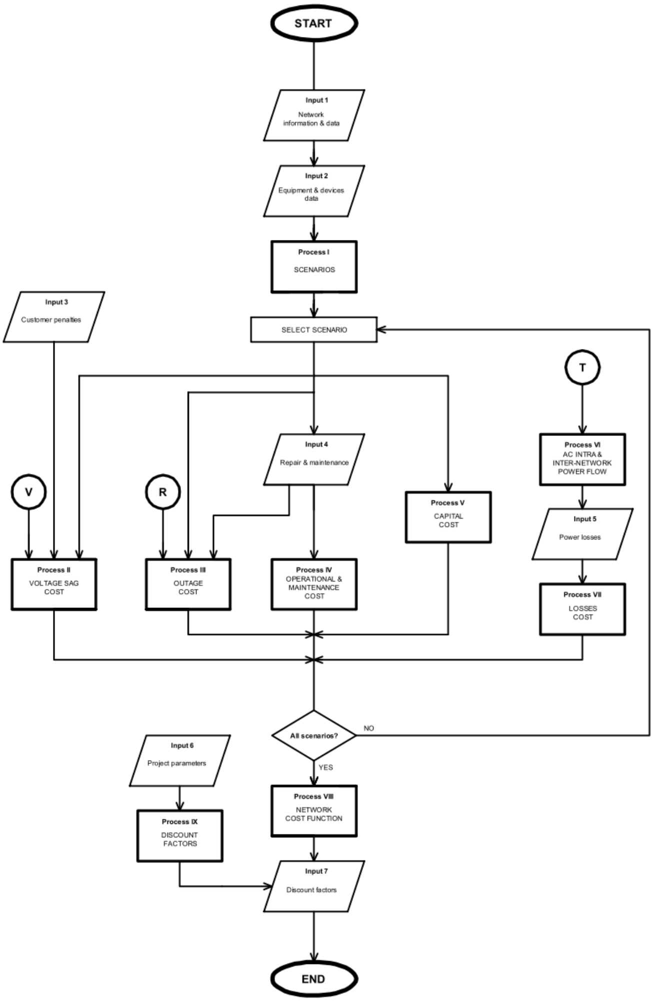

Figure 8. Flowchart of the Network Cost Module.

Input 1 (*Network information & data*): the information and data in the network in focus provided are by the local utility, by the manufacturers and from the relevant standards. This includes all the nominal and project values; catalogue information from installed equipment and devices; reliability parameters including minimal power quality requirements; limits and capacity, such as short-circuit levels, thermal capacities, nameplate values and voltage tolerance curves; as well as load demands and local generation outputs. This thesis utilized data from the tested Nordic 110-kV subtransmission network, **Appendix A**, and information surveyed and proposed in [Ant03], [Ene15a], [Eur14b], [Hei03], [Hyv08], [Kaz11], [Kjø06] and [Ren08], in addition to data from the local utility company.

Input 2 (*Equipment & device data*): the selected data from the data collected by the local utility or for the network location for the main equipment and devices within the network to serve as a parameter for the modeling and selection of scenarios to be considered in the frame of the base year. The main equipment and devices and the utilized data are listed in **Appendix B**.

Input 3 (*Customer penalties*): surveyed penalties [Hei02], according to customer category, to the utility company for a voltage sag event. Utilized values are listed in **Appendix C**.

Input 4 (*Repair & maintenance*): data for the repair and maintenance of the considered equipment, it can also include other ancillary figures to estimate the operational cost in the network, these values should be provided by the local utility, regarding technical team and material costs, and corrected, if necessary, in accordance to the local economic indices (**Appendix B.2**) [Sta15].

Input 5 (*Power losses*): set of data related to the calculation of cost of power losses and power losses, both load and no-load losses, in the equipment of the considered network (**Appendix B.2**).

Input 6 (*Project parameters*): the main driving parameters on the calculation of the discount factors: load growth, interest rate, inflation (if relevant), project lifetime (it can also be divided into two parts with different load growths).

Input 7 (*Discount factors*): the three utilized discount factors in this methodology dependent on load growth: in constant relation with load growth (k_c); linearly related to load growth (k_l); and quadratically related to load growth (k_q). These values are accordingly multiplied with the addends of the network cost function to return their present values.

R (*Input from the Reliability Module – reliability indices*) compiles all possible reliability indices [Bol06],[Iee12] based on the number of customers, the probability of unavailability, the amount of curtailed load, the unavailability, the equivalent failure rate and the equivalent repair time in all blocks and layers from each delivery point (substation).

T (*Input from the Reliability Module – topology*) compiles the information about all inter and intra-substation connections as well as inter-network connections for the tested network.

V (*Input from the Voltage Sag Module – voltage sag rate*) compiles the voltage sag distribution function for the given network in all year scenarios.

Processes

And the processes involved in this part of the algorithm are, from Figure 8:

Process I (*Scenarios*) compiles and selects collected data and defines the appropriate division of the base year into scenarios (annual scenario), considering the number of days of the four seasons of the year, the average seasonal load demand profiles, the average seasonal local generation outputs and the weather condition (adverse or normal) and the division of the day (daily scenario), considering load demand profiles, equipment failure rate and average repair time distributions, as previously described in this chapter.

Process II (*Voltage sag cost*) calculates the voltage sag cost (C_{sag}) individually for each substation in the network in focus and then sums these values to obtain the network voltage sag cost in the base year. Process II compiles information from the customers within the network, the considered penalty for a voltage sag event determined by customer category and the protection philosophy, pre-set in the voltage sag module. The network voltage sag cost function is:

$$C_{sag} = \sum_{c=1}^{4}\sum_{i=1}^{N}\sum_{s=1}^{S}\left[\mu_i \cdot \left(\mathrm{n_c} \cdot \mathrm{c_c} \cdot P_{cc}\right)_i\right]_s \qquad (2)$$

$\mathrm{c_c}$	voltage sag penalty per event according customer category [€/sag]
$\mathrm{n_c}$	number of end-customers per unit of power according customer category [cust/MW]
P_{cc}	sagged load according customer category per substation [MW/subst]
μ_i	voltage sag rate per substation [sag/season]

And the subindices *c*, *i* and *s* refer to customer category, considered substation and considered scenario, respectively. The voltage sag distribution function is further detailed in *Chapter IV*.

Process III (*Outage cost*) also calculates the outage cost individually for each substation in the network in focus and sums these values to obtain the network outage cost in the base year. This process embodies the results from the reliability assessment and the data from network equipment and devices and their relative repair costs. The outage cost function is subdivided into three components: the interruption cost (C_{interr}), which consists of the economic burden from contingencies leading to interruption for the end-customer (from the reliability analysis); the repair cost (C_{repair}), which estimates the expenses of repairing equipment during contingency (from the defined equipment failure rates); and the switching cost (C_{switch}), which calculates the cost of switching the load connected to a faulty transformer bay to the healthy bay in the substation that is directly proportional to the average switching time (this is a constant suggested by the utility that regards the operational constraints and also technological aspects of the employed protection equipment in the substation). The three cost components of the outage cost are:

$$C_{out} = C_{interr} + C_{repair} + C_{switch} \tag{3}$$

Where:

$$C_{interr} = \sum_{c=1}^{4}\sum_{i=1}^{N}\sum_{s=1}^{S}\left[\Lambda_i \cdot P_{ns_{eq}} \cdot \left(cic_p + cic_e \cdot T_i\right)\right]_{c,i,s} \tag{4}$$

$$C_{repair} = \sum_{e=1}^{E}\sum_{s=1}^{S}\left[\left(c_{team_h} \cdot U_{eq}\right) + \left(c_{repair} \cdot \lambda_b\right)\right]_{e,s} \tag{5}$$

$$C_{switch} = \sum_{c=1}^{4}\sum_{i=1}^{N}\sum_{b=1}^{B}\sum_{s=1}^{S}\left[\lambda_b \cdot P_{ns_b} \cdot \left(cic_p + cic_e \cdot \mathrm{T_{SW}}\right)\right]_{c,i,s} \tag{6}$$

c_{repair}	cost of repair [€/fault.unit]
c_{teamh}	cost of technical team, including salaries and related costs [€/h]
cic_e	customer interruption cost for non-delivered energy [€/kWh]
cic_p	customer interruption cost for non-delivered power [€/kW]
P_{nsb}	equivalent power not supplied directly connected to the transformer bay [kW]
P_{nseq}	equivalent power not supplied [kW]
T_i	average outage time [h]
$\mathrm{T_{SW}}$	switching time, subtransmission [h]
U_{eq}	equivalent unavailability [h/scenario]
λ_b	transformer bay failure rate [fault/scenario]
Λ_i	equivalent interruption rate at the delivery point [interr/scenario]

And the subindices *b* and *e* stand for the considered transformer bay and the considered equipment, respectively. The division of the outage cost equation into three parcels assists in the identification of possible discrepancies in the reliability and in the structural and technical aspects of the network under consideration. In addition, the reliability assessment is thoroughly described in *Chapter III*.

Equations (3) and (6) are only valid for subtransmission networks with disconnections between the HV and/or MV busbars. In distribution systems, where feeders incorporate n.o. disconnectors, the addend C_{switch} is included in the C_{interr} and instead of transformer bay failure rate, it should calculate feeder section equivalent failure rate. Therefore, Equation (3) would subsume C_{interr} plus C_{repair}.

Process IV (*Operational & maintenance cost*) embodies the variable and fixed costs related to the operation of the project in focus. The equipment maintenance (C_{maint}) and rents and instalments ($C_{r\&i}$) costs are estimated and grouped under this process [Hyv08] as:

$$C_{o\&m} = C_{maint} + C_{r\&i} \tag{7}$$

Process V (*Capital cost*) consists of the fixed costs of all acquisitions and investments attributed to the network planning, including constructed areas, permits, equipment and devices, for instance. In the assessment of alternatives to the current operating network, the capital cost includes only the added set of equipment to the existing network. This extends to the operational and maintenance cost as well.

Process VI (*AC intra & inter-network power flow*) calculates the necessary power flow routines to return the no-load and load power losses in all transformers, UGCs, OHLs and inter-network connections in this network. The utilized AC power flow routine is the Newton-Raphson solution method that returns the apparent power, with its components, and both voltage magnitude and phase under normal and constrained states at each busbar.

Process VII (*Losses cost*) calculates the costs attributed to no-load (C_0) and load (C_L) losses within this network:

$$C_{losses} = C_L + C_0 \tag{8}$$

Being:

$$C_L = \sum_{e=1}^{E}\sum_{s=1}^{S}\left[h_{pL} \cdot \mathrm{P_L} \cdot \left(\frac{S_p}{\mathrm{S_N}}\right)^2\right]_{e.s} \tag{9}$$

$$C_0 = \mathrm{P_0} \cdot \sum_{e=1}^{E}\sum_{s=1}^{S}\left(h_{p0}\right)_{e.s} \tag{10}$$

And:

$$h_{pL} = \mathrm{p_{pl}} \cdot \mathrm{pf}_s + \log_{\eta}(1.8) \cdot q_s \cdot \mathrm{p_{el_s}} \tag{11}$$

$$h_{p0} = \mathrm{p_{pl}} \cdot \mathrm{pf} + q_s \cdot \mathrm{p_{e0_s}} \tag{12}$$

$$\eta = {}^{\mathrm{T_p}}\!/_{8760} \tag{13}$$

h_{pL} price for equipment load losses in the considered scenario [€/kW.scenario]

h_{p0}	price for equipment no-load losses in the considered scenario [€/kW.scenario]
p_{els}	price of energy for load losses [€/kWh.scenario]
p_{e0s}	price of energy for no-load losses [€/kWh.scenario]
P_L	equipment nominal load losses [kW]
p_{pl}	price of power for load losses [€/kW.a]
P_0	equipment nominal no-load losses [kW]
pf_s	power factor in the considered scenario
q_s	number of hours in the considered scenario [h/scenario]
S_p	peak power in the considered scenario [MVA]
S_N	nominal rated power [MVA]
T_p	peak utilization time [h/a]
η	ratio between peak utilization time and year

Equations (11)–(13) are employed in transformers, UGCs and OHLs, and the suggested parameters in (8)–(13) can be found in **Appendix B**. Equation (13) is based on typical figures from linear approximations [Hyv08].

The no-load losses can be simplified and approximated over the base year, since power factor does not significantly vary throughout time at this kind of networks. However, this is a long-term cost assessment and both types of losses change by the installation or utilization of motoric load, *e.g.*, air conditioning systems, which is a current trend in Finland [Mub14]; line compensations in UGCs that can occur in meshed networks with OHLs and UGCs operating in parallel [Pih06],[Sou12]; and the high variation and multidirectionality of power flows at intra-network and inter-network levels throughout the year, including partial or total deactivation of the CHP units. Therefore, this analysis should be performed in every year scenario.

Process VIII (*Network cost function*) is the compilation of the five addends of the network cost function into the total network cost for the base year. It is represented as:

$$C_{net_p} = \sum_{s=1}^{S} \left(C_{cap} + C_{o\&m} + C_{out} + C_{\text{sag}} + C_{\text{loss}} \right)_s \tag{14}$$

Process VIII outputs each component to be paired with the corresponding discount factor.

Process IX (*Discount factors*) calculates the three discount factors: k_c, k_l and k_q. The three formulas are detailed in **Appendix D**.

Select scenario chronologically selects the defined scenarios in Process I and compiles the previously calculated scenarios.

III. The Reliability Assessment

III.1 The Three-Layer Reliability Assessment of Subtransmission Networks

The three-layer reliability assessment method is a block-layer structure that strategically groups equipment with similar functions to identify the critical zones and to generate partial and total system or substation reliability indices within a given network. The partial reliability indices assist in the notification of regions of low reliability within the network under consideration. In communion with substation reliability indices, they propose improvement and upgrades in different groups of equipment to enhance availability from the network components right through the end-customer. This method, discussed in **Publication III** and applied in **Publication II**, mainly aims to solve the reliability problems of meshed subtransmission networks, topology also typically featured in transmission systems, and can consider or neglect information from the adjacent subsystems and other connected systems. Nevertheless, as demonstrated in **Publications V** and **VII**, the three-layer reliability technique can be expanded and adjusted to distribution systems that consist of a number of topologies fulfilling similar principles and requirements.

The Three-Layer method defines that any substation within any network can be structured into three or four blocks, depending on whether there is directly connected local generation, and three layers. Moreover, this analysis is first performed at each individual substation, using the blocked structure from the perspective of the substation being investigated, and then obtained for the entire network (embodying all load-connected individual substations) in order to obtain the system reliability indices and other important figures. The block-layer structure simplifies the multidirectionality and complexity of subtransmission networks into an iterative and combinational source-to-load model.

The four blocks, denominated as blocks A, B, C and D (similarly, for distribution networks, denominated in lowercase letters), represent respectively the remote generation (within the network, away from the network in focus) and inter-system connections, including all connections with upstream systems, all connections with adjacent subsystems; the inter-substation connections within the network in focus (OHLs and UGCs); the intra-substation connections (substation arrangement and equipment); and, in particular cases, the local generation (the directly connected generation facilities to the substation under consideration). The three layers, denominated layer I, II and III (in distribution networks, in lowercase letters), refer to, respectively, the network interface (the grouping of all connections listed as block A, including the main and the secondary supplies, in parallel); the substation interface (the point between the considered substation and its direct connections, *i.e.*, lines); and to the delivery point interface (the secondary side of the considered substation). In this fashion, each of the substations in the assessed network form a unique three-layer set. A general diagram for the three-layer four-block reliability technique is depicted in Figure 9.

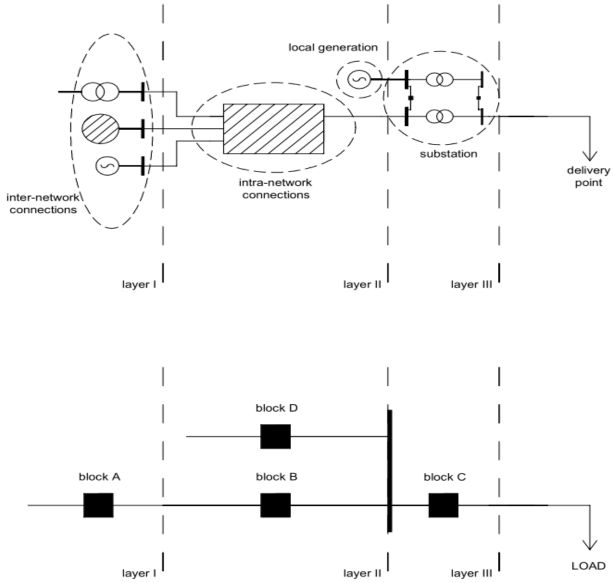

Figure 9. Schematic of the Three-Layer reliability technique from the perspective of a delivery point: (above) the considered parts of the power system and (below) how these parts are interpreted in this reliability assessment.

Each of the four blocks are featured by a number of reliability indices and other relevant parameters, set by the user, that individually illustrate the partial operation under the considered scenarios, from the point of view of each substation (*i.e.*, delivery point) and the entire network (system indices). When these four blocks are properly associated, they then constitute the three layers, representing the core structure of this method. These layers define a set of requirements in order to provide power between source and load at determined availability and quality.

It is important to highlight that this method considers failures up to the fourth order at each analysis level, thus accounting for the probability of higher-order failures [Che05],[Kha06]. This is a valid assumption, since all equipment failure rates and individual normalized unavailabilities are manifold smaller than the unity [Bil92]. Furthermore, this method considers that these network types can be operated in islanded mode. If this is not possible, it is advised that all substations be assessed as ABC-substations (local generation isolated from the system during islanded mode).

This reliability technique for subtransmission networks summarizes a complete and comprehensive power system reliability investigation from the perspective of the end-customers. In the traditional hierarchy level framework [Bil94], this technique assesses the hierarchy level two that includes the generation and the transmission functional zones. However, this thesis assesses subtransmission networks as a complete power system, including the three hierarchy levels [Bil94], where bulky generation is dispersed as distributed generation in the form of RESs, CHPs and inter-network connections.

III.1.1 Component Clustering

Clustering is a fundamental feature of the present reliability assessment technique. This technique groups components related in function and/or physical position into four levels (cells, clusters, blocks and layers) which locally depict parts of networks in a more compact, yet detailed, format. In this context, clustering has the purpose of decreasing the number of states in the reliability assessment (*i.e.*, decreasing the maximum failure order) without loss of accuracy through using the clustering techniques described, *e.g.*, in [Bil92].

Figure 10 schematizes the successive clustering phases pertained to the two parts of this developed reliability technique. The gradual association from the left to the right side of the diagram denotes a transition to more system-oriented and load-related assessment (more susceptible to total load curtailment, LC). Conversely, the associations from the right to the left side of the diagram imply a transition to more component-oriented and equipment-based assessment (more prone to partial LC events).

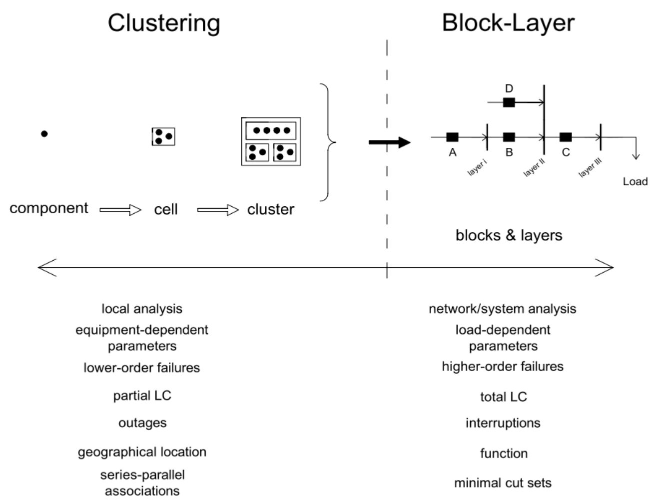

Figure 10. Levels of associations in the Three-Layer reliability technique. The horizontal line indicates evolution in clustering and association mechanisms with the list of characteristics on focus involved in them (bottom).

Firstly, network components are grouped into cells. A cell consists of bay devices, busbars or physically-connected devices, being able to gather the respective ancillary and protective equipment (*e.g.*, relays). A cell can be a transformer bay, a generator bay, a line bay, an association of substation busbars or the section of a feeder. Subsequently, cells are grouped into clusters. A cluster is determined as the association of geographically close cells of the same function. The association of line bays connecting two substations and generator bays inside a power plant form clusters.

Cells and clusters are characterized by:

- number of cells (similarly, number of clusters);
- power-transfer capacity (P_{cap});
- power-transfer utilization rate (ε_p);
- equivalent failure rate (λ_{eq});
- equivalent repair time (r_{eq});
- equivalent unavailability (U_{eq}).

Cells and clusters are not load-related entities, they rely exclusively on component information. Therefore, they need to be further associated in order to bridge equipment unreliability for the end-customer. The association of clusters and cells forms blocks that successively form layers. The specific cases applied to subtransmission networks are detailed in the following subsections along with the definition of blocks and layers in this technique.

III.1.2 Blocks

A block is defined as the set of adjacent system components with similar functions that cause partial or total interruption of power supply to the delivery point under contingency in the network. Each block is associated as individual components to subsequently return the pre-determined parameters. These values provide input to the economic assessment and to the calculation of the significant reliability indices and other system parameters.

The substations of any subtransmission network can be represented by using blocks A, B and C (ABC substation type) or, in the presence of generation units directly connected to it, blocks A, B, C and D (ABCD substation type). As previously stated, this analysis is initially performed at each individual substation and thereafter the system indices are obtained for the entire network. Each of these four blocks are characterized by:

- demanded load (P_{dem});
- power-transfer utilization rate (ε_p);
- probable power not supplied (P_{pns});
- probable power supplied (P_{ps});
- equivalent failure rate (λ_{eq});
- equivalent repair time (r_{eq});
- equivalent unavailability (U_{eq}).

These parameters are obtained from the risk assessment of each block (in all scenarios and substations) and from the statistical data obtained from the utility company and catalogues. The techniques employed to define the block structure include series and parallel associations as well as the Minimal Cut method. These methods are detailed, for instance, in [Bil92] and [Bol00]. Substation and system parameters, including customer-oriented and load-oriented indices, are calculated according to [Iee12],[Iee98]. Moreover, ε_p, P_{ps} and P_{pns} are further detailed in Section III.1.5 and all capacities, demand, losses, generation and power-related figures are dealt with as active power; whereas, it is possible to similarly state block and layer requirements in terms of reactive and apparent powers.

The four blocks are:

Block A (the inter-network connections & the remote generation)

Block A embodies all inter-network connections that can inject power into the considered subtransmission network. The three classes of interconnections are: EHV/HV connections (with the upstream transmission systems) via EHV/HV transformers; HV/HV connections (with adjacent subsystems) via overhead lines and/or underground cables; and MV/HV connections (with generation, in the case of this thesis, CHP units, within the network but outside the considered substation, *i.e.*, remote generation) via step-up transformers. Each of these connections are clusters that together constitute block A.

The availability of each connection and power transfer capacity are individually calculated by determining the series association of the bay components. Subsequently, these components are associated in parallel with other connections to compose the parameters of block A and to perform the risk assessment in this block. Figures 11–14 show block and layer in the example of substation 5 from the typical 110-kV Nordic subtransmission network, introduced in Section II.1.1.

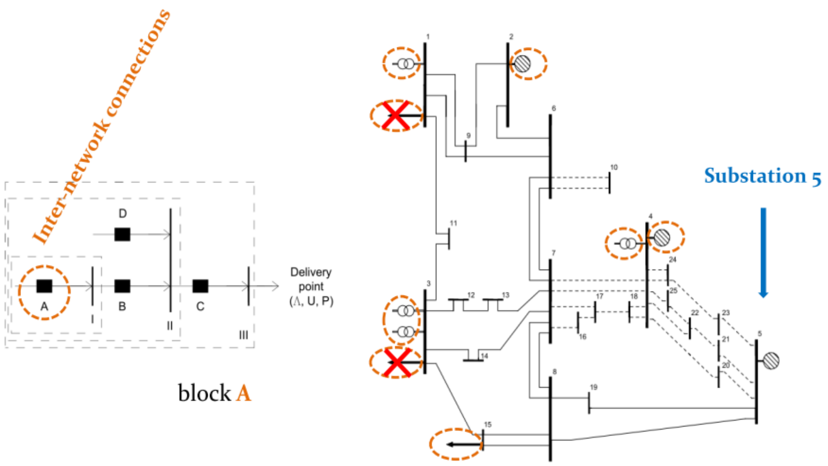

Figure 11. Inter-network connections, in orange, that constitute block A, in block-layer structure (left) and in subtransmission network diagram (right). The red crosses show connections that cannot inject power into this network.

Block B (the intra-network connections)

Block B compiles the set of equipment and components between all the possible paths between the inter-network connections, block A, and the considered substation, block C. The cells formed by the inter-substation line bays are grouped in clusters, according to their position in the network, and denominated as block B in the risk assessment. This assessment identifies combination of line clusters that cause partial or total load curtailment to each subtransmission delivery point. Figure 12 borders this area (the non-hatched area).

In urban networks with meshed topologies, as in the case of this test network, the parallel paths between source and load can be numerous. Therefore, simplifying the modeling of this block considerably decreases the computational burden in the simulation and does not compromise the accuracy of the results. This simplification is pictured in Figure 12 (hatched area) in which only the directly connected line clusters (to substation 5) will significantly affect the block reliability. In this case, block B is reduced to the hatched area in blue. Nonetheless, some certain combination of failures, particularly involving common-mode faults of OHLs in parallel with UGCs, might include risk to the substation. However, these are typically higher-order failures and will cause very low partial load curtailments at very low probabilities; these states are, therefore, negligible.

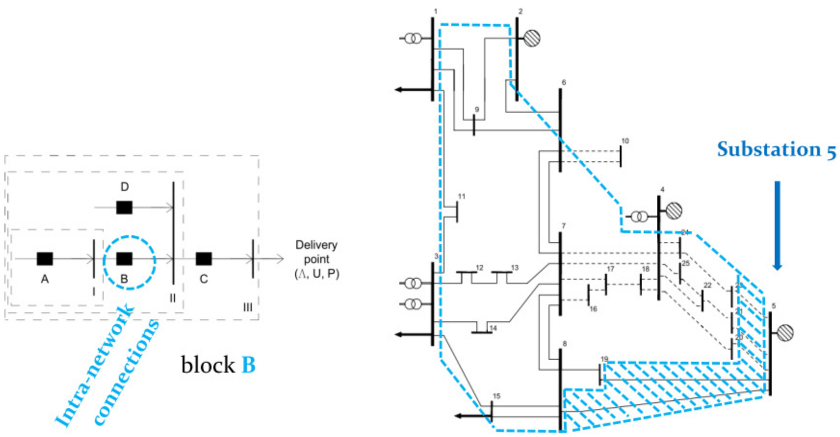

Figure 12. Intra-network connections, in blue, that constitute block B, in block-layer structure (left) and in subtransmission network diagram (right). The dashed area contains directly connected lines to substation 5 that is regarded in the model of this block.

Conversely, networks with a lower number of intra-network connections are more susceptible to lower-order failures. These networks, under low-order failures, will experience partial or total load curtailment. In this situation, full assessment of intra-network connections is necessary in this phase of the reliability analysis.

Block B is subdivided into sub-block Ba, consisting of the lines directly connected to one side of the busbar, in the substation, and sub-block Bb, to the other side (*vide* Figure 2 from Subsection II.1.1). This is the situation in which busbars are divided into two sections by a disconnector or a breaker. If this disconnector is not present, block B does not include sub-blocks. In addition, the modeling of block B should consider, how the substation in focus is connected with adjacent substations (also, if it is exclusively connected to only one substation). This can also be set as a requirement when planning networks (each substation should be connected by at least one line and to at least two different adjacent substations).

Block C (the intra-substation connections & arrangement)

Block C subsumes the substation equipment and arrangement, as illustrated in Figure 2 and located in Figure 13 below. This block associates clusters, in which include the transformer bays (including the HV/MV transformers), the line bays (connected to sides A and B of HV busbars), the HV busbars, and the circuit breakers or disconnectors between the busbars (both on the HV and the MV side), by employing the minimal cuts technique and the equivalent parameters are drawn as block C [Che05].†

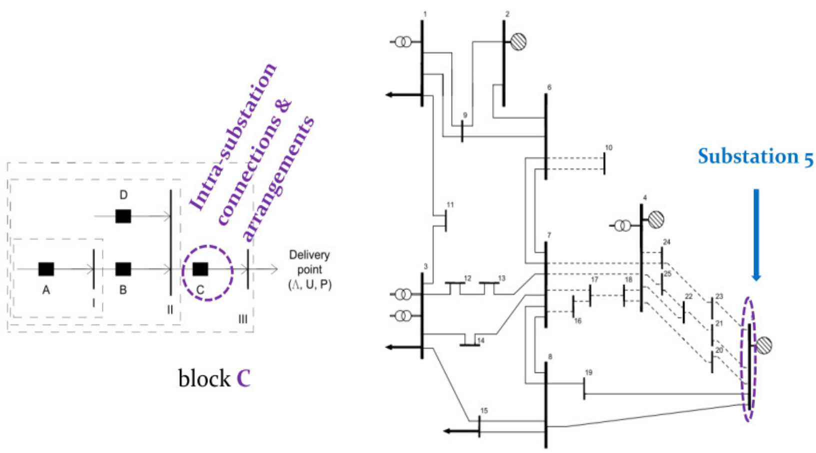

Figure 13. Intra-substation connections and arrangement, in purple, that constitute block C, in block-layer structure (left) and in subtransmission network diagram (right).

Block C addresses direct effect to the delivery point, for in most of the cases, it represents the only possible way between source and load (through the transformer bay). For a complete analysis, including reserve connection, the assessment must be expanded to distribution systems (described in Subsection III.1.6). In addition, the parameters for each of the four blocks are mutually independent, by the exception of blocks B and C. While modeling block C, the sub-blocks Ba and Bb are used in the minimal cuts technique. However, this dependency is typically very low, for it is a sum of first and second-order failures with

†In this test network, it is important to remind that both transformers are connected to each other in the MV side via a manual n.o. disconnector.

third and fourth-order values, to which block B is included, and therefore block C can be regarded as independent from block B.

Block D (the local generation)

Block D consists of the generation directly connected to the substation, *i.e.*, the local generation, as shown in Figure 14. Similarly to block A, in block D, each generation unit bay is associated in series and then associated in parallel with the adjacent generation units present in the considered substation, but connected in parallel with blocks A and B. In addition, blocks A and D, in substation analysis, are complementary, hence requiring simultaneous assessment.

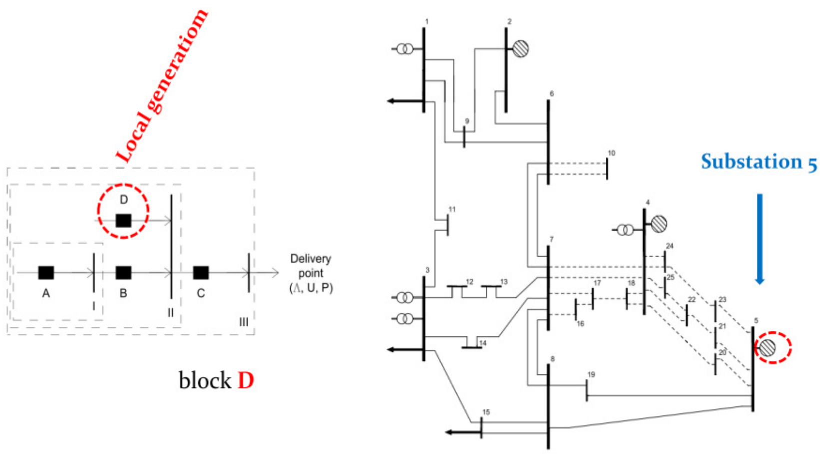

Figure 14. Local generation, *i.e.*, CHP units, in red, that constitutes block D, in block-layer structure (left) and in subtransmission network diagram (right).

The presence of generation at this point positively interferes in the substation and in the system reliabilities. An inspection of Figures 11 and 14, as remote generation (in block A), the generation in substation 5 would be the eighth parallel path for transferred power, while as local generation (in block D), it would be the second parallel path between the source and the load (from the block B and block D itself). If block A and block B were interrupted, there would still be block D to supply power to this substation. However, it is important to clarify the presence of reserve connections and the way these, via MV feeders, are assembled as well as the implemented protection philosophy in the network under consideration to better interpret the risk assessment of block D.

Block D is not present in all substations and neither in all scenarios, as for instance, in the Nordic subtransmission network, generation units work at varying outputs and in summer most of them are out of service (*vide* Figure 7 from Subsection II.3.1). As a consequence, block D is not added into the calculations and those substations are handled as ABC substations. Depending on the position of the generation, when calculating different substations, certain generation can be processed either as remote generation (block A) or local generation (block D).

III.1.3 Layers

A layer is determined as the critical convergence point of any subtransmission network through which power must flow in order to reach the end-customer. Each of the three layers in Figure 9 show the converging point of the associated blocks where partial, substation and system reliability indices and parameters are measured to estimate network performance. Similarly, each layer is characterized by the same parameters than the blocks, since, analytically, a layer is an association of blocks. In addition, a layer does not occupy a physical location; it is, nevertheless, a theoretical *loco* to measure network adequacy and security.

Each layer enunciates a set of requirements in order to set a minimal level of reliability when planning or evaluating system performance. Supplementary requirements can, whatsoever, be included in this technique, with regard to possible project needs, as for instance, the number of parallel connections and the transfer capacity of each block to support network adequacy requirements. And, similarly to blocks, layer outputs are calculated at each substation individually then averaged to obtain the system or network indices.

The analysis of each block independently identifies possible improvement of alternatives within each block, *i.e.*, locally, given the defined network requirements. For instance, it assists when selecting underground cables or overhead lines, or gas-insulated switchgear (GIS) over air-insulated switchgear (AIS). Analysis at network (system) level is targeted primarily at the investigation of *outages*. The introduction of layers facilitates the identification of zones in the considered network with low reliability (critical areas) and the overall benefits to the delivery point due to equipment upgrade or replacement. Complementarily, assessment at substation level primarily investigates the impact of *interruptions*.

The three layers are:

Layer I (the network interface)

Layer I is the represented point to where all intra-network connections with power injection possibility, including EHV/HV, HV/HV and MV/HV connections, between the considered subtransmission network and its adjacent subsystems present outside the substation under investigation. In other words, layer I is the network interface to adjacent networks and subsystems and it is analytically equivalent to block A.

The requirements for layer I, at any given scenario, are:

$$P_{loc.gen} + \sum P_{inter.net} \geq P_{dem_N} \tag{15}$$

For the entire network:

$$P_A + P_D \geq \sum P_{dem_i} \quad (16)$$

For the substations under analysis (being $P_D = 0$, for ABC substations).

P_A	generated/transferred power in block A [MW]
P_D	generated/transferred power in block D [MW]
P_{dem_i}	demanded power for the considered substations† [MW]
P_{dem_N}	demanded power for the considered network [MW]
$P_{inter.net}$	generated/transferred power by each inter-network connection with power injection capacity [MW]
$P_{loc.gen}$	generated power by the local generation [MW]

The subindices dem_N and dem_i stand for the demanded power in the considered network and the substation under analysis, respectively. These requirements must also be valid if security criteria are employed (*e.g.*, N-1 criterion), in which the sum of the healthy parallel intra-network connections and the local generation outputs must be larger than the network demand. Certain inter-network connections (blocks A and D) do not generate power, but can transfer power, hence, implying the term generated/transferred. In addition, in reliability assessment of networks in operation, each layer requirement is determined in terms of generated and transferred power; while in reliability assessment of planning networks, the layer requirements are stated in terms of generation and transfer capacities.

Equation (15) implies that the power injected from the vicinities of the subtransmission network in addition to the power generated within the network must be sufficient to supply the total demanded power in this network. Equation (16) formalizes that the sum of the local generation, if existent, plus the remote generation and connections must be able to feed the considered substation. In addition, the summation in (16) marks the substation under analysis in addition to all possible exclusively-connected substations to it.

The unavailability at layer I is:

$$U_I = A = \prod_{m=1}^{M} A_m \quad (17)$$

For both ABC and ABCD substations.

U_I	unavailability of layer I [p.u.]
A	unavailability of block A [p.u.]

Where the subindex m stands for the number of inter-network connections in the network. This thesis processes unavailabilities in normalized values, at each

†*In addition to the possible exclusively connected substations to the substation on focus.*

scenario, and exhibits them in time units. For the calculation the unavailability of blocks and layers at each scenario, the normalized unavailability is given as:

$$U = {U_s}/{T_s} \tag{18}$$

U	normalized unavailability over the scenario [p.u.]
U_s	unavailability at given scenario [h]
T_s	given scenario duration [h]

Layer II (the substation interface)

Layer II constitutes the intra-network connections, *i.e.*, lines directly connected to the substation under analysis, and the generation units directly connected to the considered substation (local generation). Layer II is also referred to as the substation interface and it is the point to where the directly connected lines and local generation deliver power.

The requirements for layer II, at any given scenario, include the requirements of layer I and:

$$P_B + P_D \geq \sum P_{dem_i} \tag{19}$$

For the substations under analysis (being $P_D = 0$, for ABC substations).

P_B	transferred power through block B [MW]

Equations (18) and (19) determine that the power transferred from block B and injected from block D to the considered substation must be sufficient to supply the demand at this substation and other possible substations exclusively connected to it. In the case local generation is not present, P_D is zero. In addition, Equations (15) and (16) must also be fulfilled in order to meet all the determined requirements at layer II.

The unavailability at layer II is:

$$U_{II} = \begin{cases} A + B - AB & ,\forall ABC \text{ substations} \\ D \cdot \left(A + B - AB \right) & ,\forall ABCD \text{ substations} \end{cases} \tag{20}$$

According to the type of substation under analysis.

U_{II}	unavailability of layer II [p.u.]
B	unavailability of block B [p.u.]
D	unavailability of block D [p.u.]

Equation (20) expresses the series and parallel association of the blocks related to layer II given substation type.

Layer III (the delivery point interface)

Layer III is the delivery point of the tested substation. It embodies the effects of all upstream equipment, arranged in the blocked structure, on the MV busbar to which the MV feeders are connected. In other words, layer III shows the reliability of the subtransmission network to the delivery point of the considered substation.

The requirements for layer III include the requirements of layers I and II in addition to:

$$P_C \geq \sum P_{dem_i} \tag{21}$$

For both ABC and ABCD substations under analysis.

P_C transferred power through block C [MW]

Equation (21) states that the power transferred through block C to the considered load point must supply the demanded power at this considered substation. Concomitantly, the requirements of layers I and II must be met to fulfill all requirements of layer III.

And the unavailability of layer III is:

$$U_{III} = U_{II} + C - U_{II}C \tag{22}$$

U_{III} unavailability of layer III [p.u.]
C unavailability of block C [p.u.]

Equation (22) is valid for both ABC and ABCD substations, using the respective unavailability for block II.

III.1.4 Delivery points

The assumptions and considerations must be clear in order to identify the parts where all reliability indices and relevant parameters are measured. Since the subtransmission network is located in an intermediate position in the power system and should not include, for computation time reasons, features of every single component in the system.

For this, the delivery points of the subtransmission network, from the perspective of each HV substation, are defined as the MV side of the primary substations [Jal10]. This point serves as the starting point for the reliability assessment of distribution networks also utilizing the block-layered structure, as demonstrated in **Publications III**, **V** and **VII**. Hence, the subtransmission delivery point does not depict the exact values for reliability to the LV end-customer; whereas, it depicts the performance of the subtransmission network and its effect on the LV end-customer. Nonetheless, the investigation of the subtransmission network is sufficient to frame an accurate reliability evaluation of the HV and MV customer connected to it. For a more comprehensive network assessment, the distribution network must be included compiling all relevant statistical data, information collected and assumptions.

The reliability analysis in this method defines that each delivery point in the network under consideration comprises a four-block three-layer structure representing any subtransmission network projected to any delivery point, as schematized in Figure 9. Moreover, the delivery point implies a set of requirements for power quantity and quality to meet standardized criteria in addition to requirements to be determined by the planner using reasonable engineering judgement to match availability, quality and cost [Wil04].

In terms of power quantity, the subtransmission delivery point requirements specify that:

- all delivery points must be continuously supplied without any level of load curtailment tolerating, for instance, a maximum of 120 min/subst.a of unavailability for each substation and 90 min/subst.a of average unavailability in the network (these values must be determined according to policy within the local utility company);
- all delivery points must be supplied given any load scenario with regard to the load profiles at each year and daily scenario set in the project.

And in terms of power quality:

- the voltage magnitude under normal operation should follow the suggested updated voltage tolerance curves in practice, such as in [Nai12];
- short circuit tolerated levels;
- and project regulation to other possible power quality issues, such as frequency regulation, balance in the phases and the protection philosophy that directly affect the propagation of small interruptions as voltage sags through the entire meshed grid.

Moreover, threshold values set for power factor and losses in the network can also be set as a delivery point requirement for the performance of the network within the operational conditions. Similarly, unavailability limits can be established for each scenario, particularly given the fact that in subarctic and temperate regions, such as Finland, winters can be long and harsh, thus implying great impact on the societal wellbeing.

These requirements are defined for the subtransmission delivery point and should be in phase with the local regulator policy. However, it is advised that stricter requirements at planning and operational stages must be set into practice in order to provide high-quality power supply to all end-customers and minimize outages and interruptions in the network.

III.1.5 Other concepts

The Three-Layer technique described implies three important concepts: (i) the probable power supplied; its complementary value, (ii) the probable power not supplied; the power transfer utilization rate; and (iii) the average number of connections.

They are:

Probable power supplied & probable power not supplied

The probable power supplied (P_{ps}) in a given block is:

$$P_{ps} = \frac{\sum_{q=0}^{Q} \left(P_{dem_x} - P_{curt} \right)_q \cdot R_q}{\sum_{q=0}^{Q} R_q}, \forall P_{curt_q} \le P_{dem_x} \quad (23)$$

And similarly, the probable power not supplied (P_{pns}) in a given block is:

$$P_{pns} = \frac{\sum_{q=0}^{Q} P_{curt_q} \cdot R_q}{\sum_{q=0}^{Q} R_q}, \forall P_{curt_q} \le P_{dem_x} \quad (24)$$

Or simply:

$$P_{dem_x} = P_{pns} + P_{ps} \quad (25)$$

P_{dem_x}	demanded power at given block [MW]
P_{curt_q}	curtailed load at risk state q [MW]
R_q	probability of the risk state q

And the subindex q stands for risk state. These two power measures, analytically estimated, are defined for each block considering all risk states leading to failure (*i.e.*, states that do not fulfill the block requirements) and are then associated and averaged accordingly to obtain the substation reliability indices. From these two quantities, this reliability technique can estimate the loss of load expectation (LOLE) and the loss of energy expectation (LOEE).

Power transfer utilization rate & average number of connections

The power transfer utilization rate (ε_p) expresses the idea of power flowing through the inter-substation connections at each substation. This value is important in the risk assessment, particularly due to the high range of UGC and OHL ratings for nominal power in HV networks.

This parameter is calculated as:

$$\varepsilon_p = \frac{\sum S_{avg}}{\sum S_N} \quad (26)$$

This rate represents the sum of the average power (S_{avg}), at a given scenario, in all inter-substation connections of a given substation, over the sum of the rated nominal power (S_N) of these connections.

In addition, the average number of inter-substation connections in the network is:

$$\bar{N}_{inter.subs} = \frac{1}{N}\sum_{i=0}^{N} N_{inter.subs_i} \qquad (27)$$

N	number of substations in the test network
$N_{inter.subs_i}$	number of inter-substation connections in substation i

These last two parameters support the reliability assessment when comparing different substations and assessing possible diagnosis in the sensitivity analysis.

III.1.6 Expansion to distribution network assessment

To include a more comprehensive aspect to the assessment of subtransmission networks, the Three-Layer Reliability Assessment was expanded and adjusted to distribution systems, as detailed in **Publication VII**. In combination with the upstream analysis, this expanded technique summarizes a complete and in-depth power system reliability investigation from the perspective of the LV customers. According to the traditional hierarchy level framework [Bil94], this technique assesses the hierarchy level 3, with the generation, transmission and distribution functional zones.

The method previously described in this chapter calculates reliability indices for the subtransmission delivery points neglecting information from downstream equipment, *i.e.*, distribution systems. These indices are partial values, for they gather the reliability situation at the MV side of the primary substations. If distribution system data are available as well as the need for further assessment, this technique can also be applied to the distribution reliability domain.

Figure 15 illustrates the block-layer structure in a generic MV feeder from the perspective of a sampled substation. The same four blocks and three layers from primary HV/MV substations are also applied to secondary MV/LV substations using lowercase digits. In the presence of reserve connections, block b is segregated by the n.o. point. Similarly, the subtransmission network and the primary substations correspond to the test feeder and the secondary substations, respectively, in the analysis at distribution level.

Conversely, this assessment comports topologies typical of distribution systems, including radial, radially-operated backed-up, looped and islanded schematics. The difference in the structure between these topologies relies on the determination of the inter-feeder points and the number of feeder sections to be considered. Moreover, all the secondary substations can also be classified as abc or abcd substation (in lowercase digits, to be distinguished from subtransmission networks) in the presence of directly connected distributed generation. However, as investigated in **Publication V**, it is not a technically trivial task to install distributed generation (as in the example of small CHP units) in feeders with other secondary substations, more specifically connected to a substation with load (customers). However, this research will include this possibility to maintain the aspect of generality in the proposed method.

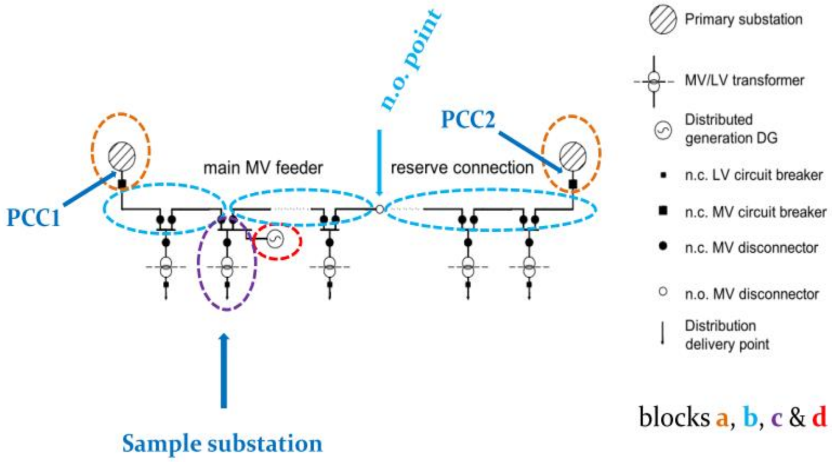

Figure 15. Block-layer model for a sampled secondary substation in backed-up MV feeder, including the four blocks taking the example of substation 5.2.

Distribution delivery point

The distribution delivery point in this context is the secondary side of the secondary MV substation. It is where layer iii is located and it is analogous to the subtransmission delivery point, described in Subsection III.1.4. In addition, this method here is simulated at each secondary substation and then for the entire MV feeder, or other feeders in the distribution network under investigation, to estimate the system reliability indices.

Blocks

At this part of the power system, the four blocks assume equivalent positions, as traced in Figure 15 depicting the secondary substation 5.2. Block a constitutes the primary substations and the remote generation units (outside the assessed substation, but still within the feeder under analysis); block b subsumes the sections of feeders between the substation and the main primary substation (block b1), between the substation and the other possible primary substations via the n.o. disconnectors (blocks b2, b3, ..., bn); block c incorporates the secondary substation under consideration; and block d the possible DG directly connected to the simulated substation.

Block a is the association of the primary substations and MV DG involved in the test feeder and is highly dependent on the feeder and distribution network topologies and operations. In radial feeders, block a is only one point, forming the main primary substation. In the other topologies presenting reserve connections, block a can be divided into more sub-blocks, each one representing the number of primary substations directly and indirectly connected to the considered feeder, also via the n.o. disconnector. In these cases, the main primary substation is defined as sub-block a1 and the others, as from sub-block a2 to an, if applicable. In other cases, a feeder can be connected to another feeder in the same primary substation, thus sharing the same primary substation (hence, only one sub-block).

The structure of block b also depends on the network topology, the feeder type and the coordination of protection involving the n.c. and n.o. disconnectors in this feeder. Sub-block b1 involves all feeder sections between the test MV substation and the main feeding point (block a1), *i.e.*, the point of common coupling, PCC1, as in Figure 15. Sub-block b21 (or higher, depending on the number of feeder paths directly connected to the test substation) includes the sections of the feeders between the substation and n.o. point and sub-block b22 from the n.o. point to the secondary feeding points, in PCC2. Block b is therefore divided into sub-blocks with the feeder sections connecting the test MV substation, the n.o. points and the PCCs. Note that the MV busbars in the intermediate substations must also integrate block b.

Layers

Similarly, the three layers for the distribution delivery points are enunciated as in Subsection III.1.2. They are defined as, for layer i:

The unavailability at layer i is:

$$U_i = a = \prod_{m=1}^{M} a_m \tag{28}$$

For both abc and abcd substations.

a	unavailability of block a [p.u.]
U_i	unavailability of layer i [p.u.]

Where the subindex *m* stands for the number of sub-blocks in the feeder (primary substations and local DG). And the requirement for layer i, at any given scenario, is:

$$P_{dg} + \sum P_{inter.feed} \geq P_{dem_F} \tag{29}$$

For the test feeder:

$$P_a + P_d \geq P_{dem_{i\,sec}} \tag{30}$$

For the substations under analysis ($P_d = 0$, for abc substations).

P_a	generated/transferred power through block a [kW]
P_d	generated/transferred power through block d [kW]
$P_{dem_{isec}}$	demanded power for the test secondary substation [kW]

P_{demF}	demanded power for the test feeder [kW]
P_{dg}	generated power by the local DG [kW]
$P_{inter.feed}$	generated/transferred power by each inter-feeder connection with power injection capacity [kW]

The requirements for layer ii, at any given scenario, are:

$$P_b + P_d \geq P_{dem_{i\,sec}} \tag{31}$$

For substations under analysis ($P_d = 0$, for abc substations).

P_b	transferred power through block b [kW]

And the unavailability at layer ii is:

$$U_{ii} = \begin{cases} b_{T_{sw}} + \prod_{m=1}^{M} \left(a_m + b_m - a_m b_m \right) & ,\forall abc\ substations \\ b_{T_{sw}} + d \cdot \prod_{m=1}^{M} \left(a_m + b_m - a_m b_m \right) & ,\forall abcd\ substations \end{cases} \tag{32}$$

For both abc and abcd substations.

U_{ii}	unavailability of layer ii [p.u.]
b	unavailability of block b [p.u.]
b_{Tsw}	unavailability of block b between zero and the switching time [p.u.]
d	unavailability of block d [p.u.]

And the requirement for layer iii, at any given scenario, is:

$$P_c \geq P_{dem_{i\,sec}} \tag{33}$$

In which:

P_c	transferred power through block c [kW]

Similarly, the unavailability of layer iii is:

$$U_{iii} = U_{ii} + c - U_{ii} c \tag{34}$$

For both abc and abcd substations, replacing the respective unavailability for layer ii.

U_{iii}	unavailability of layer iii [p.u.]
c	unavailability of block c [p.u.]

Additionally, the unavailabilities of the three layers (as well as for the four blocks) are assessed in two periods, being the instant 0 the moment when a failure occurs, and in two parts, according to the type of load curtailment, LC, as shown in the following schematic:

$$U_i, U_{ii}, U_{iii} \Rightarrow \begin{cases} total\ LC \Rightarrow & \begin{cases} 0 < t \leq \mathrm{T_{sw}} \\ \mathrm{T_{sw}} < t \leq r_{eq} \end{cases} \\ partial\ LC \Rightarrow & \begin{cases} 0 < t \leq \mathrm{T_{sw}} \\ \mathrm{T_{sw}} < t \leq r_{eq} \end{cases} \end{cases} \tag{35}$$

r_{eq} equivalent repair time [h]
$\mathrm{T_{sw}}$ switching time, distribution [h]

These sets of states are disjointed and mutually independent; therefore, they can be summed resulting in the total unavailability at each layer. The system operates without constraints for $t > r_{eq}$.

III.2 The Reliability Module

The Reliability Module in this thesis includes the reliability assessment of this research. This module calculates and evaluates relevant reliability indices and other customer-oriented parameters through several processes and risk assessments at substation and network levels, using a number of project parameters and possible ancillary algorithms, such as AC power flow routines and network planning algorithms.

Figure 16 schematizes the main inputs and outputs of this module. Input data, including number of scenarios (n), failure rates (λ), repair times (r) and the demand profiles, are processed to obtain the interruption rate distribution in this network (Λ), the unavailability (U) and the probable power not supplied (P_{pns}). From these outputs, related reliability indices and other customer-oriented figures can be estimated at any layer, block or delivery point of the network under consideration.

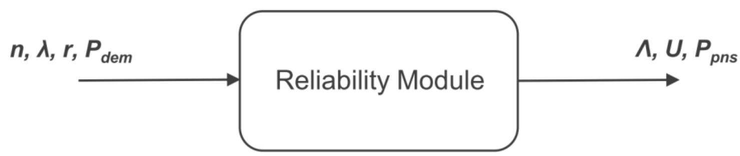

Figure 16. The Reliability Module processes related information and data from the network under consideration (including its equipment and devices, substations and customers) and returns equivalent indices and figures at each delivery point.

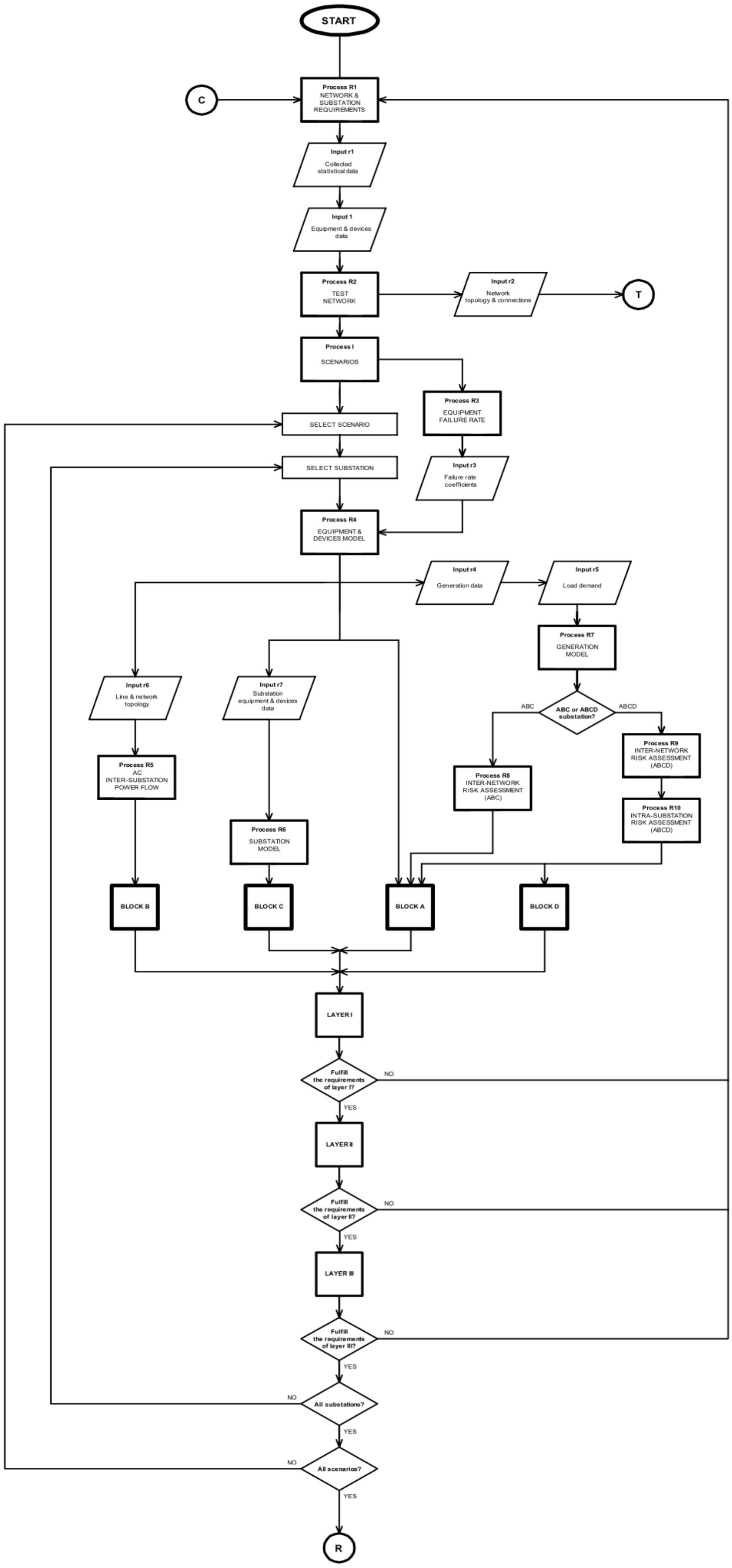

Figure 17. Flowchart of the Reliability Module.

Inputs & outputs

The inputs in the Reliability Module are (Figure 17), in addition to **Input 1** from the Network Cost Module in *Chapter II*, and input **C**, described in *Chapter IV*:

Input r1 (*Collected statistical data*): all statistical data for the region where the network is located. These data feature topographical and meteorological information, demographic, real estate and property values, obtained from relevant sources, in addition to the local utility company, such as the meteorological department and the urban development and planning department.

Input r2 (*Network topology & connections*): information of the network topology and position of substations and other equipment in the network under consideration.

Input r3 (*Failure rate coefficients*): the coefficients obtained from the distribution of equipment failure rates, according to the weather condition, season and the time of the year. The two coefficients, α and β, refer to the year scenario and to the day scenarios, respectively. These coefficients are multiplied with the annual averaged failure rate, per equipment, to return the time-dependent failure rate for any given year or daily scenarios.

Input r4 (*Generation data*): the output of the intra-network generation plants at each scenario. The EHV/HV and HV/HV inter-network connections are modeled in this thesis as supplying any power between zero and their maximum rated power.

Input r5 (*Load demand*): the load demand profiles for each delivery point, the share of customers by categories in the total demand and the number of customers by category for each scenario.

Input r6 (*Line & network topology*): data from the inter-substation connections, including the type of line (UGC or OHL) and the number of connections.

Input r7 (*Substation equipment & device data*): data from the intra-substation connections and equipment, including all the main devices (transformers, busbars and breakers) as well as protection scheme.

C (*Input from the Voltage Sag Module – short circuit*) compiles the initial symmetrical short-circuit currents and the peak short-circuit currents for each substation. In case these values exceed the specified limit, this module suggests that the network must be upgraded or redesigned.

R (*Output for the Reliability Module – reliability indices*) returns all possible reliability indices [Bol06],[Iee12] based on the number of customers, probability of unavailability, curtailed load, unavailability, equivalent failure rate and equivalent repair time in all blocks and layers from each delivery point (substation).

T (*Output for the Reliability Module – topology*) extracts the information about all inter and intra-substation connections as well as inter-network connections for the tested network.

Processes

And the processes in this part of the algorithm are (Figure 17), in addition to **Process I** from the Network Cost Module in *Chapter II*:

Process R1 (*Network & substation requirements*) compiles and selects collected data and defines the appropriate division of the base year into scenarios (annual scenario). This process should be updated in case the reliability indices do not meet the requirements enounced in each layer and block otherwise alterations must be performed in the network topology and arrangement.

Process R2 (*Test network*) selects the test subtransmission network to be assessed. This part can be linked to a robust network planning algorithm to generate possible subtransmission networks, regarding operational aspects, topographical and meteorological information about the region, technical constraints and all other major features to be considered in network planning. The methods proposed in [Mil12] and [Saa13] investigate network planning from a topographical perspective and can offer interesting features to this Reliability Module, in particular in the routing of UGCs in the urban environment.

Process R3 (*Equipment failure rate*) calculates the two failure rate coefficients: α, for the day scenarios; and, β, for the year scenarios. The equipment failure rate at given scenario is:

$$\lambda\big|_s = \alpha\beta\lambda_e \tag{36}$$

For the considered equipment and devices in this method.

α	failure rate coefficient at given day scenario
β	failure rate coefficient at given year scenario
λ_e	average annual failure rate [failure/unit.a]

This process transforms the constant failure rate into a time-variant parameter intrinsic to each class of equipment, in the context of this thesis, listed in **Appendix B**. These coefficients are obtained numerically, depending on the statistical data under observation, and include the observations listed in Section II.2.

Due to the scarcity of fault events in some local utilities, as, for instance, in HV networks consisting of short-length connections or a small number of HV transformers, as in the typical 110-kV Nordic subtransmission network, the number of failures can be below one per year. Nevertheless, previous research have confirmed the correlation between time of the day [Rid14] and time of the year [Sou15] and number of events. As a rule-of-thumb, more failures occur during daytime and adverse weather-conditions. Process R3 includes these phenomena analytically to better depict and model equipment in this model.

Process R4 (*Equipment & devices model*) models all considered devices, equipment and lines in this module. Process R4 utilizes information from the collected statistical data and catalog specifications to compile important parameters, as failure rates, repair time, nameplate values and aging. The values employed in this process are available in **Appendices A** and **B**.

Process R5 (*AC inter-substation power flow*) calculates the inter-substation power flow routines required to evaluate possible load curtailment in each substation. Similarly to the Network Cost Module, it employs the Newton-Raphson solution method (AC power flow analysis); whereas, a simple DC power flow analysis is enough for this process.

Process R6 (*Substation model*) compiles and selects collected data and defines the appropriate division of the base year into scenarios (annual scenario).

Process R7 (*Generation model*) consists of the appropriate model for the generation units, taking into consideration the type of generation, the scenario division (particularly the season in question) and the number of states for each unit. Due to the nature of CHP generation, the number of generation units in this test network and to simplify the employed model, each generation unit will either be at a given output, at each season, or out of service. The reliability model of the generation units includes the main equipment of the step-up transformer bay to which the units are connected.

Process R8 (*Inter-network risk assessment - ABC substations*) performs the risk assessment of the remote generation between the test network and its adjacent systems. This process is only assigned to the ABC substations, for these do not present local generation, and this process is run only once for all the ABC substations.

Process R9 (*Inter-network risk assessment - ABCD substations*) similarly performs the risk assessment of the remote generation between the test network and its adjacent systems including the local generation. This process is valid exclusively for ABCD substations and it must be run individually for each ABCD substation, since each of these constitute a different local generation.

Process R10 (*Intra-substation risk assessment - ABCD substations)* runs, in association with Process R9, the risk assessment individually at the substation.

This must be performed due to the presence of local generation in ABCD substations that will dampen or even mitigate load curtailment in a set of combinations of upstream equipment failure.

Blocks A, B, C and **D** incorporate the requirements and calculations involved in all the blocks of each substation, described in Subsection III.1.2.

Layers I, II and **III** entail the requirements and calculations involved in all layers of each substation, described in Subsection III.1.3.

Select scenario is the same as in the Network Cost Module.

Select substation chooses substations in numerical order (all substations are numbered) to perform the reliability assessment in this module and, similarly, stores results from the previous substations to calculate the network/system reliability indices.

III.3 The Sensitivity Analysis

The sensitivity analysis emerges as an adjunct tool to assess network performance and reliability status, under the given operation conditions, and to identify zones of low reliability and prospective areas to be diagnosed with equipment replacement or upgrade, developed and simulated in **Publications III** and **VI**. This analysis assists in the iteration of network planning algorithms in order to converge to a more robust and reliable network as well as to balance substation reliability, in reference to network reliability, within the network under examination.

The sensitivity functions are derived from the unavailability functions at the delivery point, Equation (22). These functions are the partial derivative of U_{III} in relation to each of the blocks to be evaluated. By setting all other blocks constant and deriving in relation to the analyzed block (*i.e.*, independent variable), the sensitivity function expresses the influence of this block on the delivery point at the determined operation point (*i.e.*, the other blocks set constant). This module is employed for both subtransmission and distribution systems. This subsection derives mathematically the sensitivity equations for subtransmission delivery points (the same applies to distribution delivery point indexed as lowercase digits).

Therefore, this sensitivity analysis identifies the zones of the network, from the perspective of a delivery point, that insert the highest influence on substation and network reliability at the operational point. In other words, it addresses, from the reliability point of view, the most sensitive parts of the network for upgrade and replacement, forming the most eligible areas for investment.

After inspection, the partial derivatives of the unavailability at layer III correspond to the slope of the same in the slope-interception form, when determining one block as the variable and the other blocks as constant (thus setting the operational point). These slopes, at the given operational point, show the degree of influence that an improvement in the variable block has on the delivery point (layer III).

Analytically, the partial derivatives of Equation (22) in relation to each variable (block) are:

$$m_A = \frac{\partial U_{III}}{\partial A} = 1 - B - C + BC \tag{37}$$

$$m_B = \frac{\partial U_{III}}{\partial B} = 1 - A - C + AC \tag{38}$$

$$m_C = \frac{\partial U_{III}}{\partial C} = 1 - A - B + AB \tag{39}$$

For ABC substations, and:

$$m_A = \frac{\partial U_{III}}{\partial A} = D - BC + BCD \tag{40}$$

$$m_B = \frac{\partial U_{III}}{\partial B} = D - AC - CD + ACD \tag{41}$$

$$m_C = \frac{\partial U_{III}}{\partial C} = 1 - AB - BD + ABD \tag{42}$$

$$m_D = \frac{\partial U_{III}}{\partial D} = A + B - BC + ABC \tag{43}$$

For ABCD substations, in which:

$$\forall A, B, C, D <<< 1, \qquad 0 < m_x < 1 \tag{44}$$

m_x slope of the independent variable (block) [p.u.]

Equations (34)–(43) are valid under the principle that the total unavailability is much less than one [Bil92]. This is true, for the annual outage time of all considered individual equipment in this research, normalized over the year, is much less than the unit. The slope m_x can be represented as the angle of incline from the relation:

$$\theta_x = \arctan(m_x) \qquad 0 < \theta_x < 45^\circ \tag{45}$$

θ_x angle of incline of the slope m_x [$^\circ$]

It is important, nonetheless, to add that, as in the Reliability Module, the Sensitivity Module runs for each substation individually and should be performed for each scenario. This is necessary to set the several operational points for each delivery point in every scenario. Nevertheless, it is possible to assess the average sensitivity by employing the annual unavailability at layer III.

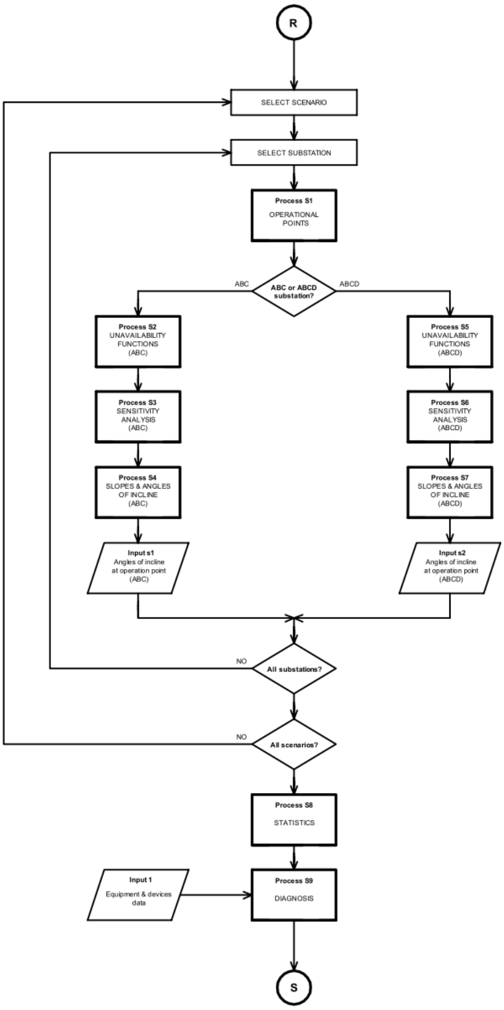

Figure 18. Flowchart of the Sensitivity Module.

Inputs & outputs

The inputs in the Sensitivity Module are (Figure 18), in addition to **Input 1** from the Network Cost Module in *Chapter II*, and input **R**, from the Reliability Module:

Input s1 (*Angle of incline at operation point – ABC substations*): angle of inclines, θ, of blocks A, B and C at the scenario operation point.

Input s2 (*Angle of incline at operation point – ABCD substations*): angle of inclines, θ, of blocks A, B, C and D at the scenario operation point.

S (*Output for the Sensitivity Module*) returns all parameters, coefficients and values related to the sensitivity analysis for each substation during all year scenarios.

Processes
And the processes in this part of the algorithm are (Figure 18):

Process S1 (*Operational points*) determines the operational point in every scenario for all delivery points. This is achieved by selecting which of the blocks will be set as the independent variable and the other blocks are fixed, thus the fixed operating point at the given conditions is determined by each scenario and substation.

Process S2 (*Unavailability functions – ABC substations*) returns the unavailability at layer III, (22), for each delivery point for ABC substations.

Process S3 (*Sensitivity analysis – ABC substations*) calculates the slopes of each block, (37)–(39), at the determined operation point for ABC substations.

Process S4 (*Slopes & angles of incline – ABC substations*) calculates the angles of incline of each block using (45) for ABC substations.

Process S5 (*Unavailability functions – ABCD substations*) returns the unavailability at layer III, (22), for each delivery point for ABCD substations.

Process S6 (*Sensitivity analysis – ABCD substations*) calculates the slopes of each block, (40)–(43), at the determined operation point for ABCD substations.

Process S7 (*Slopes & angles of incline – ABCD substations*) calculates the angles of incline of each block using (45) for ABCD substations.

Process S8 (*Statistics*) manipulates all unavailabilities obtained so far throughout this algorithm (blocks, layers, substations and network) and calculates statistical measures (mean, range, standard deviance and variance) for comparison.

Process S9 (*Diagnosis*) compiles and treats the statistical measures from Process S8 AS to determine possible alternatives for zones of low reliability or high deviation in relation to the other parts of the tested network. This process must include project parameters and definitions, network requirements established by the designing team and the costs of these possible solutions.

This process indicates the block or blocks with higher influence on the delivery point unavailability and suggests prospective solutions to improve reliability, for instance (not limited to):

- block A: including more inter-network connections, installing more generation units;
- block B: installation of underground cables;
- block C: upgrading to equipment GIS, upgrading to double-busbar substation;
- block D: installing more generation units.

In parallel with this process, a viability study must be performed in order to support and economically assess the suggested alternatives to the zones of low reliability. This thesis suggests that UGCs subsume a more reliable alternative to subtransmission networks and also constitute a more immune alternative to external factors than OHLs; however, it is, overall, in subtransmission networks, the costliest solution in the context of the Nordic countries. Moreover, in subtransmission networks, some eligible alternatives might be located downstream, *i.e.*, close to the end-customer; for example, in the distribution networks, by adding reserve connections or upgrading protection from manual to remote. Conversely, some alternatives at this level might not offer benefits, *e.g.*, installing generation plants in the MV networks might introduce complicated technical constraints and offer only minimal improvements on reliability (**Publication V**), thus being more suited to subtransmission level. This is only possible in distribution networks with smart grid features.

Select scenario is the same as in the Network Cost Module.

Select substation is the same as in the Reliability Module.

The Sensitivity Module segregates substations according to their block-layer structure (ABC or ABCD). This is necessary, for the processes involved include different equations, regarding substation type.

IV. The Voltage Sag Assessment

IV.1 The Voltage Sag Distribution Model

Faults that originate in meshed networks with several line connections propagate through multiple paths as voltage sags, molded by the electrical features of the involved network components, and may cause power quality issues to customers connected at different part of the network. Due to the intermediate location in the power system and the length of its intra-network connections, voltage sags in subtransmission account for a small number of events that propagate through its LV customers. According to the local utility company, on average one voltage sag per year originates from its subtransmission network; however, it has a high chance of reaching all of its LV customers, as subsequently demonstrated.

A voltage sag is characterized by duration and magnitude and depends on its position in the grid [Hei05]. The method developed here acknowledges these three factors to explicate a voltage sag distribution function for urban meshed subtransmission networks. These factors are used in the reliability assessment and the network planning and operation in a simplified, yet accurate manner. The distribution function is determined to be able to cope with the several scenarios and iterations of the reliability analysis, also extending to network planning algorithms, without causing any additional computational burden on the entire assessment.

IV.1.1 Considerations for the subtransmission networks

The model developed in this chapter is particularly applicable to urban meshed subtransmission networks. This implies a number of considerations that must be necessarily taken into account. These types of network are assembled in mesh, in urban areas (thus consisting of short/medium-length underground or/and overhead connections) and in the intermediate position in the power system (*i.e.*, subtransmission). It is important to mention that in meshed networks containing short or medium-length lines, the largest impedances belong to the transformers. This is easily proven by observing the average impedance between the short/medium lines (any transfer element in the network impedance matrix) and the HV/MV transformers (*e.g.*, the values given in **Appendix A.1**).

Figure 19 depicts an overall view of the Nordic power systems considered in this research which is characterized by [Hei03]:

- transmission (EHV) system: 400 kV, looped or meshed, impedance-grounded neutrals or solidly grounded;
- subtransmission (HV) system: 110 kV, meshed, impedance-grounded neutrals or ungrounded;
- primary distribution (MV) system: 20 kV, radial or radially operated, neutral compensated or ungrounded;
- secondary distribution (LV) system: 0.4 kV, radial or radially operated, solidly grounded;
- EHV/HV transformers: YNyn0d;
- HV/MV transformers: YNd11;
- MV/LV transformers: Dyn11.

In addition, circuital parameters utilized for the Nordic subtransmission network are found in **Appendix A.1**. Figure 19 also exhibits the five key points, listed from A to E, at which residual voltages are obtained from a given fault in the HV network.

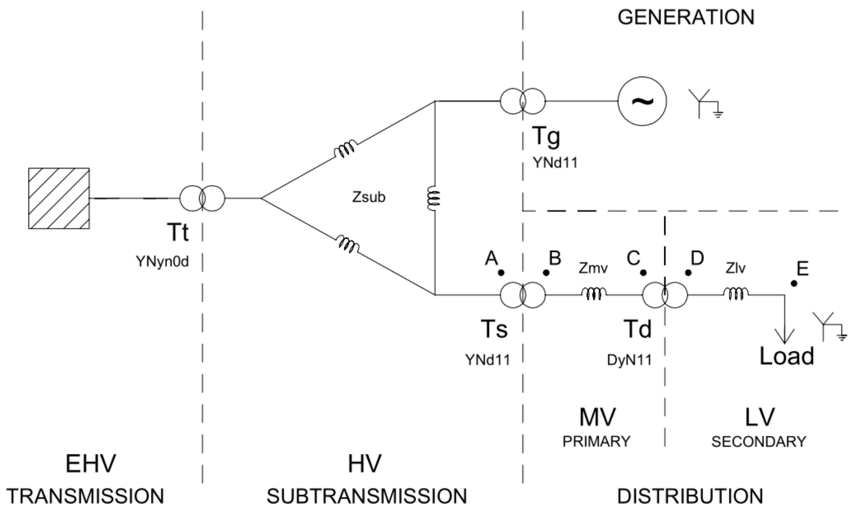

Figure 19. Diagram of the Nordic power systems and its networks and five key points in the calculation of residual voltage.†

The focus of the Voltage Sag Module is to identify the effect of voltage sags originating in the test subtransmission network on its delivery points (HV, MV and LV downstream customers). Therefore, only faults originating within this

†*D, n and y refer to delta-connected, neutral-grounded and wye-connected systems, respectively, and the uppercase letters indicate the primary side while lowercase letters, the secondary side.*

network will be computed and accounted for in this research and will be calculated at point B, *i.e.*, at the subtransmission delivery point. In addition, this module also calculates the initial symmetrical short-circuit currents and the peak short-circuit currents from the symmetrical short circuits for each substations whose limits, for this test network, is 40 kA and 100 kA respectively [Sou13],[Sou14].

Protection philosophy

An essential factor to be included in this study is the protection philosophy adopted in the network. Mostly, it is important to assess the switching time, to determine the threshold of the residual voltage from the voltage tolerance curve of voltage sags originating in the subtransmission network, and the existence of auto-reclosure, to estimate the number of trippings per fault. Additionally, instantaneous and momentary faults are cleared by RARs, temporary faults, by DARs, and longer faults are considered permanent, being out of service for the repair time.

Table II shows the number of trips for faults cleared by RAR, DAR and permanent faults. This module considers one or two trips from DAR, as common practice in several countries [Lak03] and a time-delay of between one and two minutes [Ren08]. In addition, all faults in networks that contain only underground cables are considered permanent, hence only one tripping per fault. This must be acknowledged due to the fact that auto-reclosure in networks with underground cables mechanically stresses the insulation structure of cables.

TABLE II. TOTAL NUMBER OF TRIPS (VOLTAGE SAGS) ACCORDING TO CLEARING MECHANISM

Clearing mechanism	Overhead & mixed networks	Underground networks *
RAR	*1*	–
DAR	*2 or 3*	–
Permanent	*3 or 4*	*1*

*All faults are considered permanent

Auto-reclosure is a common practice associated in avoiding long outages (thus interruptions in supply for the end-customer), particularly in cases, for instance, in transmission and subtransmission overhead networks, where a small portion of the total fault share are permanent faults [Eur14b],[Hei03]. However, permanent faults will be replaced by three or four voltage sags for a large part of the subtransmission network and depending on the customer category and weather scenario, auto-reclosure might imply higher customer related costs (outage plus voltage sag costs) than networks without auto-reclosure.

One other solution utilizing reclosure in distribution networks, named fuse saving, works by having a recloser clearing transient faults in the presence of slow fuses [Bol00]. This avoids the operation of sacrificial devices.

IV.1.2 Voltage sag propagation

Voltage sags from symmetrical short circuits propagate to the end-customer unchanged; conversely, it is not the case for unsymmetrical faults. In order to establish the residual voltage in the delivery point (in the subtransmission and distribution networks), the calculated component voltages, from **Appendix E**, must be transferred across the transformers, thus estimating the propagated residual voltages in the secondary terminals. The effect of transformer winding connections is calculated from the matrix scalar product [Hei05]:

$$\mathbf{u}_{\mathbf{sec}} = [T][A][T]^{-1}\,\mathbf{u}_{\mathbf{pri}} \tag{46}$$

Where:

$$[T] = \begin{bmatrix} 1 & 1 & 1 \\ 1 & \mathrm{a}^2 & \mathrm{a} \\ 1 & \mathrm{a} & \mathrm{a}^2 \end{bmatrix} \tag{47}$$

$$[A] = \begin{bmatrix} \mathrm{A}(1,1) & 0 & 0 \\ 0 & e^{j\varphi} & 0 \\ 0 & 0 & e^{j(-\varphi)} \end{bmatrix} \tag{48}$$

a	Fortescue operator
$\mathbf{u}_{\mathbf{pri}}$	residual voltage vector at the transformer primary terminals [p.u.]
$\mathbf{u}_{\mathbf{sec}}$	residual voltage vector at the transformer secondary terminals [p.u.]
φ	phase-shift angle of transformer class [rad]
$[A]$	transform matrix of the transformer in focus
$[T]$	sequence-to-phase component transform matrix
$[T]^{-1}$	phase-to-sequence component transform matrix

The angle φ corresponds to the phase-shift angle, specified by each transformer class, caused to the voltage sags propagated over the transformer. And the element A(1,1) from (48) corresponds to whether the subtransmission zero sequence impedances are connected to the transformer (equals one) or not (equals zero) [Hei05].

In Finland and in several other countries, the distribution systems are radial or radially-operated; therefore, the residual voltages from the voltage sags from the subtransmission network that propagate to the distribution networks will always be lower than on the secondary side of the HV/MV transformers. The voltage sag distribution function for subtransmission networks will be calculated at point B, from Figure 19, due to the fact that distribution feeders significantly vary in length (from a dozens of meters up to a dozen of kilometers) and the large number of secondary substations. This denotes a relatively conservative approach to this model and inserts independency from distribution network data. One other approach, without data of the MV and LV feeders, is to calculate residual voltages at point B and establish a pessimist scenario by setting points C, D and E, from the same figure, according to the maximum voltage drop allowed at each of these feeders, *e.g.*, 4 % in the MV and 6 % in the LV network [Hyv08].

IV.1.3 Derivation of the voltage sag distribution function

In this context, the voltage sag distribution refers to the distribution of residual voltages below the defined limit, *i.e.*, voltage sag, within the test network, either at each substation or by each fault type, in a given scenario. To each voltage sag event is attributed a penalty determined by customer category to estimate an approximate cost burden from this event.

First, the failure rates in the inter-substation connections must be estimated. Then they are translated into voltage sag rates, as the relation:

$$\lambda_{ir}\big|_{a,b} = \sum_{i=1}^{N}\sum_{r=1}^{N}\left(\frac{\lambda_{inter.subst_{ir}}\big|_{a,b}}{2}\right), \quad \forall i \neq r \tag{49}$$

And:

$$v_{ir}\big|_{a,b} = \mathrm{n_{trip}} \cdot \lambda_{ir}\big|_{a,b} \tag{50}$$

$\mathrm{n_{trip}}$	number of trips given fault duration
$\lambda_{inter.substir}$	failure rate in the inter-substation connection *ir* [occ/season]
λ_{ir}	total inter-substation failure rate [occ/season]
v_{ir}	total inter-substation post-fault residual voltage rate [occ/season]

The post-fault residual voltage rate constitutes the number of residual voltages due to faults in the network. It is imperative to distinguish this from the voltage sag rate because the latter corresponds to the residual voltages below the limits specified in the voltage tolerance curve. Both the failure rate and the post-fault residual voltage rate in (49) and (50) are distributed according to fault type, *a* (1-ph-gr, 2-ph, 2-ph-gr and 3-ph), and fault duration, *b* (momentary, temporary and permanent). The shares of fault type and duration in this study can be found in **Appendix B.1**. In addition, the denominator of (49) is 2 to indicate that half of the faults, thus the length, in the inter-substation connections is linked to the substation under consideration (**Publication I**).

The post-fault residual voltage distribution by fault type (v_a), in occ/season, is given as:

$$v_a = \sum_{b=1}^{3}\sum_{i=1}^{N}\sum_{r=1}^{N} \mathrm{P_a}\big|_{\mathrm{b}} \cdot v_{ir}\big|_{a,b} \tag{51}$$

And the in the entire network in focus (v_{net}), in occ/season:

$$v_{net} = \sum_{a=1}^{4} v_a = \sum_{i=1}^{N} v_i \quad (52)$$

$P_{a|b}$ share of fault type a given fault duration b

v_i post-fault residual voltage distribution in substation i [occ./season]

Equation (51) computes the distribution of fault shares, both according to type and duration, in all lines within the subtransmission network to return the distribution of post-fault residual voltages by each fault. The summation of these values for the four considered fault types will return the total network rate (52). From these two equations, the concept of severity coefficient must be introduced to estimate the voltage sag distribution within the test network at the delivery points.

Severity coefficient (ρ)

When calculating the propagation of a voltage sag through the transformer, the residual voltages in the secondaries are in fact the most relevant figures from the point of view of the end-customer. In the urban perimeter, the average length of distribution MV feeders is not higher than a couple of kilometers, so the voltage drop between the secondary of the HV/MV transformer and the secondary of the MV/LV transformer can be neglected. Therefore, the severity coefficients for urban subtransmission networks at these two secondaries can be approximated as being the same.

$$\rho_a = \frac{v_{net}\big|_{a,tolerance}}{v_{net}\big|_{a}} \quad (53)$$

$v_{net}|_{tolerance}$ post-fault residual voltage sag below the tolerance [occ/season]

ρ_a severity coefficient for fault type a

The severity coefficient, determined in **Publication I**, is compiled in Table III for points A and D from Figure 19. These values followed the above mentioned considerations for the Nordic power systems. For the considered time window of 60 ms to 200 ms, residual voltages above the limit of 70 % of the nominal voltage are tolerated [Nai12].

TABLE III. SEVERITY COEFFICIENT (ρ_a)

Position	**Fault type**			
	1-ph	**2-ph**	**2-ph-gr**	**3-ph**
Point A	*1*	*0.50*	*0.90*	*1*
Point D*	*0*	*0.50*	*0.95*	*1*

*Coefficient depends on the transformer winding connections

The severity coefficient is the rate of the number of post-fault residual voltage sags below the limit from the voltage tolerance curve divided by the total number of post-fault residual voltages due to faults in the network. The coefficient is distributed per fault type.

From that, the conversion from post-fault residual voltage rate to voltage sag rate is:

$$\mu_{net} = \rho_a \cdot \nu_{net}\big|_a \tag{54}$$

Similarly:

$$\mu_{net} = \sum_{a=1}^{4} \rho_a \cdot \nu_a \tag{55}$$

μ_{net} network voltage sag rate [sag/season]

Table III denotes that single-phase-to-ground faults are not perceived as voltage sags downstream to the HV/MV and MV/LV transformers due to their winding connections [Hei05], hence the coefficient for this fault type is zero. One other remark is that the coefficient increased from 0.9 to 0.95 in two-phase-to-ground faults. This is explained by the fact that a number of the voltage sags oscillate around 70 % of the nominal voltage when propagated to points B, C and D.

As an overall observation in the estimation of this coefficient, virtually all the three-phase short circuits occurring within this type of subtransmission network will propagate as voltage sags to the end-customer. This is explained by the short inter-substation connections. It is important to mention that this severity coefficient is only applied to urban meshed subtransmission networks and the focus of this technique is only to segregate residual voltages below the voltage tolerance curve under the described conditions.

IV.2 The Voltage Sag Module

The Voltage Sag Module synthesizes network data from the Reliability Module in addition to data specifically processed for this module (Figure 20). This module computes customer penalties, voltage sag rates, failure rates and demanded load and it returns the voltage sag distribution function for the tested network to serve as input for the estimation of the voltage sag cost.

Figure 21 schematizes the processes and parameters involved in this module. This part of the assessment is crucial for any systematic economic evaluation of underground and overhead networks.

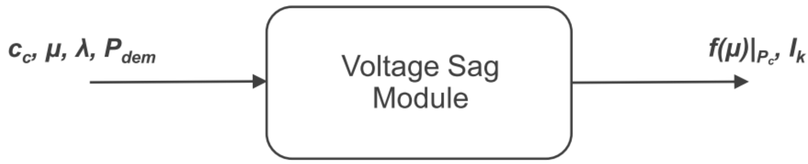

Figure 20. The Voltage Sag Module collects relevant information and data from the network under consideration and returns the distribution voltage sag functions and short-circuit levels at each delivery point given the customer category.

Inputs & outputs

The inputs and outputs of the Voltage Sag Module are (Figure 21), in addition to input **R**, described in *Chapter III*.

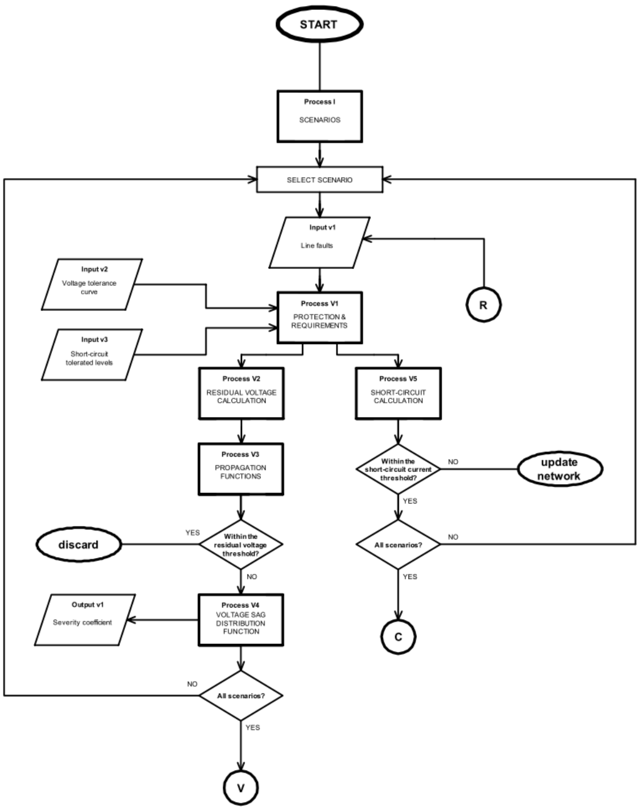

Figure 21. Flowchart of the Voltage Sag Module (left branch: voltage sags; right branch: short circuits).

Input v1 (*Line faults*): statistics from the line faults in the tested network. This input compiles information from the topology and the type of lines in each scenario.

Input v2 (*Voltage tolerance curve*): the voltage tolerance curve for the residual voltages. This is indispensable information in order to define voltage sags from the intra-network connections given sag duration and magnitude.

Input v3 (*Short-circuit tolerance levels*): the tolerated symmetrical short-circuit currents for the existing protective apparatus in the network provided by the manufacturer. This module utilizes 40 kA and 100 kA for the initial symmetrical short-circuit currents and the peak short-circuit currents.

Output v1 (*Severity coefficient*): the figures for the severity coefficient in the primary and secondary sides of the HV/MV transformers, regarding transformer class and network topology.

C (*Output for the Voltage Sag Module – short circuit*) returns the initial symmetrical short-circuit currents and the peak short-circuit currents for each substation. In case these values exceed the specified limit, this module suggests that the network must be upgraded or redesigned.

R (*Input for the Reliability Module – reliability indices*) compiles all possible reliability indices [Bol06],[Iee12] based on the number of customers, probability of unavailability, curtailed load, unavailability, equivalent failure rate and equivalent repair time in all blocks and layers from each delivery point (substation).

V (*Output for the Voltage Sag Module – voltage sag rate*) returns the voltage sag distribution function for the given network at all year scenarios.

Processes

And the processes in this part of the algorithm are (Figure 21) in addition to Process I from the Network Cost Module in *Chapter II*:

Process V1 (*Protection & requirements*) adopts the principles of the protection philosophy engaged, stores the voltage tolerance curve and sets requirements for the tested network. This process assumes the conjecture that the tested network is located in urban areas (short or medium intra-network connections, up to a couple of dozens of kilometers) and consists of either UGCs, OHLs or a mix of them. It also processes the HV/MV transformers class and the voltage sag duration within the network is equal to the circuit breaker switching time (for 110-kV networks, between 60 ms and 90 ms [And99]).

Process V2 (*Residual voltage calculation*) calculates the residual voltage sags from the four fault types considered in this study (*vide* **Appendix E**) within the subtransmission network.

Process V3 (*Propagation functions*) propagates the residual voltage calculated in Process V2 to the secondary side of the HV/MV transformer, *i.e.*, at the subtransmission delivery point, using Equations (49)–(52).

Process V4 (*Voltage sag distribution function*) constructs the voltage sag distribution function for the entire tested network firstly at the primary and secondary sides of the HV/MV transformer and, given the availability of data from the distribution networks, for the primary and secondary sides of the MV/LV transformer. The resulting values from this process are used in the determination of the severity coefficient of the network under analysis. This coefficient expressed for the four fault types studied greatly depends on the transformer vector groups present and grounding practices in the study. As common practice, Dyn transformers are used in secondary substations and YNyn or YNd transformers, in the primary substation, the values tabled in **Appendix B.1** can be utilized with minimal loss of accuracy.

Process V5 (*Short circuit calculation*) calculates the initial symmetrical short-circuit currents and the peak short-circuit currents for every substation in the network respecting the rated limits. The equations employed are detailed in **Appendix E.2**.

Select scenario is the same as in the Network Cost Module.

The Voltage Sag Module only processes faults that originate from the intra-network connections, *i.e.*, from the HV underground cables and HV overhead lines. This occurs in order to assess the differences between underground and overhead networks. Nonetheless, this model can be expanded to compute any fault originating in any main devices within the tested network (transformers, circuits breakers and busbars). Moreover, this module obtains the voltage sag distribution function for the entire tested network, unlike the other modules in which all values are first estimated for each substation individually and then averaged for the entire network.

V. Discussion

V.1 Results & Discussion

The typical 110-kV Nordic subtransmission network constitutes a rich example to be studied, for it encompasses multivariate features, both in quality and quantity, that directly affect system reliability. For instance, it embodies underground cables and overhead lines in both single and double circuits (sharing the same towers); AIS and GIS substation equipment; a vast number of inter-substation connections ranging from two to ten per substation; EHV/HV, HV/HV and MV/HV inter-network connections; as well as local generation in three substations with high output variance throughout the year.

Reliability assessment of subtransmission networks

In the assessment of the Nordic subtransmission networks, the most evident difference resulted from ABC and ABCD substations. ABCD substations (with local generation) are more reliable than the ABC ones, independently of the total number of inter-substation connections or the type of connections (UGC or OHL), as shown in **Publications II** and **III**. This is explained from the fact that under contingency in any of the inter and intra-network connections, blocks A and B respectively, the delivery points of ABCD substations will still be integrally or partially served by the local generation (block D). Moreover, this local generation, depending on the area of contingency, will also be able to supply other substations (the network must allow islanded operation mode).

Substation arrangement also has a strong influence on reliability, particularly for ABCD substations. In these, block C (the substation equipment) is the crossing point of the two possible paths from source to load (A-B-C and D-C), thus containing the largest influence. In ABC substations, block C has the same influence as the other two blocks, for they are series-connected paths from source to load. **Publication VI** detailed all the calculations about the influence of blocks, proving this statement. However, upgrading a single-busbar substation to a double-busbar substation incorporates major improvements to both substation types. This is explained by the fact that when adding parallel paths (from single to double busbar), this part of the system can still operate during a higher failure order. For instance, using data for AIS 110-kV busbars, this upgrade would mean a decrease from 68.4 min/a to 0.0089 min/a of unavailability in this equipment, hence improving the reliability of the entire block C and substation. Table IV shows the annual unavailabilities for substation 20 (ABC substation) and substation 2 (ABCD) at the substation (block C) and delivery point (layer III). These results confirm the strong influence of block C on the delivery point unavailability in both substation types.

TABLE IV. ANNUAL UNAVAILABILITY IN MIN/A – BLOCK C

Position	Substation type			
	ABC sing.	ABC doub.	ABCD sing.	ABCD doub.
Block C	*39.62*	*$2.01 \cdot 10^{-2}$*	*39.62*	*$2.01 \cdot 10^{-2}$*
Layer III*	*39.64*	*$4.19 \cdot 10^{-2}$*	*39.62*	*$2.01 \cdot 10^{-2}$*

One other alternative is to replace AIS equipment by GIS; in the case of 110-kV busbars, the improvement would decrease from 68.4 min/a to 45.6 min/a. The number of transformer bays can also change reliability. This situation was not directly investigated in this thesis, since the test network is comprised of only two-transformer bay substations. The test network in **Publication II** includes one-transformer and three-transformer bay substations. One-transformer bay substations have high unavailability, explained by the same reasons as single/double-busbar arrangement substations. Conversely, two or more bays do not differ in availability. This is so because in the case of a single transformer failure, the other transformers are dimensioned to withstand overloading, fulfilling project criteria. The improvement in this circumstance would be altering the switching time of the existing MV breaker or disconnector between the MV side of the substation.

The type of network, represented by block B, is fundamental in determining network reliability and costs. Block B is best characterized by the type and number of inter-substation connections. These features do not only affect the reliability assessment but also are strongly tied to the delineation of the voltage sag distribution in the test network. **Publication VI** elucidates the alternatives in the number of inter-substation connections and type of network.

Table V shows the impact of adding parallel inter-substation connections (5 km, OHL) between substation 2 (ABCD) and substation 20 (ABC). The annual unavailabilities for layer III converge very rapidly, mostly after installing three or more connections. The ABCD substation remained immune to alterations in block B.

TABLE V. ANNUAL UNAVAILABILITY IN MIN/A – BLOCK B

Position	Number of inter-substation connections				
	1	2	3	4	5
Block B	*1285.9*	*3.15*	*$7.7 \cdot 10^{-3}$*	*$1.9 \cdot 10^{-5}$*	*$4.6 \cdot 10^{-8}$*
Layer III (ABC)	*1325.8*	*42.76*	*39.64*	*39.62*	*39.62*
Layer III (ABCD)	*$2.0 \cdot 10^{-2}$*	*$2.0 \cdot 10^{-2}$*	*$2.0 \cdot 10^{-2}$*	*$2.0 \cdot 10^{-2}$*	*$2.0 \cdot 10^{-2}$*

The inter-network connections are the first path, from the perspective of the subtransmission system, from source to the delivery point. This results in a particular interest for improvements, as low-order failures at this point might cause interruption to the entire network, unlike the other three blocks, which have most impact on their connected substations. Block A is enunciated for the considered network and its requirements must also be set for the entire subtransmission network.

The Nordic subtransmission network contains several parallel inter-network connections with large power transfer capacity, thus including minimal risk to the network and large flexibility in injecting generated power (within its borders) into adjacent subsystems. As corroborated from Figure 9 in *Chapter III*, a low number of such connections corresponds to a high unavailability propagated to all substations within this network. Similarly, this can cause imbalances in the power flows across the network throughout the year. Table VI describes the improvements in terms of unavailability by adding parallel inter-network connections (one connection is not possible, for it does not supply the maximum load in the base year). The benefits seem marginal from installing more connections; however, the inclusion of more inter-network connections decreases the probable power not supplied by diminishing the number of risk states, thus dampening the level of load curtailment in these states, and covers all HV substations.

TABLE VI. ANNUAL UNAVAILABILITY IN MIN/A – BLOCK A

Position	**Number of inter-network connections**				
	2	**3**	**4**	**5**	**6**
Block A	*$1.6{\cdot}10^{-2}$*	*$2.8{\cdot}10^{-6}$*	*$4.8{\cdot}10^{-10}$*	*$8.3{\cdot}10^{-14}$*	*$1.4{\cdot}10^{-17}$*
Layer III (ABC)	*39.65*	*39.64*	*39.64*	*39.64*	*39.64*
Layer III (ABCD)	*$8.3{\cdot}10^{-2}$*	*$6.7{\cdot}10^{-2}$*	*$6.7{\cdot}10^{-2}$*	*$6.7{\cdot}10^{-2}$*	*$6.7{\cdot}10^{-2}$*

Sensitivity analysis

The Sensitivity Module presented in *Chapter III* contains processes to identify bottlenecks in the network reliability and propose possible remedy actions to improve both in local and system levels through angles of inclines from the block equations at the determined operational point (one block as independent variable and the others are fixed as constant). The analytical investigation proposed in this thesis for the equations steering each of the four blocks and three layers in the two types of substation confirmed that the substation equipment, block C, produces the largest influence on the delivery point, proved by the angle of incline, approximately 45° in both ABC and ABCD substations. This implies that for any given change in the availability (similarly, unavailability), the subtransmission delivery point will directly experience an equivalent change.

In ABC substations, the angles of incline of the three blocks are virtually the same, around 45°. The explanation for that relies on the fact that these blocks lay in series with each other, hence representing equal influence on the delivery point. However, the physical structure and number of components that each of these blocks consists of are extremely variable: block B is comprised of all inter-substation connections, *i.e.*, all HV lines and related bay switchgear, while block C embodies only the substation equipment. A minor alteration to the latter block would most likely affect the delivery point more than a similar alteration to the first block. Deciding the areas for network improvement, in this type of substation, depends on the economic evaluation of the alternatives and equally on the simplicity and efficacy of each prospective alternative.

In ABCD-substations, the angles of inclines of the blocks indicate large variance, block C being the most influential of the four blocks. This block constitutes a strong effect on reliability, indicating that these devices involve the best location to invest on. Particularly, the installation of double-bus substations enhances the availability to the connected customers. Block D also plays an important role, particularly in the cases when block B is out of service, and, depending on the output of the local generation (block D), it will have an effect on the reliability of adjacent substations and as far as adjacent subsystems, in cases where power is exported outside the tested network. In the particular case of the Nordic subtransmission network, this occurs during the winter season when all CHP plants operate at their maximum output.

In ABCD-substations, blocks A and B present minimal influence, because of the presence of large parallel influxes of power into this network, via substations 1 to 5 and 25. The three EHV/HV transformers are each rated at 400 MVA, and the average generation within the network varies between 200 MW and 900 MW, which is significantly higher than the average power demand of 662 MW during winter. In addition, the level of redundancy of connections in this network is rather high. The average rate of connections per substation is about 3.23, each being rated from 82 MVA to 410 MVA. In this type of substation, the enhancement of reliability does not rely on blocks A (thus block D) and B, since it would be extremely costly to include connections or generation units, but on the improvement of block C, which is prone to cause interruptions, as indicated in Table VI.

The Sensitivity Module can be utilized to promote sensible investments in the grid in network planning, attempting to match the optimum operational point from the graph in Figure 22. This is a result of the assessment at local, network and system levels with segmented structure in time (two-dimensional time analysis) and space (cells, clusters, blocks and layers), and after each iteration, the algorithm tries to match the minimal point in the classical cost *versus* reliability curve given project specifications.

In addition, in a number of cases, the fulfillment of certain network requirements, such as the N-1 criterion, can be extreme and overestimated in part of or in the entire network, thus imposing an economic burden. This module can also assist this, by simulating the network or part of it in alternative operation points, offering network downgrading or reinforcement alternatives.

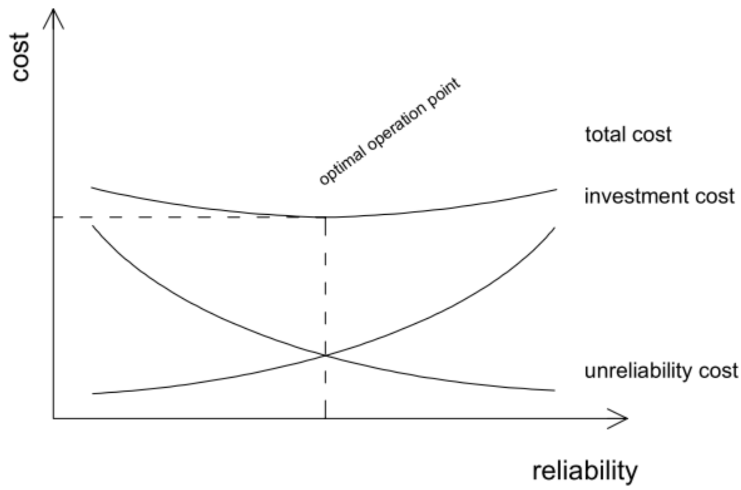

Figure 22. Classical reliability *vs.* cost curve. The curves represent how much an improvement in system reliability (x-axis) impacts on the total network cost (y-axis). In large networks, this relationship between investments and reliability tends to grow exponentially.

Reliability assessment of distribution systems

The block-layer structured reliability assessment was adjusted to distribution systems; however, several differences and particularities were observed. **Publications IV**, **V** and **VII** detailed those nuances with different approaches. The substation types were also kept unchanged, being given lowercase digits.

One of the major differences is the variety of topologies and possible feeder lengths employed in these networks. Rural distribution networks embody relatively long feeders, many times reaching distances above 10 km; on the contrary, urban distribution networks incorporate short feeders where the distances between secondary substations might be only a couple of hundred meters. Block b, *i.e.*, the feeders, must be strictly assessed at each MV substation to identify the main feeding point, the possible backup feedings and the nodes between sections of feeders. Moreover, the presence of reserve connections in radially-operated feeders greatly affects the availability to all distribution delivery points along them, as tested in **Publication VII**.

The second major difference is the apparent technical infeasibility in a number of distribution networks to include distributed generation directly connected to the MV feeders to improve reliability. The connection of CHP (the kind of eligible DG implemented in cold countries) to the primary distribution network revealed a conundrum for a fully-looped radially-operated underground network equipped with either a remote or manual disconnector. This occurs because under contingency in the feeder, the faulted feeder section waits for the related switching time to be isolated from the system, thus short-circuiting the CHP plant (this might last 15 minutes). This section of line would have to promptly be isolated, so that the CHP is still of benefit in this situation. If such fast switching were installed, the n.o. points of the network would also have to be closable in the same time frame, meaning that using distributed generation to avoid load curtailment during risk states would be negligible in terms of reliability.

From this, another major peculiarity was identified: the impact of the protection philosophy in distribution networks on the reliability of all secondary substations connected to the feeder. This is best represented by the average switching time of the MV disconnectors within the network. Depending on the disconnector technology utilized, whether it is manual, remote or automatic, the entire feeder experiences outage during the switching time. Uprating equipment, for instance, replacing strategic manual disconnectors with remote or automatic ones, can be extremely costly and might not be compensated over the project time by the savings from the outage costs. In distribution networks, feeders are connected to smaller loads, therefore the outage costs, even from longer periods of unavailability, might be still small compared to the other parts of the network cost function.

Voltage sag analysis

The voltage sag assessment in this thesis is specifically focused on urban meshed subtransmission networks due to the high probability of propagation of faults originating within them to downstream and adjacent systems, despite the presence of short/medium inter-substation connections. The largest factor influencing the number of voltage sags is the type of lines present in the network. Overhead lines in double circuits cause a very large number of faults, thus voltage sags, in particular during adverse scenarios. Underground cables, nevertheless, are relatively immune to weather-related failures, leading to low and homogeneously distributed fault and voltage sag rates.

Figure 23 confirms this with the distributions of the 110-kV Nordic network throughout the year scenarios. The tested network is comprised of about 110 km of OHL, consisting of about 93 km in double circuits, and 65 km of UGC. However, approximately 90 % of the total faults and 95 % of the total voltage sags, 0.5507 sag/a, originate in the overhead lines. Overhead lines aggregate an enormous voltage sag cost in comparison to underground cables. Networks employing auto-reclosure, not the case in this network, would probably show even higher voltage sag costs.

The calculated values for the severity coefficient were obtained for this test network and confirmed by analytical investigation from the set of equations described in **Appendix E**, for the time frame determined by the operation of the HV switchgear. For residual voltages below the limit of 70 % of the nominal voltage based at the secondary of the HV/MV substations, almost the totality of the ground faults propagate as voltage sags to the delivery points, while half of the short circuits (two-phase) propagated. The ground faults depend highly on the neutral connections in the network, and the severity coefficients in this thesis were determined for ungrounded networks. Furthermore, as previously described, single-phase-to-ground faults are not perceived as sags and the three phases, including the faulted phase, remained between 90 % and 100 % of the nominal voltage.

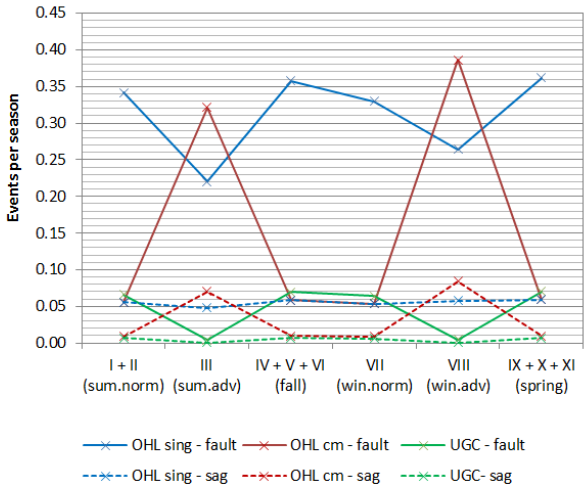

Figure 23. Distribution of voltage sags and faults originating from the Nordic subtransmission network in the eleven year scenarios (grouped in seasons), from OHL single faults, OHL common-mode faults and UGC faults.

Although symmetrical faults correspond to only 2 % and 5 % of the total failure rates in OHLs, during normal and adverse weather, respectively, and 10 % in UGCs, these faults were responsible for about 26 % of all voltage sags in this network. This share is high, since no single-phase-to-ground faults are counted and all the three-phase faults were considered as causing voltage sags. If the number of customers attached to the test subtransmission network is estimated to be approximately 200,000 MV and LV customers (consisting of 183,344 residential, 16,425 commercial & public and 137 industrial), this would result in approximately 1.72 million euros in the base year (95 % of that from OHLs).

Division of the base year

This thesis along with the associated publications showed the importance of framing network assessment into more detailed scenarios featuring load profiles and generation output, shaped by different seasons of the year, customer information and category as well as equipment parameters collected from the local utility company. Also, the division of the day into hourly-based resolution assisted the analysis of risk assessment, regarding load profile as well as time-variant failure rates.

The multidirectionality of power flows observed in meshed networks throughout the seasons determined different values for power losses when compared to a base-year analysis. Losses in the network are calculated with peak currents within the period under analysis and then squaring the rate between this peak current and the nominal current of the equipment under examination. The subdivision of the base year into several scenarios returns relatively more accurate values, not only for loss calculation, but also for outage and voltage sag costs. The total cost of losses in this network runs to around 0.5 million euros in the base year. If this value were 0.52 M€, calculated without the scenarios, in the

40-year project and 1 % of annual load growth, the loss costs would be 10.42 M€ instead of 10.02 M€. Raising the growth to 3 %, the difference between the costs with and without scenarios would rise to about 0.81 M€. This large power flow variation also determines the level of load to be curtailed under different risk states in the reliability assessment.

And, of major overall importance, the possibility to assess a project given different weather scenarios created a vast number of differences between overhead lines and underground cables, AIS and GIS, rural and urban networks, as well as subtransmission and distribution systems. This approach to the research problem, therefore, generated the need for remedial actions. It is essential, nonetheless, to process meteorological phenomena and the origin of faults from the histograms provided by electricity companies and regulators with care, particularly to avoid deviance from plausible results from data selection. This thesis interpreted weather types, as normal or adverse, using wind speed, number of rainy days and temperature (to assess whether it would be summer or winter), which are the main variables that meteorological institutes and research centers analyze, and the considered weather-related faults, from recorded events by the local utility, that greatly differ from operational and technical constraints.

Differences between UGCs & OHLs

The intrinsic features of overhead lines and underground cables in HV networks addressed several interesting findings from the analysis using the four modules of this study. The notorious influence of external factors, such as the weather and other natural phenomena, represents the largest influence on overhead networks and AIS substations; conversely, HV UGCs and GIS substations are practically immune to them. In the latter components, constructional and technical aspects as well as operational conditions incorporate the largest share of constraints. This is corroborated by data released by [Ene15a], [Eur14b], [Hyv08], [Kjø06] and the local utility company, for instance.

Publications I and **III** investigated these differences by examining exclusively underground or overhead networks and mixed networks. These differences were assessed at different points of the network (layers and blocks). In cases with mixed inter-substation connections, as is the case in the typical 110-kV Nordic subtransmission network, the natural tendency was for power to flow through the UGCs, for these are comprised of lower equivalent impedance, which compromised these connections mostly in high demand and high generation output seasons. In the case of a common-mode OHL failure that is a single failure in the double-circuited OHLs and is more likely to occur than a UGC failure (*vide* **Appendix B.1**), a large power transfer capacity is out of service (rated power from 281 to 410 MVA per OHL), thus raising the power transfer utilization rates of the remaining UGC connections (rated power from 75 to 210 MVA). These underground connections might become overloaded, thus triggering the overload line bay protection. During adverse weather conditions, such as storm or ice storm, this might cause cascading tripping. However, this is a phenomenon mostly observed in parallel or radial networks rather than in meshed.

The repair time for HV UGCs is quite large, 336 hours [Kaz11],[Sou12], in comparison to the HV OHLs, summing to 48 hours for permanent faults (only 2 %

to 5 % of the total fault distribution). The annual outage time for UGCs is 87 min/km.a, while for single-circuited and double-circuited OHLs the outage times are 7.36 min/km.a and 14.72 min/km.a, respectively. However, in substations with at least two connections, thus fulfilling the N-1 criterion, the annual outage time for block B becomes so low that the type of installed line does not affect the reliability at the delivery point. In addition, UGCs, due to the low failure rate, cause a low number of voltage sags (*vide* Figure 23).

Publication VI, on the other hand, targeted solutions particularly applied to block B in a viability analysis. The seven simulated cases showed that, in general, UGCs include large capital cost, but bring a lower voltage sag cost than from OHLs in HV networks. From this study, double-circuited OHLs correspond to the least inexpensive investments, but also have a negative impact on reliability, therefore on outage cost and particularly on voltage sag costs. The voltage sag rates and failure rates drastically increase with the length and type of connection utilized. Figure 24 breaks down the network cost into the five considered components for each of the seven simulated cases. Loss costs for the UCG cases are smaller than for the OHL cases, while investments are the opposite.

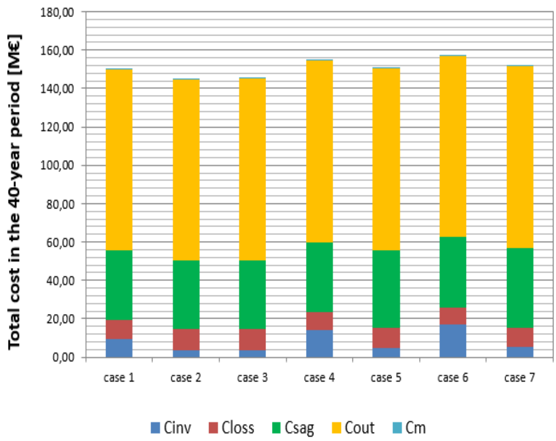

Figure 24. Total network cost over the 40-year project by case. Cases 2, 4 and 6 include UGCs to substation 15 and the other cases, OHLs to substation 15 from **Publication VI**.

The larger the number of connections is, despite line type, the higher is the availability at the delivery point. However, this improvement rapidly stagnates due to the influence of block C on the availability at layer III and to the redundancy inserted by added lines, implying that only higher-order failures will disturb the system, *i.e.*, improbable events. Another important remark is the lower total network losses when installing new UGCs; whereas, in the specific case of substation 15 (test substation in this study), this occurs to the contrary. This comes from the fact that UGCs embody lower impedances, given the same conductor cross-section, compared to OHLs, hence higher currents flow through these cables. Moreover, the installation of more parallel OHL connections increases the probability of voltage sags. However, this is highly dependent on the length and the number of circuits (for instance, single or double-circuited OHLs).

In addition, when assessing the total network cost only in the tested substation, UGC cases present a larger total cost than the cases with OHLs. However, investigating the total network cost in terms of line length, installing UGCs is not much costlier (note that the normalized rate is for the entire network, not only the tested substation). The values were, over the 40-year project time: 0.747 M€/km (case 1: two UGCs in substation 15), 0.748 M€/km (case 4: three UGCs in substation 15), 0.748 M€/km (case 6: four UGCs in substation 15) 0.721 M€/km (case 3: two double-circuited OHLs in substation 15), 0.724 M€/km (case 3: two UGCs in substation 15), 0.728 M€/km (case 5: three OHLs in substation 15) and 0.719 M€/km (case 7: four OHLs in substation 15). It is observed a difference of 0.029 M€/km was observed in the cases with four inter-substation connections.

V.2 Prospective Future Research on the Topic

The algorithm and its modules designed in this thesis the have potential to be applied to future research and other related applications. One prospective application is adapting the reliability assessment and cost functions in this work to network planning algorithms particularly focused on subtransmission network optimization. Also of value would, perhaps, be the development of a subtransmission network planning module in which topological data and real estate evaluation in the focused region are accounted for and normalized with the scenarios and parameters described in this thesis.

The developed method can be extended to assess subtransmission and distribution systems with island-mode operation possibility. Under this possibility, the investigation of the synchronization requirements should be carefully assessed as well as the coordination with adjacent systems via the reserve connections. Furthermore, this assessment should provide distinction between equipment that can and cannot operate in islanded mode. One other feature that can be developed is to include algorithm component ageing as well as maintenance strategies, creating for more diverse analysis. For that, it is indispensable to have access to detailed histograms of the failures in all main equipment and replacement/maintenance times.

V.3 Conclusions

The thesis described a comprehensive assessment of urban subtransmission networks from the perspective of power quality issues, reliability and economic impact. This work was based on the reshaping of the network cost function for the specific case of subtransmission networks by refining the reliability analysis and including the voltage sag cost.

The four modules of this thesis compiled statistical data, standards and planning requirements to evaluate existing networks and new projects in order to identify zones of low reliability and prospective areas for improvement and investment, in phase with the current regulatory recommendations. The Reliability Module includes an engineer-tailored technique to assess urban meshed subtransmission networks that, in addition, was expanded to distribution systems to provide accurate reliability indices to the end-customer. The Voltage Sag Module is comprised of the derivation of a voltage sag distribution function for the same type of network. From this, it inferred the severity coefficients, taking into consideration fault type, duration and location, as well as the intrinsic circuital parameterization of subtransmission networks. In combination, these two previous modules converge towards the Network Cost Module, *i.e.*, the network cost function itself. And as an ancillary tool, the Sensitivity Module was developed to identify and provide remedial alternatives to zones eligible for upgrade/uprate and zones of low reliability, low power quality and quantity.

As the core-structure of this analysis, the establishment of a two-dimensional time assessment of the base year brought great diversity to the analysis, thus assisting in the identification and diagnoses of low reliability or power quality in the tested network. The year scenarios proved to be fundamental in temperate regions where the weather imposes major influence on the power flows, generation, load, customer and network equipment itself. The daily scenarios geared more information from the customer and equipment behavior.

Upgrading or replacing substation equipment can be a technically challenging task and might not be viable, either economically or operationally, in several situations, despite being the most reliability-sensitive area for improvement. In network planning, networks with large loads or low reliability, for instance overhead parts of the network, should be eligible candidates for double-busbar arrangements and GIS equipment. Similarly, the cost of installing EHV/HV transformers is extremely high and does not, in this tested network, offer significant reliability improvement. However, in specific areas, for instance, the shift of the CHP plant of substation 2 directly to the transmission network via a new EHV/HV transformer brings advantages to other power quality issues, in this case, the alleviation of short-circuit levels in the subtransmission.

The choice between overhead lines and underground cables is a multilayered and complex work that requires more than just technical, operational and economical judgement to be evaluated. Several aspects must be acknowledged in this assessment; for instance, the high values of real estate in urban areas, the growing disapproval towards large industrial/utility facilities within urban areas and a growing concern about weather-related failures due to the increasing instability of meteorological phenomena predicted in the 21st Century. From the cost components employed in this research, HV underground networks have an economic disadvantage over HV overhead networks.

However, underground cables do emerge as an economically viable solution to urban meshed HV networks, bearing in mind the challenges imposed by the construction of OHLs in densely populated areas and the increasing cost of the land. The most eligible cases must be thoroughly simulated and well parameterized. The capital costs for UGCs in this study were based on installation in the ground. If tunnel installation is necessary, as it is often the situation in urban environments, these costs can be potentially higher.

From the network planning perspective, it is imperative to append that due to the high costs and penalties attributed to larger industrial and commercial customers, local regulators must establish a tight policy in order to protect all customers, regardless of category or location in the network, to guarantee societal wellbeing.

References

[Abd14] Abdi, S., Afshar, K., Ahmadi, S., Bigdeli, N., and Abdi, M. (2014). "Optimal recloser and autosectionalizer allocation in distribution networks using IPSO–Monte Carlo approach". Int. Jour. Electr. Power & Energy Syst., vol. 55, pp. 602–611.

[Aco10] Acosta, J. L., and Djokić, S. Ž. (2010). "Assessment of renewable wind resources in UK urban areas". In *Proc. 15th IEEE Mediterranean Electroctech. Conf.* (MELECON10). Valletta, Malta. April 26–28.

[Alb14] Alberta Electric System Operator (2014). *AOSE 2013 Long-Term Transmission Plan* [Report]. Available: http://www.aeso.ca as of June of 2015.

[All13] Allard, I., Olofsson, T., and Hassan, O. A. B. (2013). "Methods for energy analysis of residential buildings in Nordic countries". Renew. & Sust. Energy Reviews, vol. 22, pp. 306–318.

[Als73] Alsac, O., and Stott, B. (1973). "Optimal load flow with steady-state security". IEEE Trans. Power Apparatus & Syst., vol. PAS-93, no. 3, pp. 745–751.

[Alv01] Alves, M. F., and Fonseca, V. R. C. (2001). "Voltage sag stochastic estimate". In *Proc. 36th Indust. App. Conf.* (IAS11). Chicago, USA. September 30–October 4.

[Ama10] Amaral, T. S., Borges, C. L. T., and Rei, A. M. (2010). "Composite system well-being evaluation based on non-sequential Monte Carlo simulation". Electr. Power Syst. Research, vol. 80, pp. 37–45.

[And09] Andrade, W. S., Borges, C. L. T., and Falcao, D. T. (2009). "Integrated reliability evaluation of distribution and sub-transmission system incorporating distributed generation". In *Proc. Power Syst. Conf. & Expo.* (PSCE09). Seattle, USA. March 15–18.

[And99] Anderson, P. R. (1999). *Power System Protection* (1st ed). The Institute of Electrical and Electronic Engineers (IEEE), Inc. ISBN: 0-7803-3427-2.

[Ant03] Antila, E., Heine, P., and Lehtonen, M. (2003). "Economic analysis of implementing novel power distribution automation". In *Proc. Int. Symp. Qualit. Secur. Electr. Power Deliv. Syst. (QSEPDS03)*. Montréal, Canada. October 8–10.

[Aun06] Aung, M. T., and Milanović, J. (2006). "The influence of transformer winding connections on the propagation of voltage sags". IEEE Trans. Power Deliv., vol. 21, no. 1, pp. 262–269.

[Bak13] Bakkiyaraj, R. A., and Kumarappan, N. (2013). "Optimal reliability planning for composite electric power system based on Monte Carlo simulation using particle swarm optimization". Int. Jour. Electr. Power & Energy Syst., vol. 47, pp. 109–116.

[Bil01] Billinton, R., Fotuhi-Firuzabad, M., and Bertling, L. (2001). "Bibliography on the application of probability methods in power system reliability evaluation 1996–1999". IEEE Trans. Power Syst., vol. 16, no. 4, pp. 595–602.

[Bil04] Billinton, R., and Tang, X. (2004). "Selected considerations in utilizing Monte Carlo simulation in quantitative reliability evaluation of composite power systems". Electr. Power Syst. Research, vol. 69, pp. 205–211.

[Bil05] Billinton, R., and Acharya, J. (2005). "Consideration of multi-state weather models in reliability evaluation of transmission and distribution systems". In *Proc. Canadian Conf. Electr. & Computer Eng.* Saskatoon, Canada. May 1–4.

[Bil06] Billinton, R., and Singh, G. (2006). "Application of adverse and extreme weather: modelling in transmission and distribution system reliability evaluation". IEE Proceedings – Gen. Transm. & Distr., vol. 153, no. 1, pp. 115–120.

[Bil92] Billinton, R., and Allan, R. N. (1992). *Reliability Evaluation of Engineering Systems* (2nd ed). Plenum Press. ISBN: 0-306-44063-6.

[Bil94] Billinton, R., and Li, W. (1994). *Reliability Assessment of Electric Power Systems Using Monte Carlo Methods* (1st ed). Plenum Press. ISBN: 0-306-44781-6.

[Bil96] Billinton, R., and Allan, R. N. (1996). *Reliability Evaluation of Power Systems* (2nd ed). Plenum Press. ISBN: 0-306-45259-6.

[Bol00] Bollen, M. H. J. (2000). *Understanding Power Quality Problems* (1st ed). The Institute of Electrical and Electronic Engineers (IEEE), Inc. ISBN: 0-7803-4713-7.

[Bol06] Bollen, M. H. J., and Gu, I. Y. H. (2006). *Signal Processing of Power Quality Disturbances* (1st ed.). The Institute of Electrical and Electronic Engineers (IEEE), Inc. ISBN: 978-0-471-73168-9.

[Bol11] Bollen, M. H. J., Cundeva, S., Gordon, J. –M. R., Djokić, S. Ž., Stockman, K., Milanović, J. V., Neumann, R., and Ethier, G. (2011). "Voltage dip immunity aspects of power-electronics equipment – Recommendations from CIGRE/CIRED/UIE JWG C4.110". In *Proc. 11th Int. Conf. Electr. Power Qual. & Utilization* (EPQU11). Lisbon, Portugal. October 17–19.

[Bro09] Brown, E. R. (2009). *Electric Power Distribution Reliability* (2nd ed). CRC Press. ISBN: 978-0-8493-7567-5.

[Cha07] Chan, J. Y., and Milanović, J. V. (2007). "Severity indices for assessment of equipment sensitivity to voltage sags and short interruptions". In *Proc. Power & Energy Society Gen. Meet.* (PES07). Tampa, USA. June 24–28.

[Che05] Alsac, O., and Stott, B. (2005). "Identifying high risk N-k contingencies for online security assessment". IEEE Trans. Power Syst., vol. 20, no. 2, pp. 823–834.

[Con14] Connolly, D., Lund, H., Mathiesen, B. V., Werner, S., Möller, B., Persson, U., Boermans, T., Trier, D., Østergaard, P. A., and Nielsen, S. (2014). "Heat roadmap Europe: combining district heating with heat savings to decarbonize the EU energy system". Energy Policy, vol. 65, pp. 475–489.

[Cos11] Coster, E. J., and Houwelingen, D. van. (2011). "Integrating DG, peculiar planning challenges abound in the development of distributed generation in special horticultural areas". Transmission & Distribution World, vol. 63, no. 7, pp. 46–51.

[Cos14] Coster, E. J., and Boender, D. (2014). "Standardisation of MV substation configurations in HV/MV substations". In *Proc. 45th Cigré Session*. Paris, France. August 27–29.

[Djo05] Djokić, S. Ž., Milanović, J., Chapman, D. J., and McGranagham, M. F. (2005). "A new method for classification and presentation of voltage reduction events". IEEE Trans. Power Deliv., vol. 20, no. 4, pp. 2576–2584.

[Djo08] Djokić, S. Ž., and Bollen, M. H. J. (2008). "Dip segmentation method". In *Proc. 13th Int. Conf. Harmonics & Qual. of Power* (ICHQP08). Wollongong, Australia. September 28–October 1.

[Dug96] Dugan, R. C., McGranagham, M. F., and Beaty, H. W. (1996). *Electrical Power Systems Quality* (1st ed). McGraw-Hill, Inc. ISBN: 0-07-018031-8.

[Ene15a] Energiateollisuus. (2015). *Keskeytymistilasto 2014* [Interruption Situation 2014, from the Finnish Energy Industries, in Finnish]. Available: http://energia.fi/en/statistics-and-publications as of June of 2015.

[Ene15b] Energy Storage Association. *Energy Storage* [Case Studies]. Available: http://energystorage.org as of June of 2015.

[Ent12] Entriken, R., and Lordan, R. (2012). "Impacts of extreme events on transmission and distribution systems". In *Proc. Power & Energy Society Gen. Meet.* (PES12). San Diego, USA. July 22–26.

[Eti12] Etienne, C., and Beniston, M. (2012). "Wind storm loss estimations in the Canton of Vaud (Western Switzerland)". Nat. Hazards Earth. Syst. Sci., vol. 12, pp. 3789–3798.

[Eur11] European Commission (2011). *Smart Grids: from Innovation to Development* [Report]. Available: http://europa.eu as of June of 2015.

[Eur13] European Commission (2013). *Directive 2009/72/EC of the European Parliament and of the Council of 13 July 2009 Concerning Common Rules for the Internal Market in Electricity* [Report]. Available: http://europa.eu as of June of 2015.

[Eur14a] European Commission (2014). *Quarterly Report on European Electricity Markets* [Report]. vol. 3, no. 3. 3rd quarter of 2014.

[Eur14b] European Network of Transmission System Operators for Electricity - ENTSO-E (2014). *Nordic grid disturbance statistics 2013* [Report]. Available: http://entsoe.eu/publications as of June of 2015.

[Fin00] Fink, D. G., and Beaty, H. (2000). *Standard Handbook for Electrical Engineers* (14th ed). McGraw-Hill, Inc. ISBN: 0-07-022005-0.

[Fin13a] Finnish Energy Industries (2013). *District heating year 2012* [Report]. Available: http://energia.fi/en/statistics-and-publications as of June of 2015.

[Fin13b] Finnish Energy Industries. (2013). *Energy Year 2012: Electricity* [Report]. Available: http://energia.fi/en/statistics-and-publications as of June of 2015.

[Fin15a] Fingrid (2015). *Nordic power system and interconnections with other systems* [Article]. Available: http://www.fingrid.fi as of June of 2015.

[Fin15b] Finnish Energy Industries (2015). *Verkon rakenne* [Network construction, *in Finnish*]. Available: http://energia.fi/sahkomarkkinat/sahkoverkko as of June of 2015.

[Fin15c] Finnish Meteorological Institute (2015). *Wind Atlas*. Image captured from: http://tuuliatlas.fmi.fi as of June of 2015.

[Gau10] Gaun, A., Rechberger, G., Renner, H. and Lehtonen, M. (2010). "Enumeration based reliability assessment algorithm considering nodal uncertainties". In *the Power & Energy Society Gen. Meet.* (PES10). Minneapolis, USA. July 25–29.

[Gel09] Gellings, C. W. (2009). *The Smart Grid: Enabling Energy Efficiency and Demand Response* (1st ed.). CRC Pres. ISBN: 978-1-4398-1574-8.

[Goe05] Goel, L., Gupta, R., and Ercan, M.F. (2005). "Comparison of subtransmission system reliability worth for diverse systems by including health considerations". Electr. Power Syst. Research, vol. 74, pp. 65–72.

[Goe07] Goel, L., and Gupta, R. (2007). "Well-being reliability worth indices due to different customer outage cost functions". In *Proc. Int. Power Eng. Conf.* (IPEC07). Singapure. December 3–6.

[Gön08] Gönen, T. (2008). *Electric Power Distribution System Engineering* (2nd ed). CRC Press. ISBN: 978-1-4200-6200-7.

[Gon13] González-Fernámdez, R. A., Silva, A. M. L., Resende, L. C., and Schilling, M. T. (2013). "Composite system reliability evaluation based on Monte Carlo simulation and Cross-Entropy methods". IEEE Trans. Power Syst., vol. 28, no. 4, pp. 4598–4606.

[Gos08] Goswani, A. K., Gupta, C. P., and Singh, G. K. (2008). "An analytical approach for stochastic assessment of voltage sags in distribution systems". In *Proc. IEEE Region 10 Conf.* (TENCON08). Hyderabad, India. November 19–21.

[Gra94] Grainger, J. J., and Stevenson Jr., W. D. (1994). *Power System Analysis* (1st ed). McGraw-Hill, Inc. ISBN: 0-07-061293-5.

[Gre13] Green, R. C., Wang, L., Alam, M., and Singh, C. (2013). "Intelligent state space pruning for Monte Carlo simulation with applications in composite power system reliability". Eng. App. Artif. Intelligence, vol. 26, pp. 1707–1724.

[Gud11] Gudžius, S., Gecys, S., Markevicius, L. A., Miliune, R., and Morkvenas, A. (2011). "The model of smart grid reliability evaluation". Elektronika ir Elektrotechnika, vol. 10, no. 116, pp. 25–28.

[Haa13] Haakana, J. (2013). *Impact of Reliability of Supply on Long-Term Development Approaches to Electricity Distribution Networks*. Doctoral Dissertation. Dept. Electrical Engineering, Lappeenranta University of Technology. Lappeenranta, Finland.

[Had15] Haddadian, G., Khalili, N., Khodayar, M., and Shahiedehpour, M. (2015). "Security-constrained power generation scheduling with thermal generating units, variable energy resources, and electric vehicle storage for V2G deployment". Int. Jour. Electr. Power & Energy Syst., vol. 73, pp. 498–507.

[Ham15] Hamzeh, M., Vahidi, B., and Askarian-Abyaneh, H. (2015). "Reliability evaluation of distributed transformers with high penetration of distributed generation". Int. Jour. Electr. Power & Energy Syst., vol. 73, pp. 163–169.

[Haj14] Hajian-Hoseinabadi, H., Golshan, M. E. H., Shayanfar, H. A. (2014). "Composite automated distribution system reliability model considering various automated substation". Int. Jour. Electr. Power & Energy Syst., vol. 54, pp. 211–220.

[Hei02] Heine, P., Pohjanheimo, P., Lehtonen, M., and Lakervi, E. (2002). "A method for estimating the frequency and cost of voltage sags". IEEE Trans. Power Syst., vol. 17, no. 2, pp. 290–296.

[Hei03] Heine, P., and Lehtonen, M. (2003). "Voltage sag distributions caused by power system faults". IEEE Trans. Power Syst., vol. 18, no. 4, pp. 1367–1373.

[Hei05] Heine, P. (2005). *Voltage Sags in Power Distribution Networks*. Doctoral Dissertation. Dept. Electrical Engineering, Helsinki University of Technology. Espoo, Finland.

[Hel15] Helen Sähköverkko (2015). *Sähköverkko* [The Electricity Grid, *in Finnish*]. Available: http://www.helen.fi as of June of 2015.

[Hum13] Humayun, M., **Sousa, B. J. O.**, Degefa, M., Kazemi, S., and Lehtonen, M. (2013). "Markov model based assessment for redundancy mitigation in high voltage grids using demand response". Int. Rev. Electr. Eng., vol. 8, no. 4, pp. 1349–1362.

[Hum15] Humayun, M., **Sousa, B. J. O.**, Safdarian, A., Ali, M., Degefa, M. Z., Lehtonen, M., and Fotuhi-Firuzabad, M. (2015). "Optimal capacity management of substation transformers over long-run". IEEE Trans. Power Syst., vol. PP, no. 99, pp. 1–10, [*in Press*].

[Hyv08] Hyvärinen, M. (2008). *Electrical Networks and Economies of Load Density*. Doctoral Dissertation. Dept. Electrical Engineering, Helsinki University of Technology. Espoo, Finland.

[Iec01] IEC 60909-0 (2001). *Short-Circuit Current in Three-Phase A.C. Systems – Part 0: Calculation of Currents* [Standard]. (1st ed.) International Electrotechnical Commission (IEC).

[Iee07] IEEE Std 493-2007 (2007). *Design of Reliable Industrial and Commercial Power Systems* [Standard]. (Revision of IEEE Std 493-1997). The Institute of Electrical and Electronic Engineers (IEEE), Inc. ISBN: 0-7381-5301-X.

[Iee12] IEEE Std 1366-2012 (2012). *IEEE Guide for Electric Power Distribution Reliability Indices Systems* [Standard]. The IEEE Power & Energy Society. ISBN: 978-0-7381-7275-0.

[Iee98] IEEE Std 493-1997 (1998). *Design of Reliable Industrial and Commercial Power Systems* [Standard]. (1st ed.). The Institute of Electrical and Electronic Engineers (IEEE), Inc. ISBN: 1-55937-969-3.

[Int08] International Energy Agency (2008). *Combined Heat and Power: Evaluating the Benefits of Greater Global Investment* [Report]. Available: http://www.iea.org as of June of 2015.

[Int14] International Energy Agency (2014). *The IEA CHP and DHC Collaborative – CHP/DHC Country Scorecard: United States* [Report]. Available: http://www.iea.org as of June of 2015.

[Jal10] Jalilzade, S., and Bagheri, A. (2010). "A new approach for subtransmission system expansion planning with genetic algorithm". In *Proc. Int. Congr. on Ultra Modern Telecom. & Contr. Syst. & Workshops* (ICUMT10). Moscow, Russia. October 18–20.

[Jal14a] Jalali, M., Zare, K., and Hagh, M. T. (2014). "A multi-stage MINLP-based model for sub-transmission system expansion planning considering the placement of DG units". Int. Jour. Electr. Power & Energy Syst., vol. 63, pp. 8–16.

[Jal14b] Jalali, M., Zare, K., and Hagh, M. T. (2014). "Dynamic expansion planning of sub-transmission substations and defining associated service area". Electr. Power Syst. Research, vol. 116, pp. 218–230.

[Jär11] Järventausta, P., Verho, P., Partanen, J., and Kronman, D. (2011). "Finnish Smart Grids: a migration from version one to the next generation". In *Proc. 21st Conf. Electr. Distr.* (CIRED11). Frankfurt, Germany. June 6–9.

[Juá06] Juárez, E. E., and Hernández, A. (2006). "An analytical approach for stochastic assessment of balanced and unbalanced voltage sags in large systems". IEEE Trans. Power Deliv., vol. 21, no. 3, pp. 1493–1500.

[Kah12] Kahrobaeian, A., and Mohamed, Y. A.-R. I. (2012). "Smart control interface for robust operation of DG units in grid connected and islanded modes". In *Proc. IEEE PES Innov. Smart Grid Tech.* (ISGT12). Washington, USA. January 16–20.

[Kan08] Kanokbannakorn, W., and Saengsuwan, T. (2008). "The studies of a transmission system and distribution system voltage sags correlations". In *Proc. 5th Int. Conf. Electr. Eng., Electronics, Computer, Telecomm. & Inf. Tech.* (ECTI-CON08). Krabi, Thailand. May 14–17.

[Kar05] Karady, G. G., Saksena, S., Shi, B., and Senroy, N. (2005). *Effects of Voltage Sags on Lodas in a Distribution System* [Report]. Available: http://www.pserc.wisc.edu as of June of 2015.

[Kar11] Karaliolios, P., Sun, Y., Slootweg, J. G., and Kling, W. L. (2011). "Standardisation of MV substation configurations in HV/MV substations". In *Proc. Power & Energy Society Gen. Meet.* (PES11). San Diego, USA. July 24–29.

[Kaz11] Kazemi, S. (2011). *Reliability Evaluation of Smart Distribution Grids*. Doctoral Dissertation. Dept. Electrical Engineering, Aalto University. Espoo, Finland.

[Kha06] Khaitan, S., and McCalley, J. D. (2006). *System Topology Based Identification of High Risk N-k Contingencies* [Report]. Available: http://www.ece.cmu.edu as of June of 2015.

[Kil14] Kile, H., Uhlen, K, and Kjølle, G. (2014). "Scenario selection in composite reliability assessment of deregulated power systems". Int. Jour. Electr. Power & Energy Syst., vol. 63, pp. 124–131.

[Kjø06] Kjølle, G. H., Gjerde, O., Hjartsjø, B. T., Engen, H., Haarla, L., Koivisto, L., and Lindblad, P. (2006). "Protection system fault – a comparative review of fault statistics". In *Proc. 9th Int. Conf. Prob. Methods Appl. Power Syst.* (PMAPS06). Stockholm, Sweden. June 11–15.

[Kjø08] Kjølle, G. H., Samdal, K., Singh, B., and Kvitastein, O. A. (2008). "Customer costs related to interruption and voltage problems: methodology and results". IEEE Trans. Power Syst., vol. 23, no. 3, pp. 1030–1038.

[Küf13] Küfeoğlu, S, and Lehtonen, M. (2013). "A novel hybrid approach to estimate customer interruption costs for industry sectors". Scient. Research Eng., vol. 5, no. 10A, pp. 34–40.

[Küf15a] Küfeoğlu, S, and Lehtonen, M. (2015). "Comparison of different models for estimating the residential sector customer interruption costs". Electr. Power Syst. Resear., vol. 122, pp. 50–55.

[Küf15b] Küfeoğlu, S, and Lehtonen, M. (2015). "Interruption costs of service sector electricity customers, a hybrid approach". Int. Jour. Electr. Power & Energy Syst., vol. 64, pp. 588–595.

[Lak03] Lakervi, E., and Holmes, E. J. (2003). *Electricity Distribution Network Design* (2nd ed). The Institution of Electrical Engineers. ISBN: 0-86341-308-0.

[Lec07] Leckebusch, G. C., Donat, M., and Ulbrich, U. (2007). "European property damage potentials: development and application of simple storm regression model to global and regional simulations". In *RT6.2 Meeting*, Helsinki, Finland, April 26–27.

[Li05a] Li, W. (2005). *Probabilistic Transmission System Planning* (1st ed). John Wiley & Sons, Inc. ISBN: 978-0-470-63001-3.

[Li05b] Li, W. (2005). *Risk Assessment of Power Systems: Models, Methods and Applications* (1st ed.). The Institute of Electrical and Electronics Engineers, Inc. ISBN: 0-471-63168-X.

[Li11] Li, W. (2011). *The Smart Grid: Enabling Energy Efficiency and Demand Response* (1st ed.). CRC Pres. ISBN: 978-1-4398-1574-8.

[Mac10] MacIlwain, C. (2010). "Supergrid: is a vast undersea grid bringing wind-generated electricity from the North Sea to Europe in a feasible proposition or an overpriced fantasy?". Nature, vol. 468, pp. 624–625.

[Mah13] Mahapatra, K., Gustavsson, L., Haavik, T., Aabrekk, S., Svendsen, S., Vanhoutteghem, L., Paiho, S., and Ala-Juusela, M. (2013). "Business models for full service energy renovation of single-family houses in Nordic countries". App. Energy, vol. 112, pp. 1558–1565.

[Mal10] Mallette, M., and Venkataramanan, G. (2010). "Financial incentives to encourage demand response participation by plug-in hybrid electric vehicle owners". In *Proc. Energy Conv. Congr. 6 Expo.* (ECCE10). Atlanta, USA. September 12–16.

[Mar13] Martínez-Lacañina, P. J., Villa-Jaén, A., and Martínez-Ramos, J. L. (2013). "Hybrid procedure including subtransmission systems and substations for reliability assessment". IET Gen., Trans. & Distr., vol. 7, no. 12, pp. 1461–1472.

[Men08] Mendes, W. R., Samesima, M. I., and Moura, F. A. (2008). "Influence of power transformer winding connections on the propagation of voltage sags through electric system". In *Proc. 5th Int. Conf. on European Electr. Market* (EEM08). Lisbon, Portugal. May 28–30.

[Men14] Mena, R., Hennebel, M., Li, Y. –F., Ruiz, C., and Zio, E. (2015). "A risk-based simulation and multi-objective optimization framework for the integration of distributed renewable generation and storage". Renew. & Sust. Energy Reviews, vol. 37, pp. 778–793.

[Mil09] Millar, R. J., Hyvärinen, M., Lehtonen, M., and Hämäläinen, P. (2009). "Urban distribution networks – some general planning observations". In *Proc. 20st Conf. Electr. Distr.* (CIRED09). Prague, Czech Republic. June 8–11.

[Mil12] Millar, R. J., Kazemi, S., Lehtonen, M., and Saarijärvi, E. (2012). "Impact of MV connected microgrids on MV distribution planning". IEEE Trans. Smart Grid, vol. 3, no. 4, pp. 2100–2108.

[Moa13] Moazzami, M., Hemmati, R., Fesharaki, F. H., and Rad, S. R. (2013). "Reliability evaluation for different power plant busbar layouts by using sequential Monte Carlo simulation". Int. Jour. Electr. Power & Energy Syst , vol. 53, pp. 987–993.

[Mok10] Mokhlis, H., Li, H. Y., and Khalid, A. R. (2010). "The application of voltage sags pattern to locate a faulted section in distribution network". Int. Review of Electr. Eng., vol. 5, no. 1, pp. 173–179.

[Mub14] Mubbashir, A., Safdarian, A., and Lehtonen, M. (2014). "Demand response potential of residential HVAC loads considering user preferences". In *Proc. IEEE PES European Innov. Smart Grid Tech.* (ISGT14). Istanbul, Turkey. October 12–15.

[Nai12] Naidu, S. R., Andrade, G. V., and Costa, E. G. (2012). "Voltage sag performance of a distribution system and its improvement". IEEE Trans. Industr. App., vol. 48, no. 1, pp. 218–224.

[Nor08] Nordel (2008). *Annual Statistics 2008* [Report]. Available: https://www.entsoe.eu as of June of 2015.

[Nor11] Nordic Energy Regulators (2011). *Economic regulation of electricity grids in Nordic countries* [Report]. Available: http://nordicenergyregulators.org as of June of 2015.

[Nor15] Nord Pool Spot (2015). *The Power Market* [Concept]. Available: http://www.nordpoolspot.com as of June of 2015.

[Olg05] Olguin, G. (2005). *Voltage Dip (Sag) Estimation in Power Systems Based on Stochastic Assessment and Optimal Monitoring*. Doctoral Dissertation.

Dept. Energy & Environment, Chalmers University of Technology. Gothenburg, Sweden.

[Ond14] Onda, H., Yamamoto, S., Takeshit, H., Okamoto, S., and Yamanaka, N. (2014). “Peak load shifting and electricity charges reduction realized by electric vehicle storage virtualization”. In *Proc. 2nd AASRI Conf. Power & Energy Syst*. (PES13). Jeju Island, South Korea. December 27–28.

[Per13] Perrier, N., Agard, B., Baptiste, P., Frayret, J.-M., Langevin, A., Pellerin, R., Riopel, D., and Trépanier, M. (2013). “A survey of models and algorithms for emergency response logistics in electric distribution systems. Part I: Reliability planning with fault considerations”. Comp. & Operations Research, vol. 40, pp. 1895–1906.

[Pih06] Pihkala, A. (2006). *Helsingin 110 ja 400 kV Sähkönsiirtoverkon Kehittäminen* [The Development of the 110 and 400-kV Networks of Helsinki, *in Finnish*]. Master’s Thesis. Dept. Electrical Engineering, Helsinki University of Technology. Espoo, Finland.

[Pin11] Pindoriya, N. M., Jirutitijaroen, P., Srinivasan, D., and Singh, C. (2011). “Composite reliability evaluation using Monte Carlo simulation and Least Squares support vector classifier”. IEEE Trans. Power Syst., vol. 26, no. 4, pp. 2483–2490.

[Ras15] Rassaei, F., Soh, W., and Chua, K. (2015). “Demand response for residential electric vehicles with random usage patterns in smart grids”. IEEE Trans. Sust. Energy, vol. PP, no. 99, pp. 1–10, [*in Press*].

[Ren08] Renner, H., Heine, P., and Schmaranz, R. (2008). “Structural differences of European rural networks and their influence on supply reliability”. In *Proc. Power Qualit. & Supply Reliab. Conf. (PQ08)*. Pärnu, Estonia. August 27–29.

[Rid14] Ridzuan, M. I. M., Hernando-Gil, I., Djokić, S., Langella, R., and Testa, A. (2014). “Incorporating regulator requirements in reliability analysis of smart grids. Part 1: Input data and models”. In *Proc. IEEE PES European Innov. Smart Grid Tech*. (ISGT14). Istanbul, Turkey. October 12–15.

[Roc15] Rocchetta R., Li, Y. F., and Zio, E. (2015). “Risk assessment and risk-cost optimization of distributed power generation systems considering extreme weather conditions”. Reliab. Eng. & Syst. Safety, vol. 136, pp. 47–61.

[Saa13] Saarijärvi, E. (2013). *Geographical Perspectives on the Development of Power Distribution Systems in Sparsely Populated Areas*. Doctoral Dissertation. Dept. Electrical Engineering, Aalto University. Espoo, Finland.

[Saf14] Safdarian, A., Fotuhi-Firuzabad, M., Aminifar, F., and Lehtonen, M. (2014). “A new formulation for power system reliability assessment with AC constraints”. Int. Jour. Electr. Power & Energy Syst., vol. 56, pp. 298–306.

[Sal12] Salehi, J., and Haghifam, M. -R. (2012). “Long term distribution network planning considering urbanity uncertainties”. Int. Jour. Electr. Power & Energy Syst., vol. 42, pp. 321–333.

[Sha11] Shah, J., Wollenberg, B. F., and Mohan, N. (2011). “Decentralized power flow control for a smart micro-grid”. In *Proc. Power & Energy Society Gen. Meet.* (PES11). San Diego, USA. July 24–29.

[Sha13] Shayeghi, H., and Bagheri, A. (2013). “Dynamic sub-transmission system expansion planning incorporating distributed generation using hybrid DCGA and LP technique”. Int. Jour. Electr. Power & Energy Syst., vol. 48, pp. 111–122.

[Sie14] Siemens Energy Sector (2008). *Power Engineering Guidelines* [Report] (ed. 7.1) Available: http://www.energy.siemens.com as of June of 2015.

[Sil07] Silva, A. M. L., Resende, L. C., Manso, L. A. F., and Miranda, V. (2007). “Composite reliability assessment based on Monte Carlo Simulation and Artificial Neural Networks”. IEEE Trans. Power Syst., vol. 22, no. 3, pp. 1202–1209.

[Sin10] Sinhuber, P., Rohlfs, W., and Sauer, D. U. (2010). “Conceptional considerations for electrification of public city buses – energy storage system and charging stations”. In *Proc. Emobility – Electr. Power Train*. Leipzig, Germany. November 8–9.

[Sin12] Sinhuber, P., Rohlfs, W., and Sauer, D. U. (2012). “Study on power and energy demand for sizing the energy storage systems for electrified local public transport buses”. In *Proc. IEEE Vehicle Power & Propul. Conf.* (VPPC12). Seoul, South Korea. October 9–12.

[Sou12] **Sousa, B. J. O.** (2012). *Economic Assessment of Fault Current Limitation and Power Flow Control Techniques in Subtransmission Networks*. Master’s Thesis. Dept. Electrical Engineering, Aalto University. Espoo, Finland.

[Sou13] **Sousa, B. J. O.**, Pihkala, A., and Lehtonen, M. (2013). “Evaluation of fault current limitation techniques in urban meshed 110-kV subtransmission networks”. In *Proc. 4th IEEE PES Innov. Smart Grid Tech. Europe* (ISGT13). Lyngby, Denmark. October 6–9.

[Sou14] **Sousa, B. J. O.**, Pihkala, A., and Lehtonen, M. (2014). “Optimal allocation and assessment of superconducting fault current limiter in an urban meshed 110-kV subtransmission network”. In *Proc. 45th Cigré Session*. Paris, France. August 27–29.

[Sou15] **Sousa, B. J. O.**, Millar, J. R., and Lehtonen, M. (2015). “Influence of voltage sags and outage costs on realistic radial and backed-up 20-kV rural and urban networks”. In *Proc. 12th IEEE African Cont. Conf.* (AFRICON15). Addis Ababa, Ethiopia. September 14–17.

[Sta15] Statistics Finland (2015). *Rakennuskustannusindeksi* [Building cost index, *in Finnish*]. Available: http://www.stat.fi as of June of 2015.

[Sto15] Stockholms Ström (2015). *Svenska kraftnät – Stockholm* [Swedish Grid – Stockholm, *in Swedish*]. Available: http://www.stockholmsstrom.net as of June of 2015.

[Tor15] Torchio, M. F. (2015). “Comparison of district heating CHP and distributed generation CHP with energy, environmental and economic criteria for Northern Italy”. Energy Conv. & Management, vol. 92, pp. 114–128.

[Und06] Underbrink, A. (2006). “Risk analysis in distribution and transmission networks”. In *Proc. Int. Conf. on Prob. Methods Appl. to Power Syst.* (PMAPS06), Stockholm, Sweden, June 11–15.

[Uni14] United States Department of Energy (2014). *Smart Grid System Report 2014* [Report]. Available: http://energy.gov/ as of June of 2015.

[Vél10] Véliz, F. F. C., Borges, C. L. T., and Rei, A. M. (2010). “A comparison of load models for composite reliability evaluation by nonsequential Monte Carlo simulation”. IEEE Trans. Power Syst., vol. 25, no. 2, pp. 649–656.

[Wan10] Wang, Y., Huang, Y., Ma, C., and Xiao, X. (2010). “Voltage sag stochastic estimate”. In *Proc. Asia-Pacific Power & Energy Eng. Conf.* (APPEEC10). Chengdu, China. March 28–31.

[Wil00] Willis, H. L., and Scott, W. G. (2000). *Distributed Power Generation: Planning and Evaluation* (1st ed). Marcel Dekker, Inc. ISBN: 0-8247-0336-7.

[Wil04] Willis, H. L. (2004). *Power Distribution Planning Reference Book* (2nd ed). CRC Press. ISBN: 978-0-8247-4875-3.

[Won91] Wong, K. P., and Fung, C. C. (1991). "A knowledge-based approach for circuit allocation in subtransmission substations under maintenance condition". In *Proc. Int. Conf. Adv. in Power Contr., Operation & Management* (APSCOM91). Hong Kong. November 5–8.

[Yas12] Yasir, M., Kazemi, S., Lehtonen, M., and Fotuhi-Firuzabad, M. (2012). "A novel approach for assessing the impacts of voltage sag events on customer operations". In *Proc. Power Qualit. & Supply Reliab. Conf. (PQ12)*. Tartu, Estonia. June 11–13.

[Zha12] Zhang, P., Qian, K., Zhou, C., and Stewart, B. G. (2012). "Demand response for optimization of power systems demand due to EV charging load". In *Proc. Asia-Pacific Power & Energy Eng. Conf.* (APPEEC12). Shanghai, China. March 27–29.

Appendices

A. The Urban Nordic 110-kV Meshed Subtransmission Network Parameters

A.1. Inter-network & inter-substation connections

Connection data

Line name	Line type	Unit price [€/km]	Nominal power [MVA]	R [Ω/ph.km]	X [Ω/ph.km]	B [mho/ph.km]
ug1	*UGC*	*457 500* [a]	*75*	*0.125*	*0.138*	$47.1\cdot10^{-6}$
ug2	*UGC*	*493 500* [a]	*134*	*0.053*	*0.116*	$66.0\cdot10^{-6}$
ug3	*UGC*	*793 500* [a]	*210*	*0.022*	*0.101*	$103.7\cdot10^{-6}$
oh1s	*OHL*	*277 723* [a]	*281*	*0.049*	*0.270*	$3.6\cdot10^{-6}$
oh1d [b]	*OHL*	*365 146* [a,b]	*562* [b]	*0.025* [b]	*0.135* [b]	$7.2\cdot10^{-6}$ [b]
oh2s	*OHL*	*362 381* [a]	*410*	*0.027*	*0.260*	$4.2\cdot10^{-6}$
oh2d [b]	*OHL*	*481 383* [a,b]	*820* [b]	*0.014* [b]	*0.130* [b]	$8.4\cdot10^{-6}$ [b]

[a] Prices based in [Hyv08] and adjusted to present values [Sta15]
[b] Double circuits, data for both circuits

Inter-network connections

Connection Name	Connection type	Insulation type	Nominal power [MVA]	R [Ω]	X [Ω]
Transf. 1	*EHV/HV*	*AIS*	*380, 420, 470, 430* [c]		
Transf. 3a	*EHV/HV*	*AIS*	*380, 420, 470, 430* [c]	*1*	*80*
Transf. 3b	*EHV/HV*	*AIS*	*380, 420, 470, 430* [c]		
Transf. 4	*EHV/HV*	*GIS*	*350, 390, 430, 400* [c]		
CHP 2	*MV/HV*	*indoors*	*770* [d]		
CHP 4	*MV/HV*	*indoors*	*275* [d]	*1.5*	*40*
CHP 5	*MV/HV*	*indoors*	*188* [d]		
Interconn. 1	*HV/HV*	*overhead*	*281*		
Interconn. 3	*HV/HV*	*overhead*	*281*	*0.1*	*0.54*
Interconn. 15	*HV/HV*	*overhead*	*281*		

[c] For summer, fall, winter & spring respectively
[d] Maximum nominal output

Inter-substation connections

Connection name [e]	Line used	Total length [km]	Length in common-mode [km]	Nominal power [MVA]
4 - 7.1	*ug3*	*6.00*	—	*210*
4 - 7.2	*ug3*	*6.00*	—	*210*
4 - 18.1	*ug2*	*1.95*	—	*134*
4 - 18.2	*ug2*	*2.24*	—	*134*
4 – 20	*ug2*	*3.60*	—	*134*
4 – 22	*ug2*	*3.89*	—	*134*
4 - 24.1	*ug2*	*2.08*	—	*134*
4 - 24.2	*ug2*	*2.59*	—	*134*
4 – 25	*ug2*	*4.08*	—	*134*
5 – 20	*ug2*	*3.09*	—	*134*
5 – 21	*ug2*	*2.25*	—	*134*
5 – 23	*ug2*	*3.15*	—	*134*
6 - 10.1	*ug1*	*4.10*	—	*75*
6 - 10.2	*ug1*	*4.04*	—	*75*
7 – 16	*ug2*	*4.50*	—	*134*
7 – 17	*ug2*	*4.50*	—	*134*
16 – 17	*ug2*	*1.00*	—	*134*
17 – 18	*ug2*	*1.64*	—	*134*
21 -22	*ug2*	*0.99*	—	*134*
22 -25	*ug2*	*1.47*	—	*134*
23 – 24	*ug2*	*1.53*	—	*134*
110-kV underground cables:		64.71		
1 - 9.1	*oh1d*	*3.01*	*3,01*	*281*
1 - 9.2	*oh1d*	*3.01*	*3,01*	*281*
1 – 11	*oh1s & oh1d*	*4.56*	*1.62*	*281*
2 – 6	*oh2d*	*8.60*	*8.60*	*410*
2 – 9	*oh2d*	*3.93*	*3.93*	*410*
3 – 11	*oh1s & oh1d*	*8.24*	*1.62*	*281*
3 – 12	*oh1d*	*4.82*	*4.82*	*281*
3 – 15	*oh1s & oh1d*	*8.37*	*0.78*	*281*
3 – 14	*oh1d*	*5.06*	*5.06*	*281*
5 – 8	*oh1d*	*6.99*	*6.99*	*281*
5 – 19	*oh1d*	*3.37*	*3.37*	*281*
6 - 7.1	*oh1d*	*4.70*	*4.70*	*281*
6 - 7.2	*oh1d*	*4.70*	*4.70*	*281*
6 – 9	*oh2d*	*4.80*	*4.80*	*410*
7 - 8.1	*oh1d*	*6.08*	*6.08*	*281*
7 - 8.2	*oh1d*	*6.08*	*6.08*	*281*
7 – 13	*oh1d*	*1.80*	*1.80*	*281*
7 – 14	*oh1d*	*5.06*	*5.06*	*281*
8 - 15.1	*oh1d*	*3.72*	*3.72*	*281*
8 - 15.2	*oh1d*	*3.72*	*3.72*	*281*
8 – 19	*oh1d*	*3.61*	*3.61*	*281*
12 – 13	*oh1d*	*5.47*	*5.47*	*281*
110-kV overhead lines:		109.63	92.48	

[e] Name from the substations connected by the line

A.2. Generation Output & Load Demand

Graph 1 combines the sum of the output of all CHP plants and the average load demand of substations in the Nordic subtransmission network in the year scenarios. This thesis assumes that CHP outputs are invariable in the course of a day.

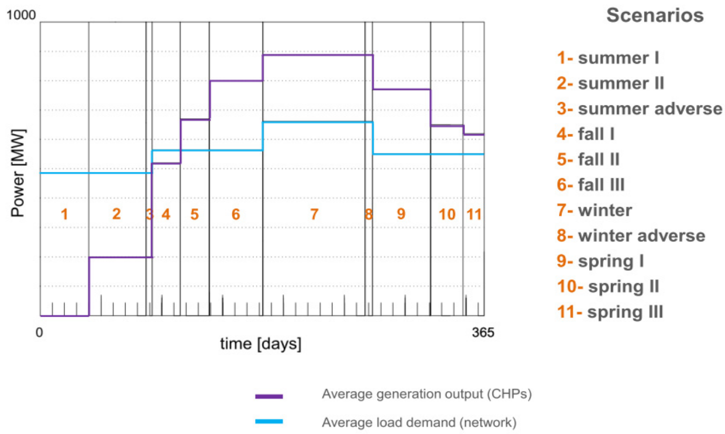

Graph 1 Generation output and demanded load of the Nordic subtransmission network.

Conversely, load demand does vary in the course of a day and must be modeled using the load profile graphic to be computed in this assessment. Each substation is modeled according to customer category and power consumption and an hourly-based distribution, based on statistical data collected by the utility company. Load is per unit and should be multiplied by the average seasonal load demand.

Graph 2 depicts the load profile of typical urban customers measured in the MV/LV transformers. The load is averaged over the year and in combination with Graphic 1, the demanded load for each scenario is obtained.

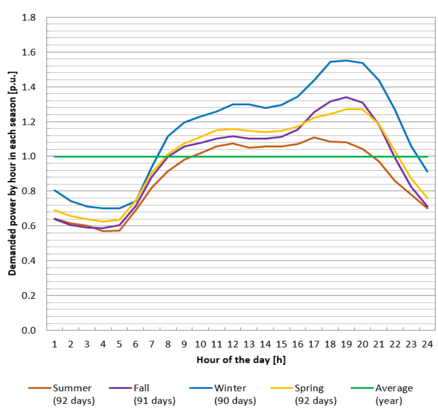

Graph 2 Typical urban load profile in the four seasons of the year.

B. Equipment & Device Data

B.1. Fault statistics & related coefficients

Component statistics & failure rate coefficients (α, β)

Line name	Failure rate [occ/a]	Repair time [h/occ]	Coefficient α [f]		Coefficient β [g]		
			day	*night*	*normal*	*sum.adv*	*win.adv*
110-kV UGC [km]	*0.0043*	*336*	*1.478*	*0.522*	*1*	*1*	*1*
110-kV OHL – single circuit [km]	*0.0171*	*48*	*1*	*1*	*0.765*	*8.57*	*8.57*
110-kV OHL – CM [km]	*0.0101*	*48*	*1*	*1*	*0.250*	*25.14*	*25.14*
indoor – GIS							
110-kV circuit breaker	*0.0022*	*100*	*1*	*1*	*1*	*1*	*1*
110-kV busbar	*0.0038*	*200*	*1*	*1*	*1*	*1*	*1*
MV circuit breaker	*0.0022*	*50*	*1*	*1*	*1*	*1*	*1*
EHV/HV transformer	*0.0018*	*300*	*1.443*	*0.557*	*1*	*1*	*1*
HV/MV transformer	*0.0179*	*300*	*1*	*1*	*1*	*1*	*1*
outdoor – AIS							
110-kV circuit breaker	*0.0034*	*100*	*1*	*1*	*0.660*	*9.95*	*13.60*
110-kV busbar	*0.0057*	*200*	*1*	*1*	*0.660*	*9.95*	*13.60*
MV circuit breaker	*0.0034*	*50*	*1*	*1*	*0.660*	*9.95*	*13.60*
EHV/HV transformer	*0.0020*	*300*	*1*	*1*	*0.881*	*4.83*	*4.83*
HV/MV transformer	*0.0226*	*300*	*1*	*1*	*0.791*	*7.73*	*7.73*

[f] Values filled as 1 indicate lack of statistical data, thus no variation in the timespan of a day
[g] Values filled as 1 indicate lack of statistical data, thus no variation in the timespan of a year

Fault shares

Line type	Share of Fault Type, *a* [%]			
	1-ph	2-ph	2-ph-gr	3-ph
110-kV underground cable [km]	*90*	*0*	*0*	*10*
110-kV overhead line – normal weather [km]	*82*	*2*	*14*	*2*
110-kV overhead line – adverse weather [km]	*75*	*5*	*15*	*5*

Line type	Share of Fault Duration, *b* [%]			
	Normal weather		Adverse weather	
	momentary & temporary	permanent	momentary & temporary	permanent
110-kV underground cable [km] [h]	*0*	*100*	*0*	*100*
110-kV overhead line – single line [km]	*84.62*	*15.38*	*87.24*	*12.76*
110-kV overhead line – common mode [km]	*0*	*100*	*99.01*	*0.99*
HV/MV transformer	*84.21*	*15.79*	*84.21*	*15.79*

[h] Due to the protection philosophy, all faults are considered permanent in underground networks

B.2. General parameters

General data	
Annual interest rate (i)	6 %
Annual load growth (g)	1 %
Project time (T)	40 years
Review period (T')	0 years *(or 20 years)*
Losses calculation	
Peak utilization time (T_p)	4500 h/a *(HV/MV transformer)*
	5000 h/a *(HV line)*
Power factor (pf)	0.94†
Price of energy losses, load (p_{els})	0.04 €/kWh†
Price of energy losses, no-load (p_{els})	0.03 €/kWh†
Price of power losses, load (p_{pl})	5 €/kWh.a *(HV/MV transformer)*
	5 €/kWh.a *(HV line)*

†*Values are valid for the year or within each scenario, in case of variation.*

C. Customer Categories & Penalties

Load distribution

Substation Type	Share of the energy [%]				Customer interruption costs	
	Agricultural	Commercial & Public	Industrial	Residential	cic_e [€/kWh]	cic_p [€/kW]
Industrial	*0*	*40*	*55*	*5*	*2.90*	*23.46*
Rural	*30*	*10*	*0*	*60*	*0.59*	*7.84*
Suburban mixed	*0*	*20*	*5*	*75*	*0.92*	*9.34*
Urban	*0*	*60*	*10*	*30*	*1.88*	*18.43*
Urban core [i]	*0*	*80*	*10*	*10*	*2.28*	*22.47*

[i] Values from [Hyv08]

Penalty for voltage sag event

Customer category	Penalty [€/sag.cust]
Agricultural	*1*
Commercial & Public	*170*
Residential	*1*
Industrial [j]	*1060*

[j] Values from [Hei02]

D. Discount Factors (*k_c*, *k_l* & *k_q*)

This Appendix delineates the three discount factors utilized in this thesis to determine the present value of future cash flows over the estimated project time including their relationship with annual load growth and annual interest rate, in which:

$$\gamma_0 = \frac{1}{1+i}, \quad \gamma_1 = \frac{(1+g)}{1+i}, \quad \gamma_2 = \frac{(1+g)^2}{1+i}$$

They are:

Discount factor for constant cash flow (k_c), independent from load growth

$$k_c = \frac{1}{i} \cdot \left(1 - \gamma_0^T\right)$$

Discount factor in linear relationship with annual load growth (k_l)

$$k_l = \gamma_1 \frac{\gamma_1^T - 1}{\gamma_1 - 1} + \gamma_0 \gamma_1^{T'} \cdot \frac{\left(\gamma_0^{T-T'} - 1\right)}{\left(\gamma_0 - 1\right)}$$

Discount factor in quadratic relationship with annual load growth (k_q)

$$k_q = \gamma_2 \frac{\gamma_2^T - 1}{\gamma_2 - 1} + \gamma_0 \gamma_2^{T'} \cdot \frac{\left(\gamma_0^{T-T'} - 1\right)}{\left(\gamma_0 - 1\right)}$$

These three discount factors are used accordingly to depict the constant, linear and quadratic relationship to the annual load growth. These discount factors are accordingly multiplied with the components of the network cost function. The annual load growth is the translation of electric current from the network circuital parameterization to be associated in terms of monetary values.

Power losses are quadratically-related to load growth, due to the i^2 (square current) multiplier. Capital costs, rents and maintenance are independent from load growth. Therefore, they are written in terms of present values by multiplying them by the constant discount factors. The other costs from the network cost function are linearly-related to the annual load growth. They are, consequently, multiplied by the linear discount factor.

E. Residual Voltages from Symmetrical & Asymmetrical Faults

This Appendix contains the residual voltages from the four types of faults considered in this thesis and the currents from symmetrical short circuits. These equations were derived based on [Gra94], [Bol00] and [Iec01], including the assumption of fault impedance as zero for the residual voltage calculations, and employing the impedance matrices for sequence components. The equations for residual voltages are employed to meshed and larger networks; nevertheless, they can be also extended to radial and looped networks, despite the existence of more straightforward techniques for the calculation in these simpler topologies.

E.1. Residual voltages

The superindices A, B, C, 0, + and - stand for phases A, B and C and zero, positive and negative sequences, respectively. The subindices i and r refer to the substation that experiences the voltage sag and the substation at which the fault occurs, respectively, where:

a	Fortescue operator
U_{res}	residual voltage during the voltage sag [p.u.]
U_0	pre-fault voltage [p.u.]
z_{ir}	transfer element of the impedance matrix [p.u.]
z_{rr}	diagonal element of the impedance matrix [p.u.]

Residual voltages from single-phase-to-ground faults (1-ph-gr), phase A faulted

$$U^A_{res_i} = U^A_{0_i} - \frac{\left(z^0_{ir} + z^+_{ir} + z^-_{ir}\right)}{z^0_{rr} + z^+_{rr} + z^-_{rr}} \cdot U^A_{0_r}$$

$$U^B_{res_i} = U^B_{0_i} - \frac{\left(z^0_{ir} + \mathrm{a}^2 z^+_{ir} + \mathrm{a} z^-_{ir}\right)}{z^0_{rr} + z^+_{rr} + z^-_{rr}} \cdot U^A_{0_r}$$

$$U^C_{res_i} = U^C_{0_i} - \frac{\left(z^0_{ir} + \mathrm{a} z^+_{ir} + \mathrm{a}^2 z^-_{ir}\right)}{z^0_{rr} + z^+_{rr} + z^-_{rr}} \cdot U^A_{0_r}$$

Residual voltages from phase-to-phase short circuits (2-ph), phases B and C short-circuited

$$U^A_{res_i} = U^A_{0_i} + \frac{\left(z^+_{ir} - z^-_{ir}\right)}{z^+_{rr} + z^-_{rr}} \cdot U^A_{0_r}$$

$$U^{B}_{res_i} = U^{B}_{0_i} + \frac{\left(\text{-a}^2 z^{+}_{ir} + \text{a} z^{-}_{ir}\right)}{z^{+}_{rr} + z^{-}_{rr}} \cdot U^{A}_{0_r}$$

$$U^{C}_{res_i} = U^{C}_{0_i} + \frac{\left(\text{-a} z^{+}_{ir} + \text{a}^2 z^{-}_{ir}\right)}{z^{+}_{rr} + z^{-}_{rr}} \cdot U^{A}_{0_r}$$

Residual voltages from two-phase-to-ground faults (2-ph-gr), phases B and C faulted

$$U^{A}_{res_i} = U^{A}_{0_i} - \frac{\left(z^{0}_{ir} \cdot z^{-}_{rr} + z^{-}_{ir} \cdot z^{0}_{rr} - z^{+}_{ir}\right)}{\Delta} \cdot U^{A}_{0_r}$$

$$U^{B}_{res_i} = U^{B}_{0_i} - \frac{\left(z^{0}_{ir} \cdot z^{-}_{rr} + \text{a} z^{-}_{ir} \cdot z^{0}_{rr} - \text{a}^2 z^{+}_{ir}\right)}{\Delta} \cdot U^{A}_{0_r}$$

$$U^{C}_{res_i} = U^{C}_{0_i} - \frac{\left(z^{0}_{ir} \cdot z^{-}_{rr} + \text{a}^2 z^{-}_{ir} \cdot z^{0}_{rr} - \text{a} z^{+}_{ir}\right)}{\Delta} \cdot U^{A}_{0_r}$$

in which:

$$\Delta = z^{+}_{rr} \cdot \left(z^{0}_{rr} + z^{-}_{rr}\right) + z^{0}_{rr} \cdot z^{-}_{rr}$$

Residual voltage from three-phase short circuits (3-ph), for the three-phases

$$U_{res_i} = U_{0_i} - \frac{z_{ir}}{z_{rr}} \cdot U_{0_r}$$

E.2. Currents from symmetrical short circuits

Parameters in the calculation of the initial symmetrical short-circuit current (I_k'') and peak short-circuit current (I_p) from symmetrical short circuits:

c	voltage factor accounting voltage level
R/X	resistance-reactance ratio at the short-circuit point [Ω]
U_n	nominal voltage [kV]
Z_k	short-circuit impedance at the short-circuit point [Ω]
κ	factor accounting decay of DC component

Initial symmetrical short-circuit current (I_k'')

$$I_k'' = \frac{cU_n}{\sqrt{3}Z_k}$$

Peak short-circuit current (I_p)

$$I_p = 1.15k\sqrt{2}I_k''$$

where:

$$\kappa = 1.02 + 0.98 \cdot e^{-(3R/X)}$$

This thesis is the end of my five-year journey at Aalto University and the result of my research in the field of reliability in power systems. The thesis develops a four-module method to assess reliability and economically evaluate a dynamic, multivalent and intermediate part of the power system: the subtransmission network.

In the context of this research and also raising other power quality issues, I focused my work on meshed subtransmission networks in urban areas of temperate/subarctic regions introducing multiscenarios in a bi-dimensional quasi-chronological time assessment over a given project time.

Aalto-DD 167/2015

9 789526 064956

ISBN 978-952-60-6495-6 (printed)
ISBN 978-952-60-6496-3 (pdf)
ISSN-L 1799-4934
ISSN 1799-4934 (printed)
ISSN 1799-4942 (pdf)

Aalto University
School of Electrical Engineering
Department of Electrical Engineering and Automation
www.aalto.fi

BUSINESS +
ECONOMY

ART +
DESIGN +
ARCHITECTURE

SCIENCE +
TECHNOLOGY

CROSSOVER

DOCTORAL
DISSERTATIONS